Synthesis of Some New Pyrene-Based Hydrazinyl-Thiazole Derivatives via a One-Pot Strategy: Biological Evaluation and Molecular Docking Studies

Pramod Dinkar Jawalepatil,*[a†] Amol Maruti Jadhav,*[b†] Pritam Bhagwan Bhosale,[c] Pooja Singh,[d] Hyun Ho Choi,*[b,e] Sang Yong Nam,*[b,e] Mahesh N. Waman,[f] Gajanan N. Wadje,[f] Satish U. Deshmukh*[f]

[a] *Department of Chemistry, Balbhim Arts, Science and Commerce College Beed.431122, MS, India.*

E-mail: pramodjawalepatil@gmail.com

[b] *Research Institute of Green Energy, and Convergence Technology (RIGET), Gyeongsang National University, Jinju 52828, South Korea.*

E-mail: amolj848@gmail.com

[c] *Department of Veterinary Medicine, Research Institute of Life Science, Gyeongsang National University, 501 Jinju-daero, Jinju, 52828, Republic of Korea*

[d] *Division of Applied Life Science, (BK21 Four), Plant Molecular Biology and Biotechnology Research Center (PMBBRC), Gyeongsang National University (GNU), 501 Jinju-Daero, Jinju, 52828, Republic of Korea*

[e] Department of Materials Engineering and Convergence Technology, Gyeongsang National University, Jinju 52828, Republic of Korea.

E-mail: hh.choi@gnu.ac.kr, walden@gnu.ac.kr

[f] *Department of Chemistry, Deogiri College, Aurangabad, Maharashtra 431005, India*

E-mail: satishud@gmail.com

*Author to whom correspondence should be addressed.

† These authors contributed equally to this work.

Supporting Information

Table of Contents

General procedure.....S3

Spectral data of the compounds (**4a-4o**).....S4

Fig. S1-S2. ^{1}H NMR and ^{13}C NMR spectra of (**4a**)……S12

^{1}H NMR, ^{13}C NMR, ^{19}F NMR, FTIR and LC-MS spectra explanation.....S13-S14

Materials and methods, Computational methods and *In Vitro* Cytotoxicity Assay……..S15-S16

Fig. S3. Target predicted for compound by SwissTargetPrediction online tool……..S17

Fig. S4. Cytotoxic effects of compounds (**4h**, **4j**, **4k**, **4l** and **4n**)…….S18

Fig. S5. Molecular docking 2D interaction maps of synthesized compounds (**4a–4o**)…..S18-S19

Fig. S6. Cytotoxic efficiency of the synthesized compounds (**4g)** and (**4m**)……S20

Fig. S7-S8. Molecular docking 3D interaction maps of (**4h**, **4j**, **4k**, **4l** and **4n**)…….S21-S22

Fig. S9-S74 ^{1}H NMR, ^{13}C NMR, ^{19}F NMR, FTIR and LC-MS spectra of (**4a-4o**)…….S23

General procedure:

Synthesis of (E)-4-(4-chlorophenyl)-2-(2-(pyren-1-ylmethylene)hydrazinyl)thiazole (4a–4o)

A mixture of pyrene-1-carbaldehyde (**1a**, 1.0 mmol), thiosemicarbazide (**2a**, 1.0 mmol), and *p*-chlorophenacyl bromide (**3a**, 1.0 mmol) was dissolved in a 10 mL mixture of water and ethanol (H_2O:EtOH, 1:1, v/v). Indium(III) chloride ($InCl_3$, 10 mol%) was then added, and the reaction mixture was refluxed under continuous stirring for 2–4 h. The reaction progress was monitored by thin-layer chromatography (TLC) using hexane/ethyl acetate (7:3) as the mobile phase. After completion, the mixture was cooled to room temperature, and the resulting precipitate was collected by filtration, washed with cold ethanol, and dried under reduced pressure. The crude product was further purified by recrystallization from ethanol to afford compound **4a** in 98% yield. Following this procedure, derivatives **4b–4o** were synthesized in good to excellent yields.

Spectral data of the compounds (**4a-4o**)

(*E*)-4-(4-chlorophenyl)-2-(2-(pyren-2-ylmethylene) hydrazinyl) thiazole **(4a)**

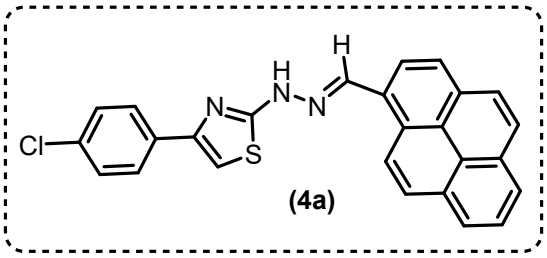

Solid; Dark brown color; Yield 98%; m.p: 282-284 °C; IR (ν_{max}) cm^{-1}: 3211 ($N–H_{str}$), 2972 ($C–H_{str}$), 1540($C=N_{str}$) 1622 ($Ar\text{-}C=C_{str}$), 1080 ($C–S_{str}$); ^1H NMR (300 MHz, DMSO-d_6) δ 12.48 (s, 1H), 9.08 (s, 1H), 8.75 (d, J = 9.5 Hz, 1H), 8.51 (s, 1H), 8.34 (s, 2H), 8.23 (d, J = 5.2 Hz, 3H), 8.15 – 8.09 (m, 2H), 7.92 – 7.89 (m, 2H), 7.48 (d, J = 1.7 Hz, 3H). ^{13}C NMR (75 MHz, DMSO-d_6) δ 168.73, 140.71, 133.97, 132.52, 131.92, 131.42, 130.70, 129.12, 128.66, 128.29, 127.64, 127.08, 126.47, 126.09, 125.69, 125.35, 125.03, 124.74, 124.35, 122.86, 105.14; LC-MS calcd for $C_{26}H_{16}ClN_3S$ $[M + H]^+$ 437.08, found 438.03; Elemental Analysis: C, 71.31; H, 3.68; Cl, 8.09; N, 9.60; S, 7.32.

(E)-2-(2-(pyren-1-ylmethylene) hydrazineyl)-4-(p-tolyl) thiazole **(4b)**

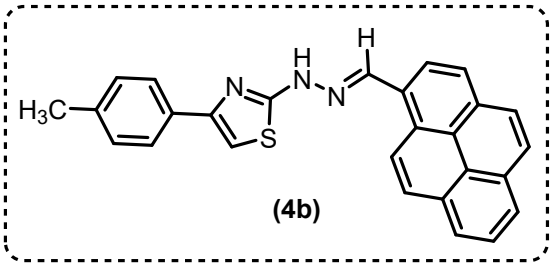

Solid; Dark yellow color; Yield 96%; m.p: 285-287 °C; IR (ν_{max}) cm^{-1}: 3270 ($N–H_{str}$), 2980 ($C–H_{str}$), 1557($C=N_{str}$) 1611 ($Ar\text{-}C=C_{str}$), 1050 ($C–S_{str}$); ^1H NMR (300 MHz, DMSO-d_6) δ 9.07 (s, 1H), 8.76 (d, J = 9.5 Hz, 1H), 8.50 (d, J = 8.2 Hz, 1H), 8.40 – 8.33 (m, 4H), 8.23 (q, J = 9.0 Hz, 2H), 8.16 – 8.09 (m, 1H), 7.80 (d, J = 8.1 Hz, 2H), 7.32 (s, 1H), 7.25 (d, J = 8.0 Hz, 2H), 2.34 (s, 3H). ^{13}C NMR (75 MHz, DMSO-d_6) δ 168.50, 140.52, 137.37, 132.42, 131.79, 131.43, 130.71, 129.69, 129.08, 128.54, 128.25, 127.91, 127.60, 127.08, 126.45, 125.95, 125.09, 124.76, 124.36,

122.88, 121.95, 103.40, 39.97, 21.30; LC-MS calcd for $C_{27}H_{19}N_3S$ $[M + H]^+$ 417.13, found 488.08; Elemental Analysis: C, 77.67; H, 4.59; N, 10.06; S, 7.68.

(E)-4-(4-nitrophenyl)-2-(2-(pyren-1-ylmethylene) hydrazinyl) thiazole **(4c)**

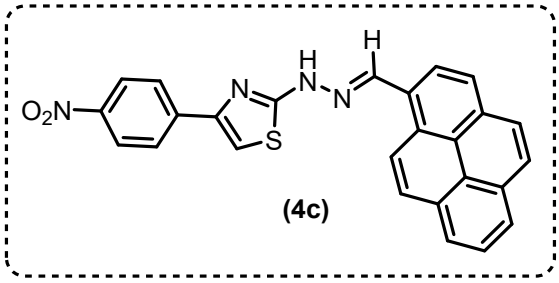

(4c)

Solid; Dark yellow color; Yield 96%; m.p: 287-289 °C; IR (ν_{max}) cm^{-1}: 3125 ($N–H_{str}$), 3020 ($C–H_{str}$), 1553 ($C=N_{str}$) 1595 ($Ar\text{-}C=C_{str}$), 1100 ($C–S_{str}$); ^1H NMR (300 MHz, DMSO-d_6) δ 12.57 (s, 1H), 9.10 (s, 1H), 8.77 (d, J = 9.5 Hz, 1H), 8.52 (d, J = 8.3 Hz, 1H), 8.38 (d, J = 1.0 Hz, 2H), 8.36 (s, 2H), 8.33 (s, 1H), 8.30 (s, 1H), 8.25 (d, J = 5.1 Hz, 2H), 8.18 (s, 1H), 8.15 (d, J = 2.2 Hz, 2H), 7.81 (s, 1H). ^{13}C NMR (75 MHz, DMSO-d_6) δ 167.80, 146.65, 139.81, 135.50, 130.91, 130.33, 129.89, 128.32, 127.69, 127.12, 126.70, 126.24, 126.02, 125.68, 125.10, 124.82, 124.01, 123.80, 123.25, 121.77, 121.41, 119.40, 105.04; LC-MS calcd for $C_{26}H_{16}N_4O_2S$ $[M + H]^+$ 448.10, found 448.94; Elemental Analysis: C, 69.63; H, 3.60; N, 12.49; O, 7.13; S, 7.15.

(E)-4-(3-nitrophenyl)-2-(2-(pyren-1-ylmethylene) hydrazinyl) thiazole **(4d)**

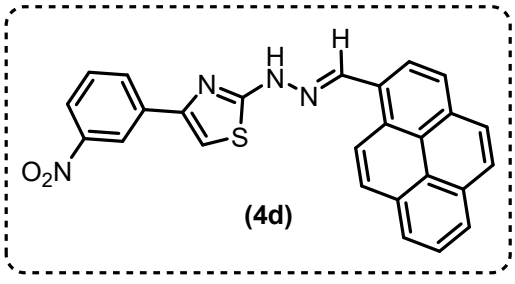

(4d)

Solid; Dark yellow color; Yield 93%; m.p: 284-286 °C; IR (ν_{max}) cm^{-1}: 3264 ($N–H_{str}$), 3010 ($C–H_{str}$), 0000 1510 ($C=N_{str}$) 1590 ($Ar\text{-}C=C_{str}$), 1065 ($C–S_{str}$); ^1H NMR (300 MHz, DMSO-d_6) δ 12.56 (s, 1H), 9.06 (s, 1H), 8.76 (d, J = 9.4 Hz, 1H), 8.71 (s, 1H), 8.50 (d, J = 8.2 Hz, 1H), 8.37 (s, 2H), 8.34 (d, J = 3.2 Hz, 3H), 8.23 (d, J = 5.5 Hz, 2H), 8.14 (s, 1H), 8.11 (d, J = 7.5 Hz, 1H), 7.72 (d, J = 4.1 Hz, 2H). ^{13}C NMR (75 MHz, DMSO-d_6) δ 167.95, 147.75, 139.91, 135.61, 130.97, 130.43,

129.69, 128.12, 127.59, 127.32, 126.90, 126.44, 126.07, 125.48, 125.11, 124.76, 124.09, 123.74, 123.35, 121.87, 121.51, 119.43, 106.04; LC-MS calcd for $C_{26}H_{16}N_4O_2S$ $[M + H]^+$ 448.10, found 448.94; Elemental Analysis: C, 69.63; H, 3.60; N, 12.49; O, 7.13; S, 7.15.

(E)-4-(4-fluorophenyl)-2-(2-(pyren-1-ylmethylene) hydrazineyl) thiazole **(4e)**

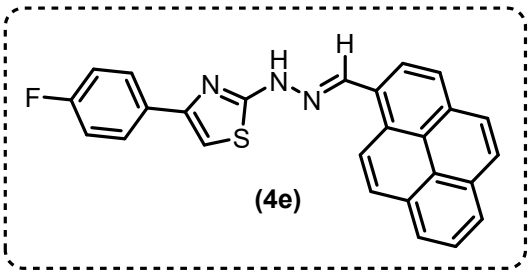

(4e)

Solid; light green color; Yield 89%; m.p: 277-279 °C; IR (ν_{max}) cm^{-1}: 3275 ($N–H_{str}$), 3018 ($C–H_{str}$), 1560 ($C=N_{str}$) 1614 ($Ar\text{-}C=C_{str}$), 1048 ($C–S_{str}$); ^1H NMR (300 MHz, DMSO-d_6) δ 9.08 (s, 1H), 8.76 (d, J = 9.4 Hz, 1H), 8.50 (d, J = 8.2 Hz, 1H), 8.36 (d, J = 7.9 Hz, 4H), 8.23 (d, J = 5.0 Hz, 2H), 8.12 (t, J = 7.6 Hz, 1H), 7.98 – 7.91 (m, 2H), 7.39 (s, 1H), 7.31 – 7.24 (m, 2H). 13C NMR (75 MHz, DMSO-d_6) δ 168.69, 140.63, 131.80, 131.42, 130.69, 129.06, 128.53, 128.05, 127.55, 127.06, 126.44, 126.07, 125.76, 124.86, 124.35, 122.85, 116.09, 115.81, 104.08; LC-MS calcd for $C_{26}H_{16}FN_3S$ $[M + H]^+$ 421.10, found 421.97; Elemental Analysis: C, 74.09; H, 3.83; F, 4.51; N, 9.97; S, 7.61.

(E)-4-(3-bromophenyl)-2-(2-(pyren-1-ylmethylene) hydrazineyl) thiazole **(4f)**

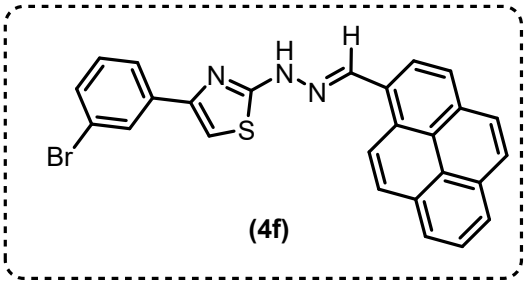

(4f)

Solid; Dark brown color; Yield 92%; m.p: 278-280 °C; IR (ν_{max}) cm^{-1}: 3155 ($N–H_{str}$), 2992 ($C–H_{str}$), 1545 ($C=N_{str}$) 1606 ($Ar\text{-}C=C_{str}$), 1030 ($C–S_{str}$); ^1H NMR (300 MHz, DMSO-d_6) δ 12.49 (s, 1H), 9.07 (s, 1H), 8.76 (d, J = 9.5 Hz, 1H), 8.50 (d, J = 8.2 Hz, 1H), 8.36 (dd, J = 8.1, 2.6 Hz, 4H), 8.23 (q, J = 9.0 Hz, 2H), 8.16 – 8.09 (m, 2H), 7.92 (d, J = 7.8 Hz, 1H), 7.57 (s, 1H), 7.52 (m, 1H),

7.41 (t, J = 7.9 Hz, 1H); ^{13}C NMR (75 MHz, DMSO-d_6) δ 167.52, 158.36, 130.81, 130.59, 130.20, 129.72, 128.09, 127.56, 127.28, 126.94, 126.53, 126.10, 125.48, 125.10, 124.80, 124.05, 123.78, 123.39, 113.51, 101.20; LC-MS calcd for $C_{26}H_{16}BrN_3S$ $[M + H]^+$ 481.02, found 481.90; Elemental Analysis: C, 64.74; H, 3.34; Br, 16.56; N, 8.71; S, 6.65.

(E)-4-(4-methoxyphenyl)-2-(2-(pyren-1-ylmethylene) hydrazineyl) thiazole **(4g)**

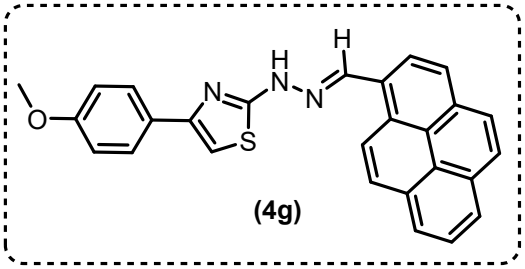

(4g)

Solid; Brown color; Yield 95%; m.p: 279-281 °C; IR (ν_{max}) cm^{-1}: 3198 (N–H_{str}), 3031 (C–H_{str}), 1556 (C=N_{str}) 1626 (Ar-C=C_{str}), 1053 (C–S_{str}); ^{1}H NMR (300 MHz, DMSO) δ 9.06 (s, 1H), 8.75 (d, *J* = 9.4 Hz, 1H), 8.49 (d, *J* = 8.2 Hz, 1H), 8.35 (d, *J* = 7.8 Hz, 4H), 8.23 (t, *J* = 7.0 Hz, 2H), 8.11 (t, *J* = 7.6 Hz, 1H), 7.83 (d, *J* = 8.7 Hz, 2H), 7.22 (s, 1H), 6.99 (d, *J* = 8.8 Hz, 2H), 3.80 (s, 3H). ^{13}C NMR (75 MHz, DMSO-d_6) δ 168.72, 149.41, 140.78, 137.36, 131.84, 131.37, 130.68, 129.08, 128.60, 128.26, 127.90, 127.74, 127.25, 127.05, 126.45, 126.07, 125.76, 124.96, 124.34, 122.73, 114.47, 105.93, 55.61; LC-MS calcd for $C_{27}H_{19}N_3OS$ $[M + H]^+$ 433.12, found 434.54; Elemental Analysis: C, 74.80; H, 4.42; N, 9.69; O, 3.69; S, 7.40.

(E)-4-(4-(methyl sulfonyl) phenyl)-2-(2-(pyren-1-ylmethylene) hydrazineyl) thiazole **(4h)**

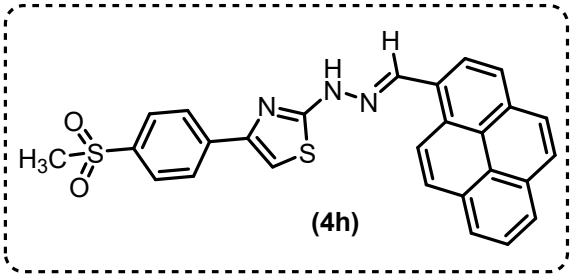

(4h)

Solid; Light green color; Yield 91%; m.p: 275-277 °C; IR (ν_{max}) cm^{-1}: 3221 (N–H_{str}), 3004 (C–H_{str}), 1564 (C=N_{str}) 1591 (Ar-C=C_{str}), 1084 (C–S_{str}); ^{1}H NMR (300 MHz, DMSO-d_6) δ 12.53 (s, 1H), 9.07 (s, 1H), 8.75 (d, J = 9.5 Hz, 1H), 8.50 (d, J = 8.2 Hz, 1H), 8.35 (dd, J = 8.1, 2.5 Hz, 4H), 8.23 (q, J = 9.0 Hz, 2H), 8.14 (t, J = 7.9 Hz, 3H), 7.98 (d, J = 8.5 Hz, 2H), 7.71 (s, 1H), 3.25 (s,

3H). ^{13}C NMR (75 MHz, DMSO-d_6) δ 168.93, 149.54, 140.90, 139.69, 131.87, 131.41, 130.68, 129.11, 128.59, 128.31, 127.96, 127.44, 127.07, 126.54, 126.10, 125.76, 125.06, 124.73, 124.34, 122.84, 107.91, 44.09; LC-MS calcd for $C_{27}H_{19}N_3O_2S_2$ $[M + H]^+$ 481.09, found 482.04; Elemental Analysis: C, 67.34; H, 3.98; N, 8.73; O, 6.64; S, 13.31.

(E)-4-([1,1'-biphenyl]-4-yl)-2-(2-(pyren-1-ylmethylene) hydrazineyl) thiazole **(4i)**

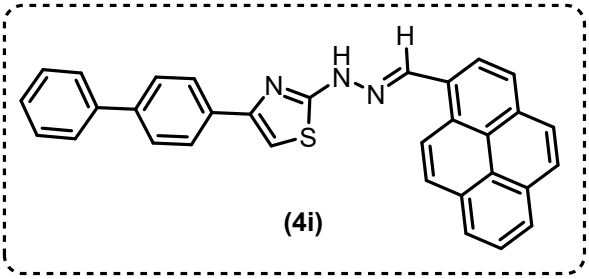

(4i)

Solid; Dark brown color; Yield 88%; m.p: 288-290 °C; IR (ν_{max}) cm^{-1}: 3197 (N–H_{str}), 3027 (C–H_{str}), 1560 (C=N_{str}) 1602 (Ar-C=C_{str}), 1060 (C–S_{str}); ^{1}H NMR (300 MHz, DMSO) δ 12.51 (s, 1H), 9.09 (s, 1H), 8.76 (d, J = 9.5 Hz, 1H), 8.51 (d, J = 8.2 Hz, 1H), 8.35 (dd, J = 8.0, 4.0 Hz, 4H), 8.22 (q, J = 9.0 Hz, 2H), 8.15 – 8.09 (m, 1H), 8.00 (d, J = 8.3 Hz, 2H), 7.73 (dd, J = 7.7, 5.5 Hz, 4H), 7.52 – 7.45 (m, 3H), 7.38 (t, J = 7.3 Hz, 1H). ^{13}C NMR (75 MHz, DMSO-d_6) δ 168.65, 140.58, 140.11, 139.58, 134.23, 131.80, 131.43, 131.11, 130.84, 130.08, 129.07, 128.55, 128.27, 127.94, 127.46, 126.95, 126.75, 126.32, 126.07, 125.77, 125.03, 124.76, 124.36, 122.87, 104.55; LC-MS calcd for $C_{32}H_{21}N_3S$ $[M + H]^+$ 479.15, found 480.02; Elemental Analysis: C, 80.14; H, 4.41; N, 8.76; S, 6.68.

(E)-4-(naphthalen-2-yl)-2-(2-(pyren-1-ylmethylene) hydrazineyl) thiazole **(4j)**

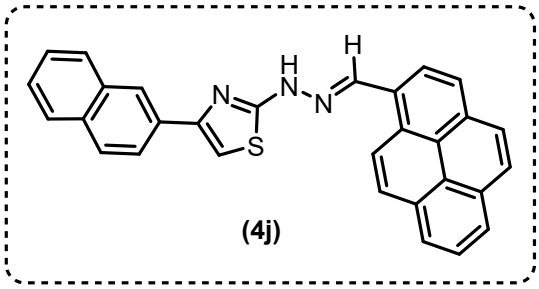

(4j)

Solid; Dark green color; Yield 90%; m.p: 287-289 °C; IR (ν_{max}) cm^{-1}: 3213 (N–H_{str}), 3025 (C–H_{str}), 1555 (C=N_{str}) 1602 (Ar-C=C_{str}), 1078 (C–S_{str}); ^{1}H NMR (300 MHz, DMSO-d_6) δ 12.52 (s, 1H),

9.09 (s, 1H), 8.78 (d, J = 9.4 Hz, 1H), 8.52 (d, J = 8.2 Hz, 1H), 8.44 (s, 1H), 8.39 – 8.32 (m, 5H), 8.23 (d, J = 5.1 Hz, 2H), 8.13 (d, J = 7.5 Hz, 1H), 7.98 (dd, J = 9.6, 5.4 Hz, 3H), 7.57 – 7.49 (m, 3H). ^{13}C NMR (75 MHz, DMSO-d_6) δ 168.68, 140.60, 133.67, 132.95, 131.81, 131.43, 130.71, 129.08, 128.35, 127.57, 127.00, 126.48, 126.08, 125.77, 125.07, 124.55, 122.89, 105.14; LC-MS calcd for $C_{30}H_{19}N_3S$ $[M + H]^+$ 453.13, found 454.02; Elemental Analysis: C, 79.44; H, 4.22; N, 9.26; S, 7.07.

(E)-2-(2-(pyren-1-ylmethylene) hydrazineyl)-4-(4-(trifluoro methoxy) phenyl) thiazole **(4k)**

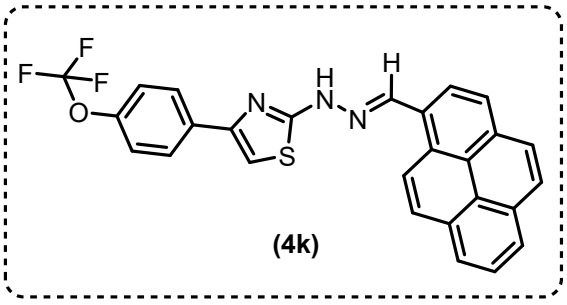

Solid; Drown color; Yield 92%; m.p: 276-278 °C; IR (ν_{max}) cm^{-1}: 3130 (N–H$_{str}$), 3034 (C–H$_{str}$), 1564 (C=N$_{str}$) 1630 (Ar-C=C$_{str}$), 1055 (C–S$_{str}$); ^{1}H NMR (300 MHz, DMSO-d_6) δ 12.54 (s, 1H), 9.07 (d, J = 3.7 Hz, 1H), 8.75 (d, J = 9.4 Hz, 1H), 8.50 (d, J = 8.2 Hz, 1H), 8.35 (dd, J = 7.9, 3.5 Hz, 4H), 8.23 (q, J = 9.0 Hz, 2H), 8.12 (t, J = 7.6 Hz, 1H), 8.03 (t, J = 5.9 Hz, 2H), 7.49 (s, 1H), 7.43 (d, J = 8.2 Hz, 2H). ^{13}C NMR (75 MHz, DMSO-d_6) δ 168.80, 140.71, 134.39, 131.83, 131.40, 130.68, 130.04, 129.15, 128.62, 128.28, 127.84, 127.51, 127.06, 126.45, 126.08, 125.75, 125.05, 124.73, 122.84, 121.58, 105.38; LC-MS calcd for $C_{27}H_{16}F_3N_3OS$ $[M + H]^+$ 487.10, found 488.02; Elemental Analysis: C, 66.25; H, 3.31; F, 11.09; N, 8.62; O, 3.28; S, 6.58.

(E)-2-(2-(pyren-1-ylmethylene) hydrazineyl)-4-(4-(trifluoromethyl) phenyl) thiazole **(4l)**

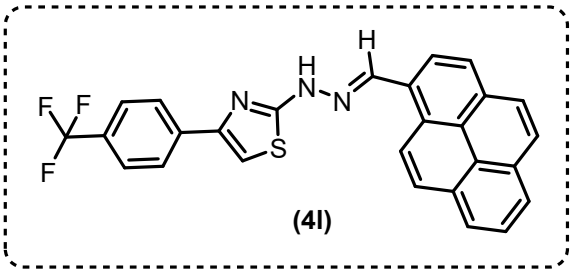

Solid; Dark brown color; Yield 91%; m.p: 279-281 °C; IR (ν_{max}) cm^{-1}: 3198 ($N–H_{str}$), 3012 ($C–H_{str}$), 1564 ($C=N_{str}$) 1621 ($Ar-C=C_{str}$), 1061 ($C–S_{str}$); ^1H NMR (300 MHz, DMSOd_6) δ 12.54 (s, 1H), 9.07 (d, J = 3.7 Hz, 1H), 8.75 (d, J = 9.4 Hz, 1H), 8.50 (d, J = 8.2 Hz, 1H), 8.35 (dd, J = 7.9, 3.5 Hz, 4H), 8.23 (q, J = 9.0 Hz, 2H), 8.12 (t, J = 7.6 Hz, 1H), 8.03 (t, J = 5.9 Hz, 2H), 7.49 (s, 1H), 7.43 (d, J = 8.2 Hz, 2H). 13C NMR (75 MHz, DMSO-d_6) δ 167.90, 148.68, 139.82, 137.82, 130.86, 130.42, 129.70, 128.74, 128.09, 127.44, 127.05, 126.90, 126.48, 125.57, 125.09, 124.75, 124.04, 123.74, 123.36, 106.13; LC-MS calcd for $C_{27}H_{16}F_3N_3S$ $[M + H]^+$ 471.10, found 472.46; Elemental Analysis: C, 68.78; H, 3.42; F, 12.09; N, 8.91; O, S, 6.80.

(E)-4-(4-fluoro-3-(trifluoromethyl) phenyl)-2-(2-(pyren-1-ylmethylene) hydrazineyl) thiazole **(4m)**

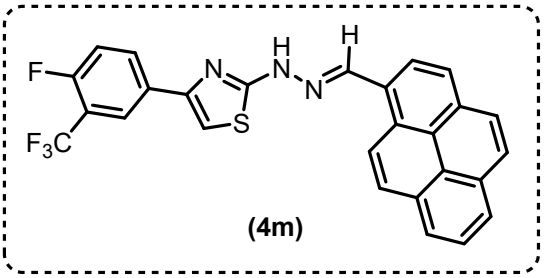

(4m)

Solid; Light brown color; Yield 93%; m.p: 285-287 °C; IR (ν_{max}) cm^{-1}: 3190 ($N–H_{str}$), 3025 ($C–H_{str}$), 1545 ($C=N_{str}$) 1618 ($Ar-C=C_{str}$), 1050 ($C–S_{str}$); ^1H NMR (300 MHz, DMSO) δ 12.54 (s, 1H), 9.04 (d, J = 5.9 Hz, 1H), 8.73 (d, J = 9.4 Hz, 1H), 8.48 (d, J = 8.2 Hz, 1H), 8.33 (dd, J = 7.7, 3.7 Hz, 4H), 8.27 – 8.18 (m, 4H), 8.10 (t, J = 7.6 Hz, 1H), 7.66 – 7.52 (m, 2H). ^{13}C NMR (75 MHz, DMSO-d_6) δ 168.96, 148.44, 140.99, 138.28, 132.29, 132.90, 131.42, 129.15, 128.59, 128.33, 127.91, 127.44, 127.10, 126.50, 126.12, 125.97, 125.78, 125.10, 124.74, 122.86, 106.01; LC-MS calcd for $C_{27}H_{15}F_4N_3S$ $[M + H]^+$ 490.40, found 489.49; Elemental Analysis: C, 66.25; H, 3.09; F, 15.53; N, 8.58; S, 6.55.

(E)-4-(2,4-difluorophenyl)-2-(2-(pyren-1-ylmethylene) hydrazineyl) thiazole **(4n)**

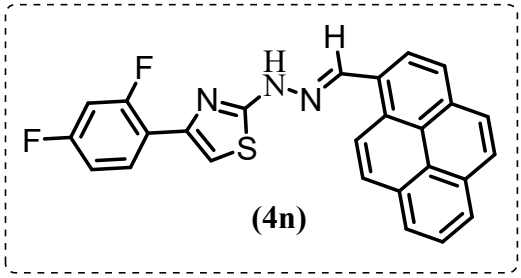

(4n)

Solid; Brown color; Yield 92%; m.p: 281-283 °C; IR (ν_{max}) cm^{-1}: 3214 ($N–H_{str}$), 2992 ($C–H_{str}$), 1540 ($C=N_{str}$) 1612 ($Ar\text{-}C=C_{str}$), 1075 ($C–S_{str}$); ^1H NMR (300 MHz, DMSO-d_6) δ 12.45 (s, 1H), 9.06 (s, 1H), 8.74 (d, J = 9.4 Hz, 1H), 8.49 (d, J = 8.2 Hz, 1H), 8.34 (dd, J = 6.9, 3.2 Hz, 4H), 8.21 (q, J = 9.0 Hz, 2H), 8.09 (m, 2H), 7.36 (m, 1H), 7.28 (d, J = 2.5 Hz, 1H), 7.20 (td, J = 8.5, 2.3 Hz, 1H). ^{13}C NMR (75 MHz, DMSO-d_6) δ 167.08, 143.07, 139.75, 130.84, 130.42, 129.70, 128.08, 127.56, 127.30, 126.90, 126.51, 126.08, 125.46, 125.08, 124.76, 124.01, 123.74, 123.36, 121.84, 104.04; LC-MS calcd for $C_{26}H_{15}F_2N_3S$ $[M + H]^+$ 439.10, found 440.05; Elemental Analysis: C, 71.06; H, 3.44; F, 8.65; N, 9.56; S, 7.29.

(E)-4-(3-fluorophenyl)-2-(2-(pyren-1-ylmethylene) hydrazineyl) thiazole **(4o)**

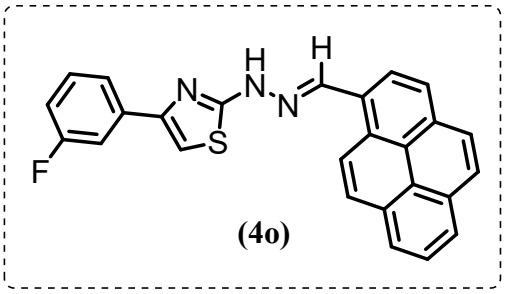

(4o)

Solid; Light green color; Yield 90%; m.p: 277-279 °C; IR (ν_{max}) cm^{-1}: 3237 ($N–H_{str}$), 2998 ($C–H_{str}$), 1560 ($C=N_{str}$) 1608 ($Ar\text{-}C=C_{str}$), 1052 ($C–S_{str}$); ^1H NMR (300 MHz, DMSO-d_6) δ 12.48 (s, 1H), 9.07 (s, 1H), 8.74 (d, J = 9.4 Hz, 1H), 8.49 (d, J = 8.2 Hz, 1H), 8.37 – 8.33 (m, 4H), 8.22 (d, J = 5.3 Hz, 2H), 8.14 – 8.08 (m, 1H), 7.76 (d, J = 7.9 Hz, 1H), 7.68 (dd, J = 7.1, 4.9 Hz, 1H), 7.54 (s, 1H), 7.47 (dd, J = 8.0, 6.4 Hz, 1H), 7.15 (m, 1H). ^{13}C NMR (75 MHz, DMSO-d_6) δ 168.68, 140.72, 137.47, 131.83, 131.55, 130.94, 130.69, 129.09, 128.55, 128.28, 127.90, 127.51, 127.06, 126.46, 126.08, 125.76, 125.01, 124.73, 124.35, 122.84, 122.07, 105.83; LC-MS calcd for $C_{26}H_{16}FN_3S$ $[M + H]^+$ 421.10, found 422.00; Elemental Analysis: C, 74.06; H, 3.83; F, 4.51; N, 9.97; S, 7.61.

Fig. S1. ^{1}H NMR Chemical shifts of compound **(4a)**

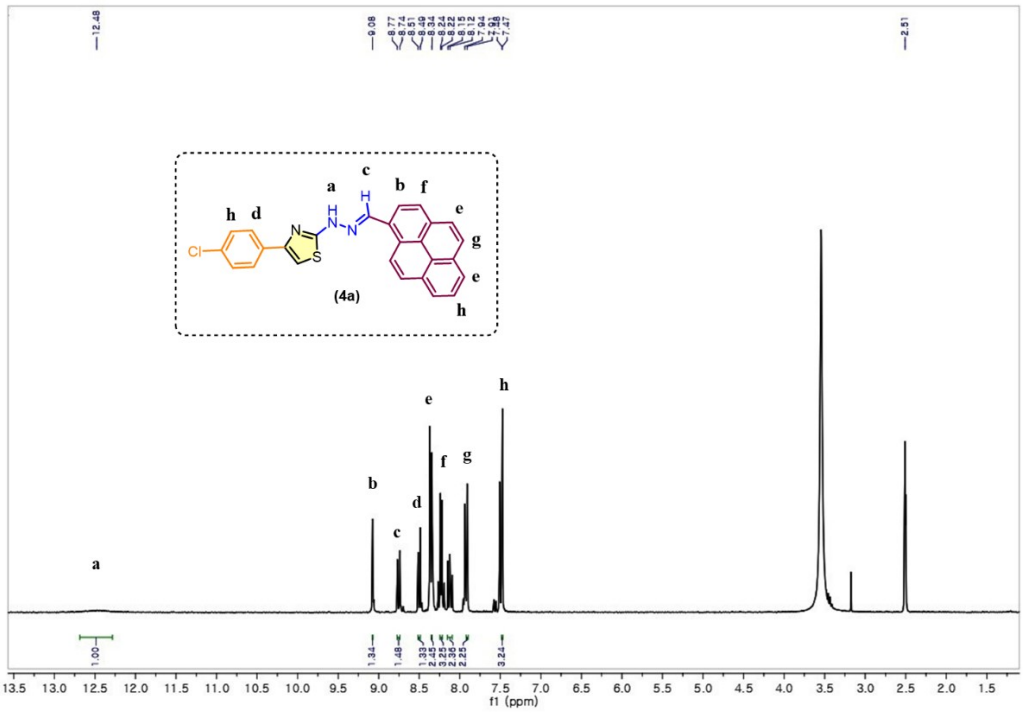

Fig. S2. ^{13}C NMR Chemical shifts of compound (**4a**)

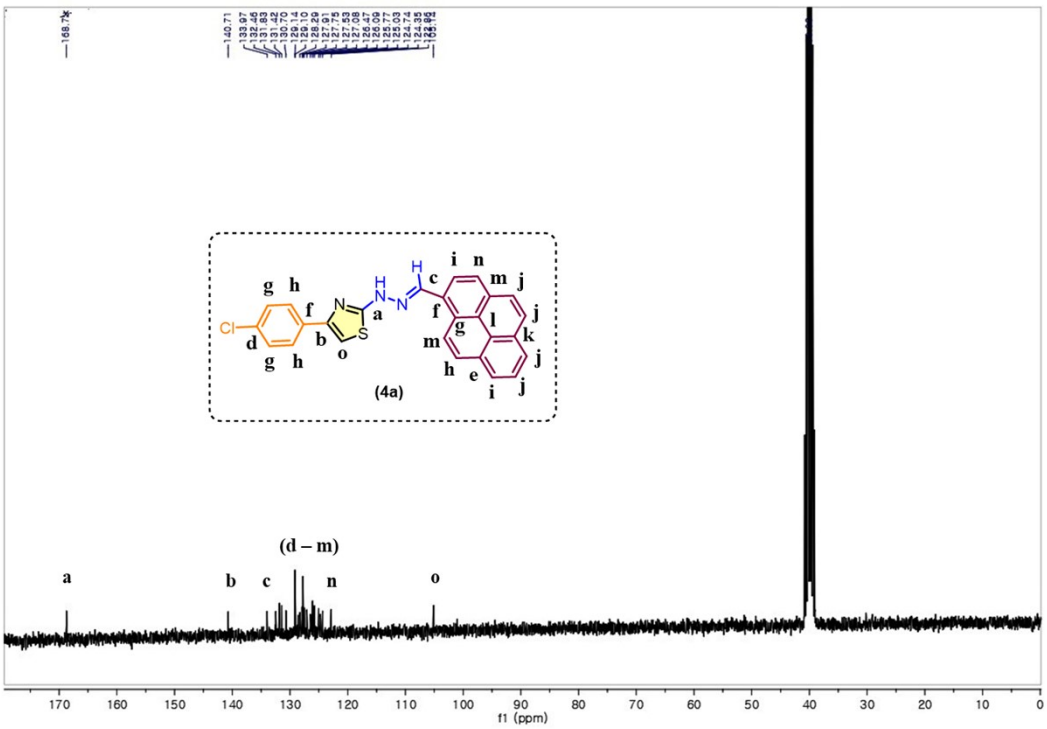

The structural confirmation and purity assessment of compound **4a** were supported by both IR and LC-MS analyses. The IR spectrum of compound **4a** displayed characteristic absorption bands corresponding to key functional groups. A broad band around 3330 cm^{-1} was attributed to N–H stretching of the hydrazone moiety, while bands in the 3050–3020 cm^{-1} range indicated aromatic C–H stretching. A prominent absorption between 1615–1590 cm^{-1} was assigned to C=N stretching, confirming the formation of the hydrazone linkage. Additional bands at 1500–1450 cm^{-1} and 1250–1150 cm^{-1} were associated with aromatic C=C and C–N stretching vibrations, respectively. The presence of a chloro substituent was supported by a peak in the 1100–1000 cm^{-1} region due to C–Cl stretching, and bands observed between 750–700 cm^{-1}. Further confirmation was obtained via LC-MS analysis, as shown in supporting information (**4a)**. The chromatogram revealed a major peak at a retention time of 4.92 minutes, accounting for approximately 94.57% of the total area, indicating high purity. The corresponding mass spectrum showed a dominant molecular ion peak at m/z 440.989, consistent with the $[M+H]^+$ ion of compound (**4a)**. Minor peaks at m/z 504.445 may represent sodium or potassium adducts, while peaks at m/z 848.256 and 941.281 could be attributed to dimeric species or instrumental artifacts. The high-resolution mass data and strong base peak intensity further confirmed the successful synthesis and structural integrity of compound (**4a)**. Collectively, these analytical results validate the purity and identity of compound (**4a)**, supporting its suitability for further structural and biological studies. The structural elucidation of compound **4a** was confirmed by detailed ^1H and ^{13}C NMR spectral analysis recorded at (300 MHz in DMSO-d_6). In the ^1H NMR spectrum (**Fig. S1**), a clear broad peak was seen at (δ 12.48 ppm), which is due to the NH proton of the hydrazone part, and it appears further down the scale because of hydrogen bonding and electronic effects. A characteristic singlet at δ 9.08 ppm was assigned to the methine proton (HC=N) of the azomethine linkage, further confirming its formation. The aromatic region δ 7.47–8.77 ppm, exhibited multiple signals corresponding to the protons of the pyrene-1-carbaldehyde and phenyl rings, showing a pattern consistent with the substitution and conjugation effects in the aromatic system. In the ^{13}C NMR spectrum (100 MHz) displayed well-resolved signals for all carbon environments in compound **4a** (**Fig. S2**). The azomethine carbon (C=N) appeared as a deshielded signal at δ 168.79 ppm, consistent with its electron-deficient character. Aromatic carbon signals were observed within the expected range of δ 105.14–140.71 ppm, including both quaternary (non-protonated) and protonated sp^2-hybridized carbons of the polycyclic and substituted aromatic systems.

This spectral profile agrees with the proposed structure, confirming the successful formation and structural integrity of compound **4a**. Additionally, the structures of the fluorinated derivatives (**4e**, **4k-4o**) were confirmed by ^{19}F NMR spectroscopy, which revealed distinct signals corresponding to the type and position of fluorine substituents. Compound **4e** showed a single peak at δ –114.52 ppm, which is typical for a monofluorophenyl group, while compound **4k** had a peak at δ –56.67 ppm from the trifluoromethoxy group. For compound **4l**, a peak at δ –60.85 ppm confirmed a para-trifluoromethyl group. Compound **4m** had two peaks at δ –60.32 and –115.14 ppm, linked to CF_3 and F atoms, respectively. Single signals were seen at δ –109.80 ppm and –113.08 ppm for compounds **4n** and **4o**, which match the expected patterns for para- and meta-fluorinated aryl rings. Overall, the ^{19}F NMR data confirm that the fluorinated groups were successfully added and support the findings from the **^{1}H** and **^{13}C NMR** spectra in verifying the identity and purity of these made derivatives.

Materials and methods

All of the reagents and solvents were pure and were acquired from Sigma Aldrich in Bangalore, Karnataka, India. A Bruker-300 spectrometer was used to obtain nuclear magnetic resonance (NMR, Bruker-300 spectrometer at 300 MHz, Germany) spectra for ^{1}H and ^{13}C in a deuterated dimethyl sulfoxide (DMSO-d6). A Bruker Vector 22 spectrometer was used to record Fourier-transform infrared (FT-IR, Bruker Vector 22 spectrometer, New York, NY, USA) spectra with a resolution of 4 cm^{-1} throughout a 400–4000 cm^{-1} range. A liquid chromatography–quadrupole ion trap mass spectrometer (LC-QIT-MS) with an electrospray ionisation source (Thermo Finnigan, San Jose, CA, USA) was used to record the mass spectra. Automatic melting points (Stuart SMP40) were used to record melting points. The chemicals' purity and the status of the reaction were examined using a G plate of silica gel TLC (Merck, Germany). All melting points are uncorrected and were measured with open capillaries on an Electrothermal-9100 (Japan) device. At Gyeongsang National University's Department of Veterinary Medicine, Research Institute of Life Science, Republic of Korea, cytotoxic activities and measurements were conducted. The MCF-7 human breast cell line was collected from the Korea cell line bank. Gibco (BRL Life Technologies, Grand Island, NY, USA) supplied the fetal bovine serum (FBS), antibiotics penicillin/ streptomycin (P/S), phosphate-buffered saline (PBS), and ‘Dulbecco’s modified ‘Eagle’s medium (DMEM).

Computational methods

Using SwissTargetPrediction, possible macromolecular targets were found for 15 synthesised compounds [56,57]. Monoamine oxidase A (MAO-A) was found to be a significant target. Neurological diseases and the advancement of cancer are associated with the dysregulation of MAO-A, a flavin-dependent mitochondrial enzyme that catalyses the oxidative deamination of monoamine neurotransmitters, including serotonin, norepinephrine, and dopamine [58]. MAO-A coupled to the clorgyline crystal structure (PDB ID: 1O5W, 3.2 Å resolution) was used for molecular docking experiments [59]. Protein preparation involved removal of crystallographic water and irrelevant heteroatoms, retention of the FAD cofactor, addition of hydrogen atoms at physiological pH, and CHARMm-based minimization[60]. The active site was defined around the co-crystallized clorgyline, and ligand preparation included protonation and tautomer optimization at pH 7.4. Docking was carried out using the CDOCKER algorithm, which generated multiple

ligand conformations ranked by interaction energy[61]. Key residues involved in ligand binding included Tyr69, Ile180, Phe208, Gln215, Tyr407, and Tyr444, supporting hydrophobic and π–π stacking interactions, while Asn181 and Gln215 contributed potential hydrogen bonds. The FAD isoalloxazine ring was also preserved as a critical catalytic site. Redocking of clorgyline reproduced its binding pose with RMSD < 2.0 Å, validating the protocol. The synthesized compounds showed favorable docking scores and stable interactions, suggesting promising inhibitory potential against MAO-A.

In Vitro Cytotoxicity Assay

The conventional MTT assay was used to assess the produced compounds cytotoxicity *in vitro*. Using the specified chemicals, the MCF-7 breast cancer cell line was treated (**4g**, **4h**, **4j**, **4k**, **4l**, **4m**, **4n**). In summary, MCF-7 cells were seeded in 48-well plates at a density of 3×10^4 cells per well. They were then treated for 24 hours with either vehicle control (dimethyl sulfoxide, DMSO) or each of the following compounds: (0, 1.56, 3.125, 6.25, 12.5, 25, 50, and 100 μM). Each well received an MTT solution, which was then incubated for two hours at 37 °C. Following incubation, the purple formazan crystals that resulted were dissolved in 200 μL of DMSO after the supernatants were carefully removed. A PowerWave HT microplate spectrophotometer (BioTek, Winooski, VT, USA) was used to detect absorbance at 540 nm after the plates had been shaken for 15 minutes. In GraphPad version 8.0.2, Bonferroni-adjusted multiple comparisons were used for statistical analyses.

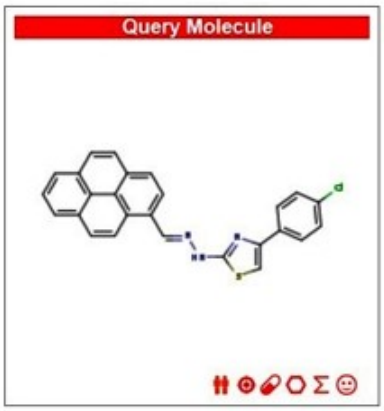

Export results:

Show 15 entries Search:

Target	Common name	Uniprot ID	ChEMBL ID	Target Class	Probability*	Known actives (3D/2D)
Monoamine oxidase B	MAOB	P27338	CHEMBL2039	Oxidoreductase		131 / 222
Monoamine oxidase A	MAOA	P21397	CHEMBL1951	Oxidoreductase		79 / 136
Dihydroorotate dehydrogenase	DHODH	Q02127	CHEMBL1966	Oxidoreductase		17 / 3
Hexokinase type IV	GCK	P35557	CHEMBL3820	Enzyme		120 / 0
Neuropeptide Y receptor type 2	NPY2R	P49146	CHEMBL4018	Family A G protein-coupled receptor		49 / 0
Hypoxia-inducible factor 1 alpha	HIF1A	Q16665	CHEMBL4261	Transcription factor		17 / 0
Cannabinoid receptor 2	CNR2	P34972	CHEMBL253	Family A G protein-coupled receptor		900 / 0
Adenosine kinase	ADK	P55263	CHEMBL3589	Enzyme		26 / 0
MAP kinase p38 alpha	MAPK14	Q16539	CHEMBL260	Kinase		572 / 0

Fig. S3. Target predicted for compound by SwissTargetPrediction online tool

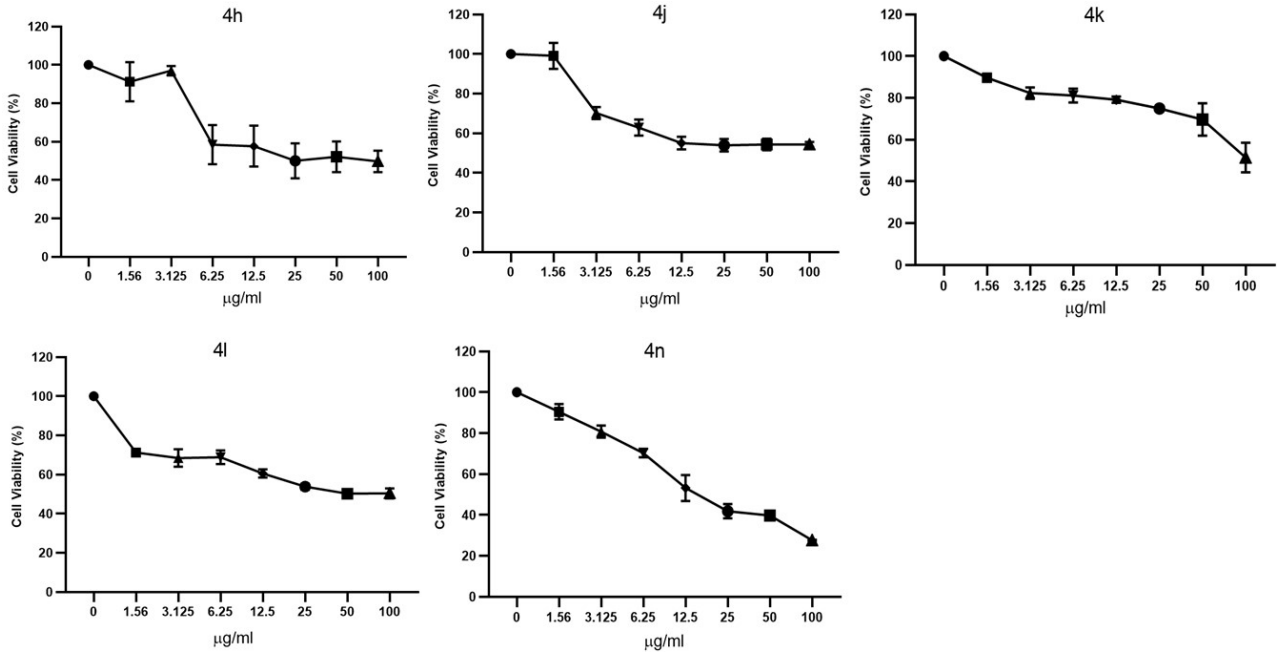

Fig. S4. Cytotoxic effects of compounds **4h**, **4j**, **4k**, **4l** and **4n** on the MCF-7 breast cancer cells.

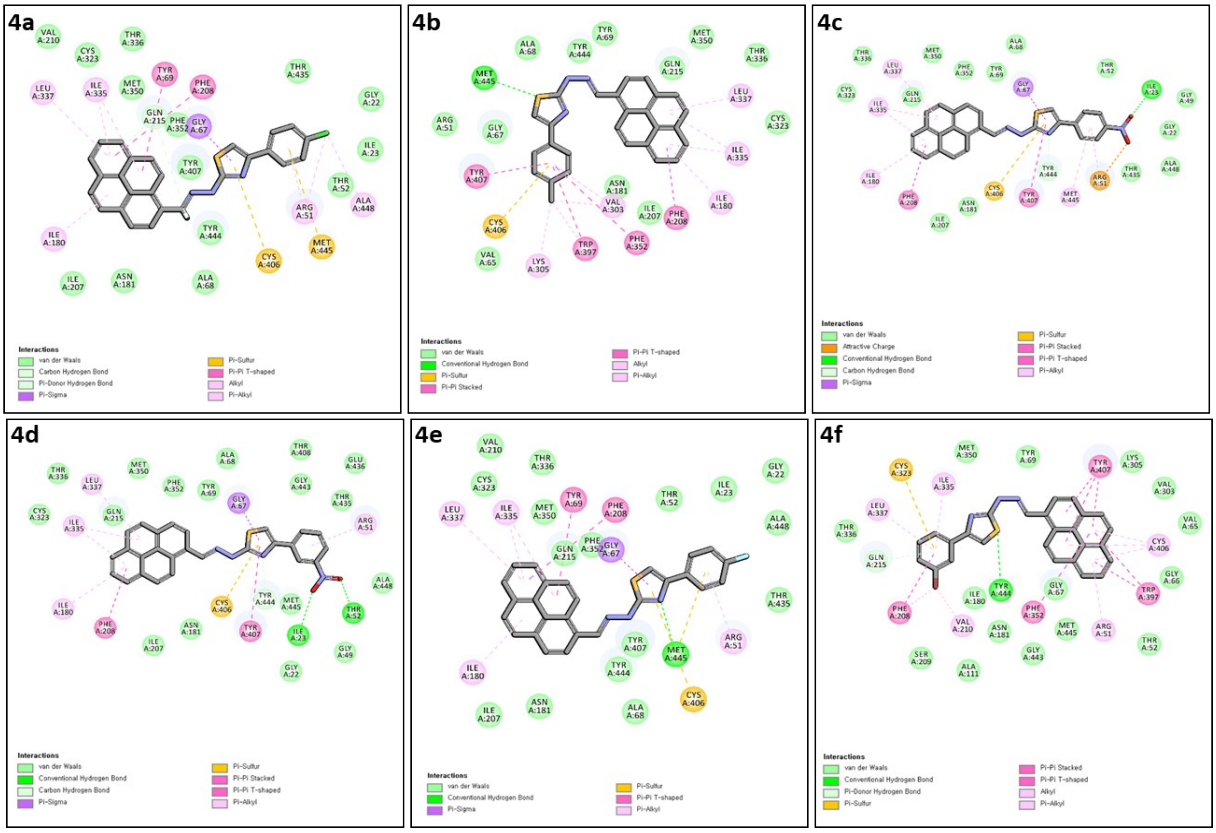

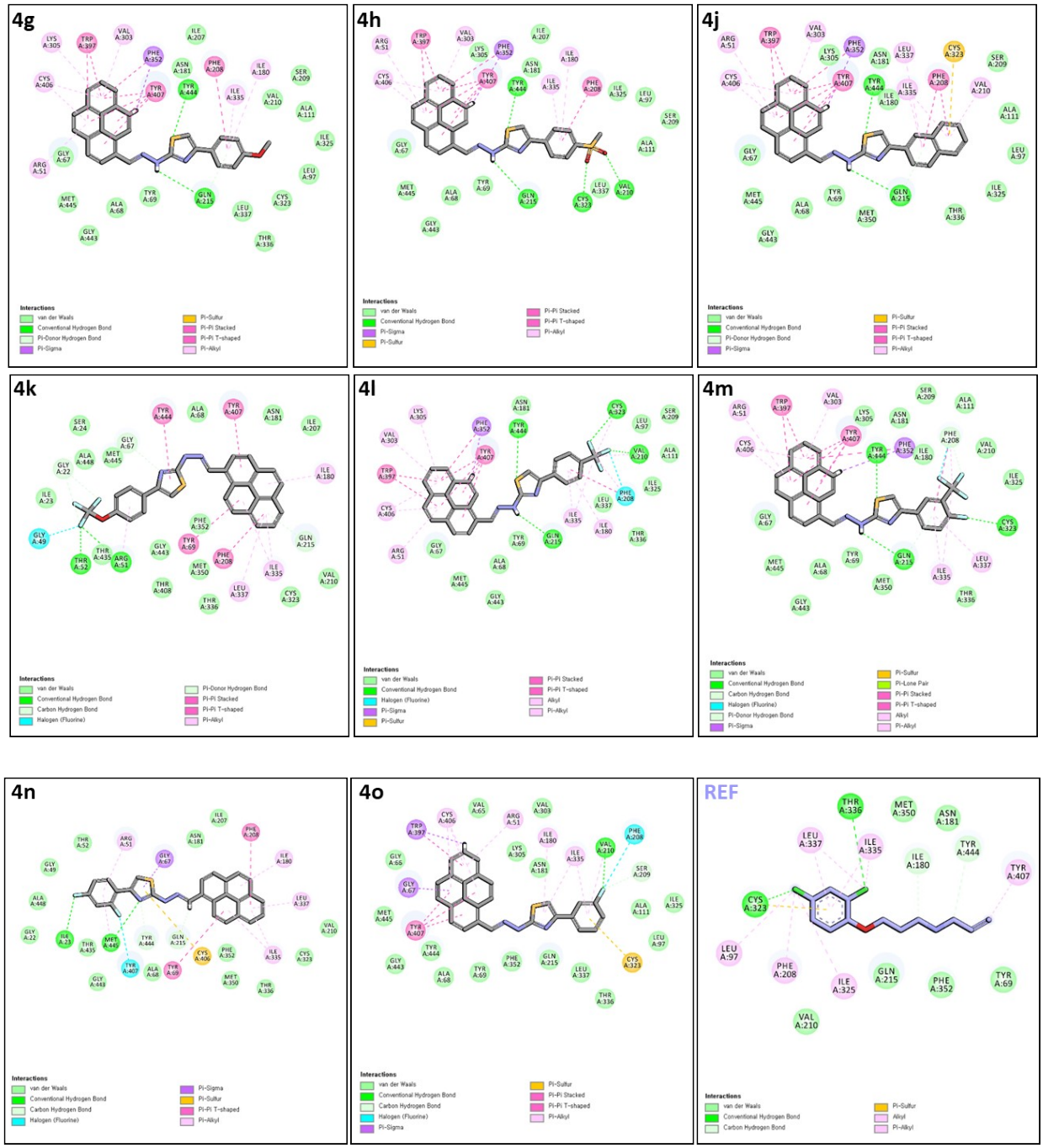

Fig. S5. Molecular docking 2D interaction maps of synthesized compounds (**4a-4o**) and the reference compound. Hydrogen bonds are shown as green lines, while hydrophobic contacts are indicated in orange.

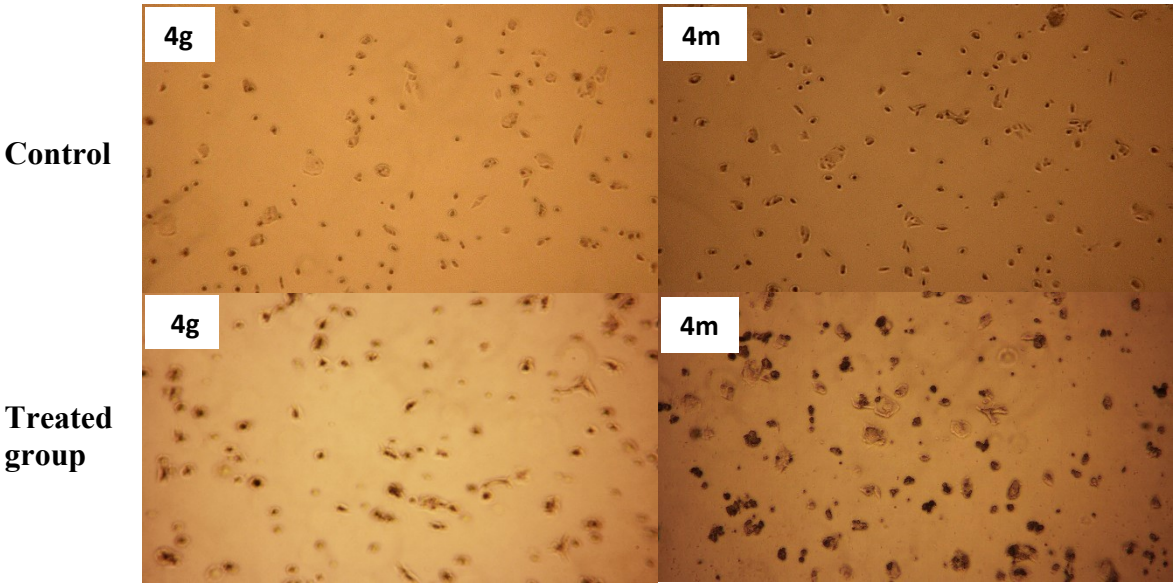

Fig. S6. Cytotoxic efficiency of the synthesized compounds (**4g)** and (**4m)** against (MCF-7) Cell line

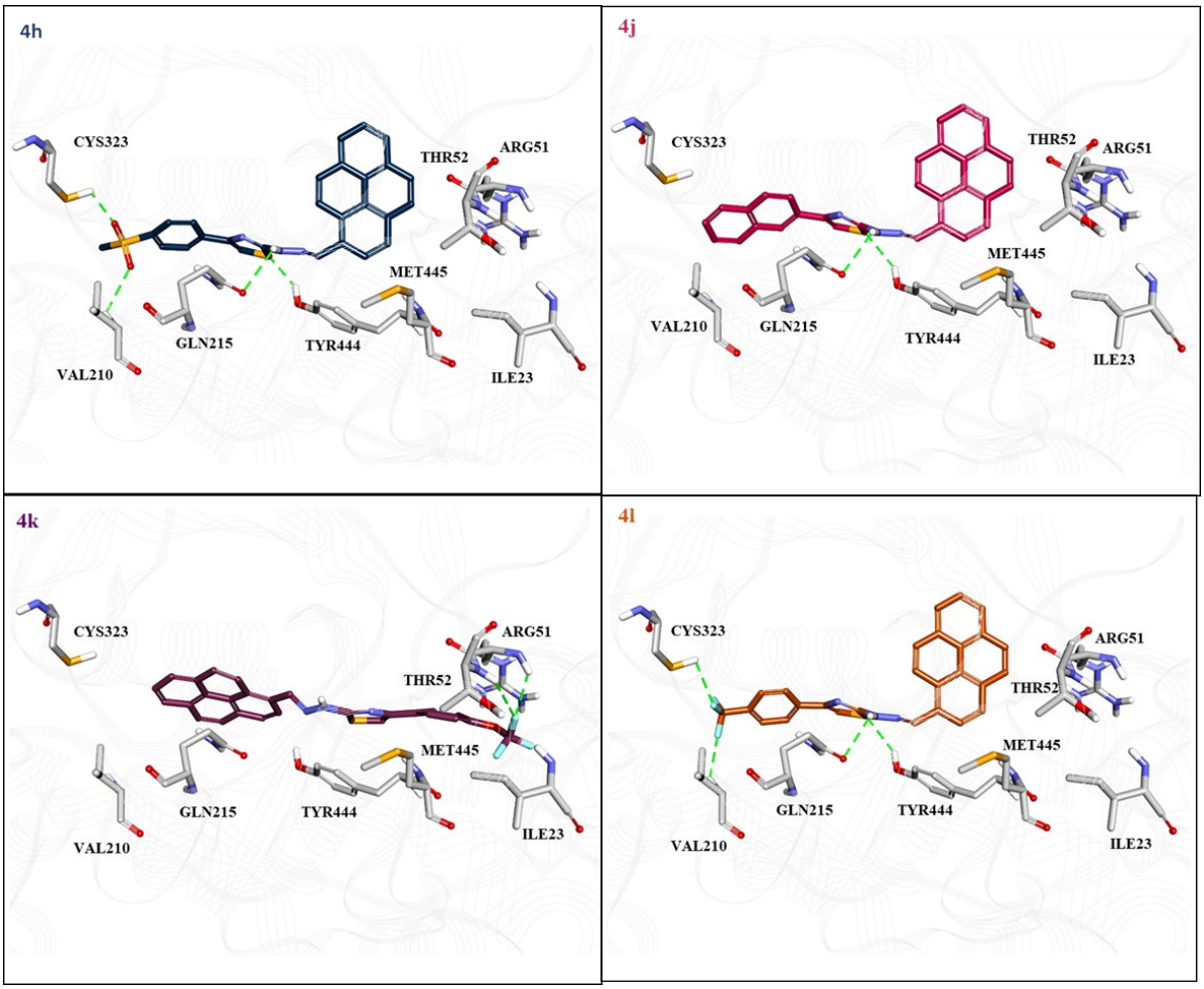

Fig. S7. Molecular docking 3D interaction maps of synthesized compounds (**4h**, **4j**, **4k**, and **4l**)

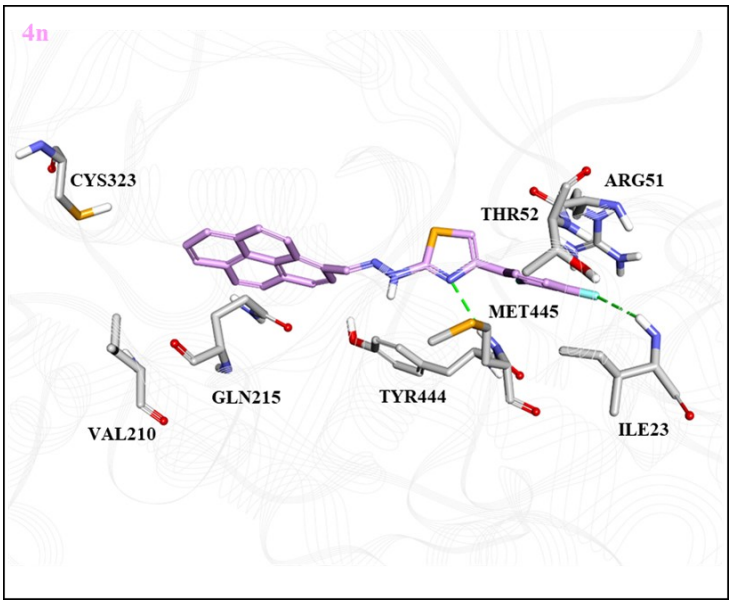

Fig. S8. Molecular docking 3D interaction maps of synthesized compound (**4n)**

Fig. S9. ^{1}H NMR and Fig. S10. ^{13}C NMR spectra of (4a)

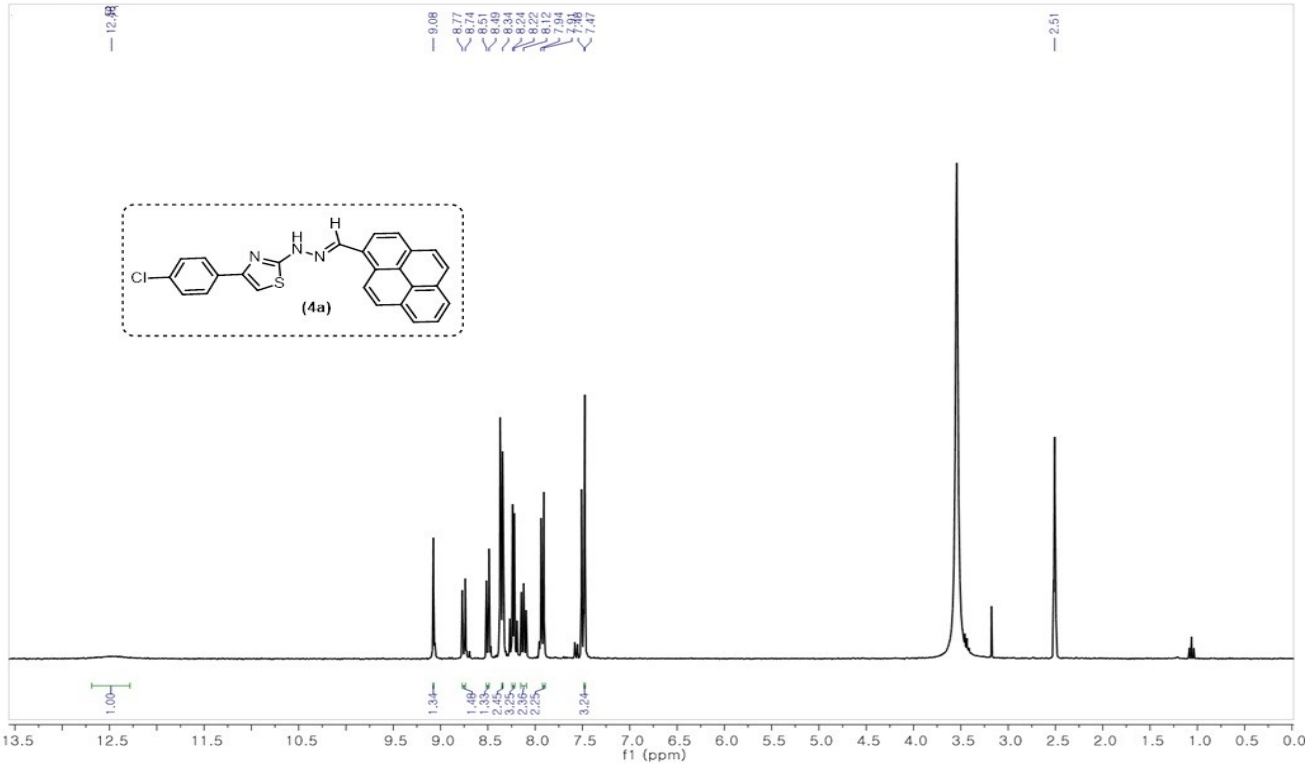

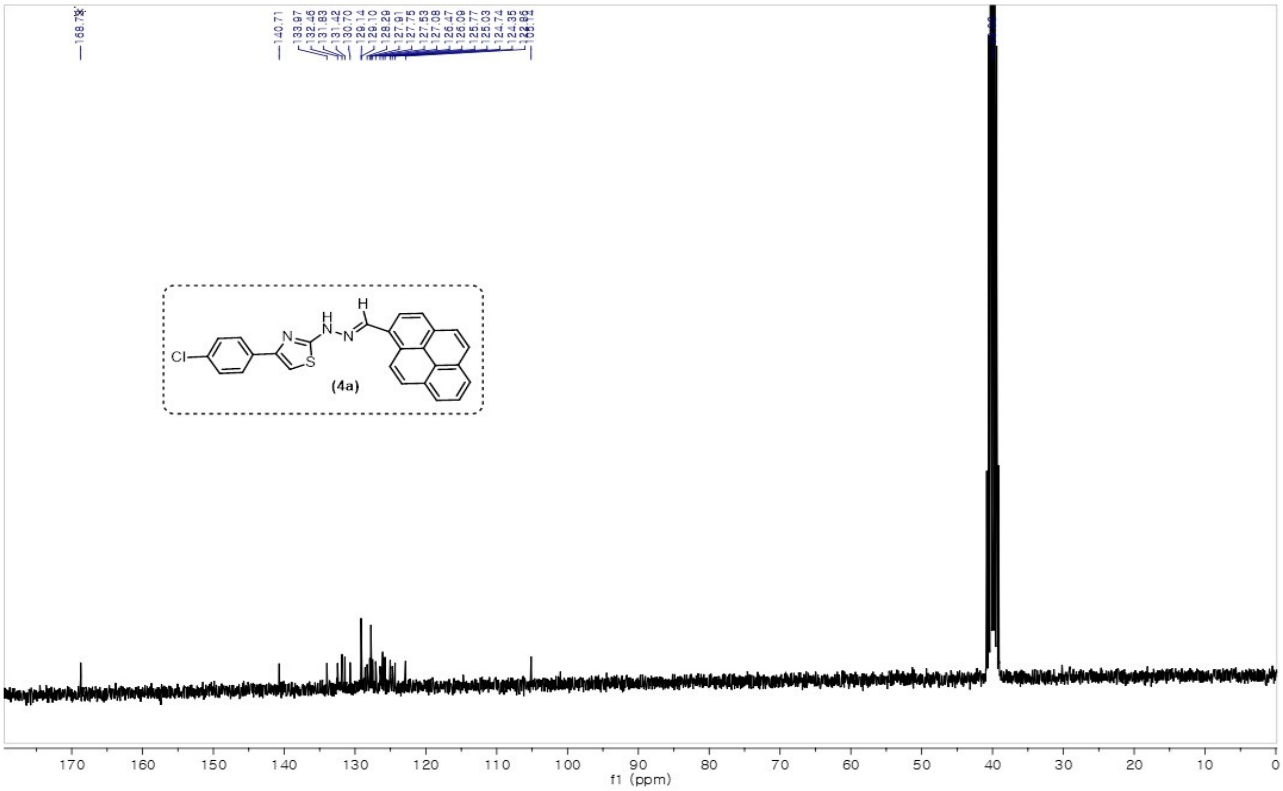

Fig. S11. IR Spectrum of compound (4a)

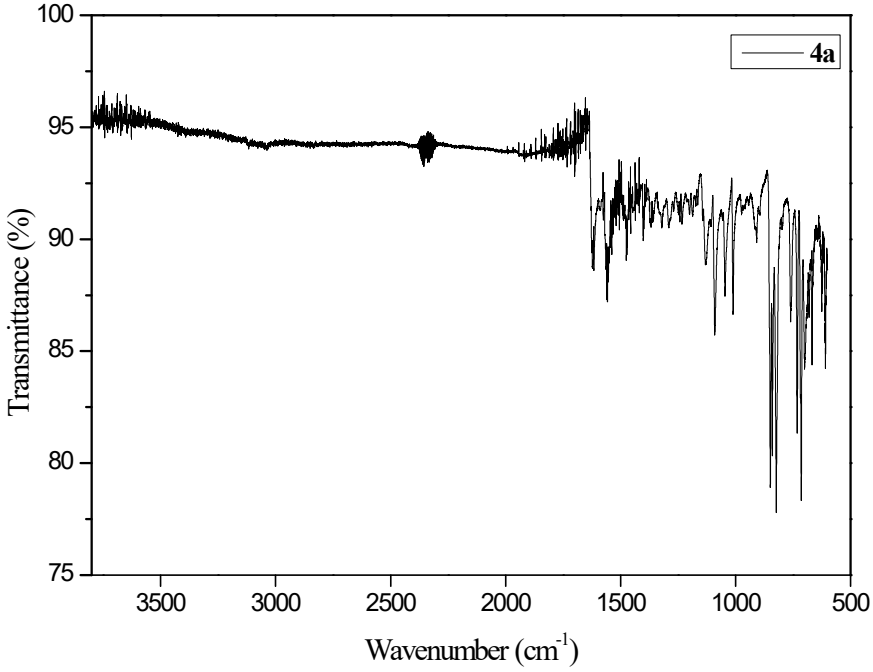

Fig. S12. LC-MS data of compound (4a)

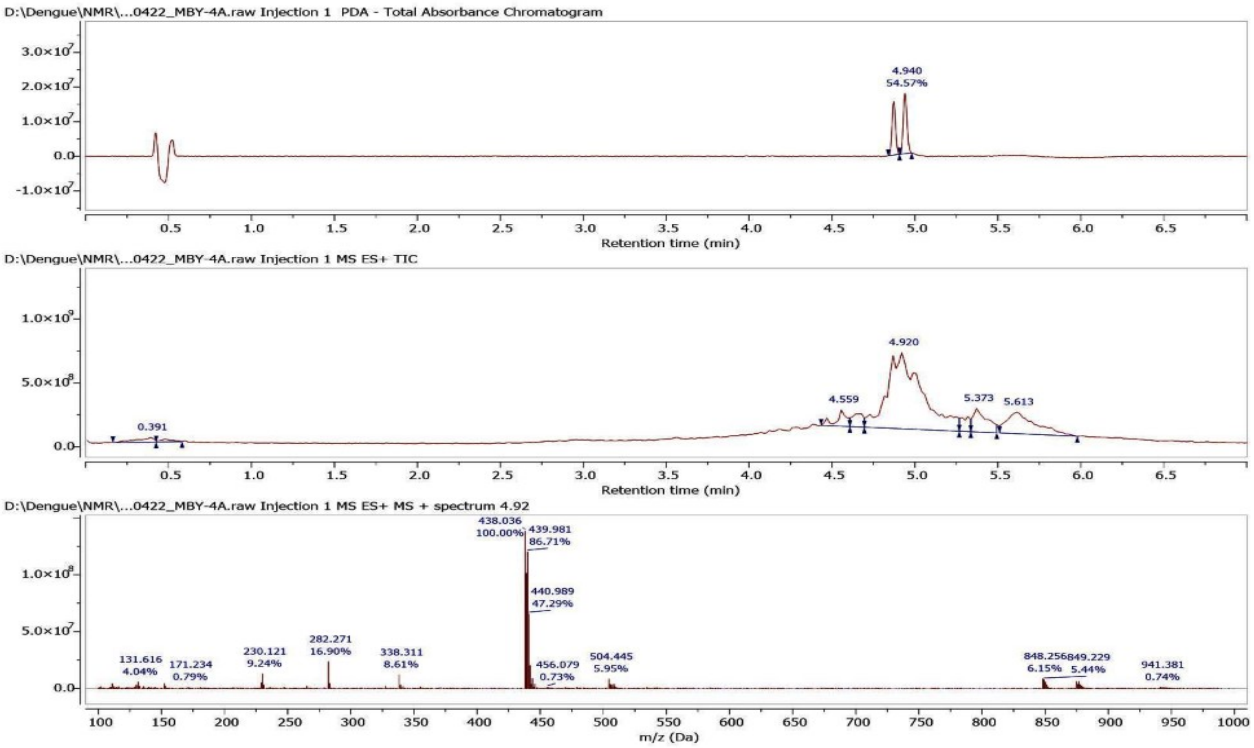

Fig. S13. ^{1}H NMR and Fig. S14. ^{13}C NMR spectra of (4b)

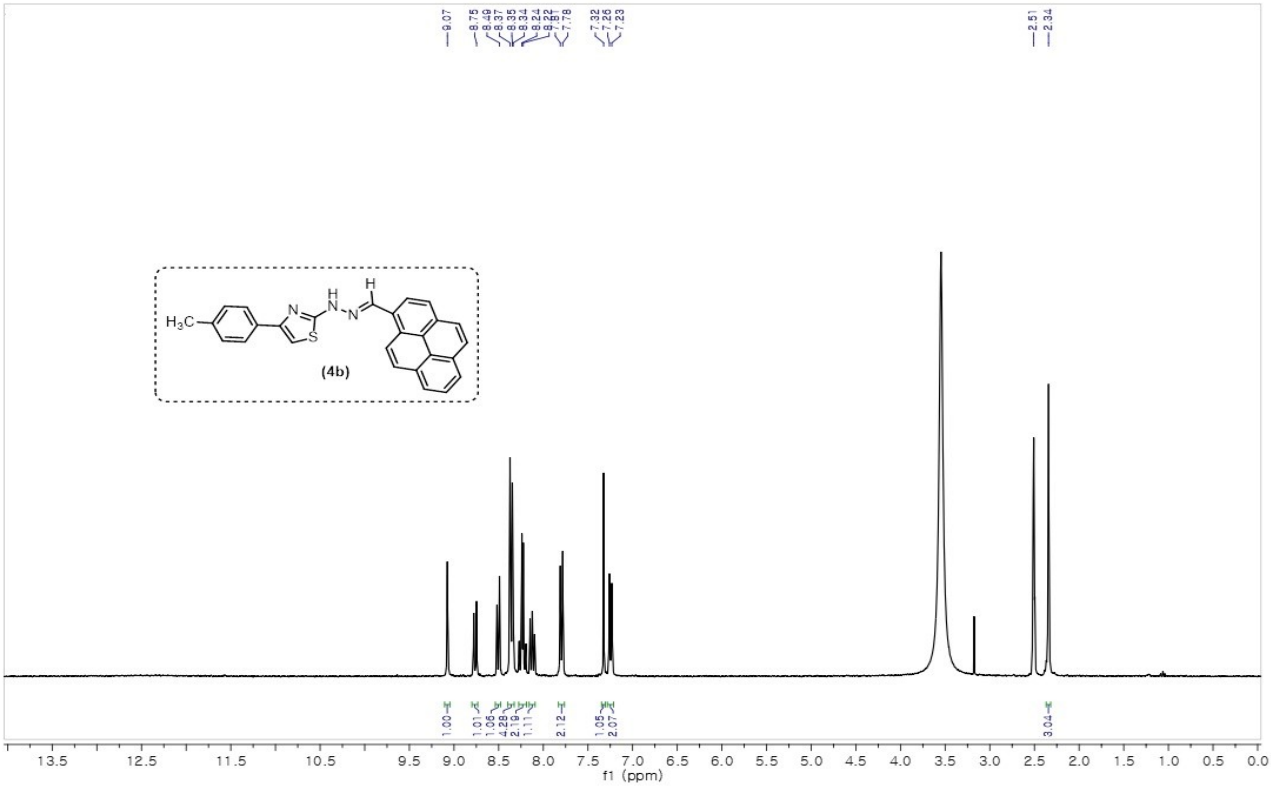

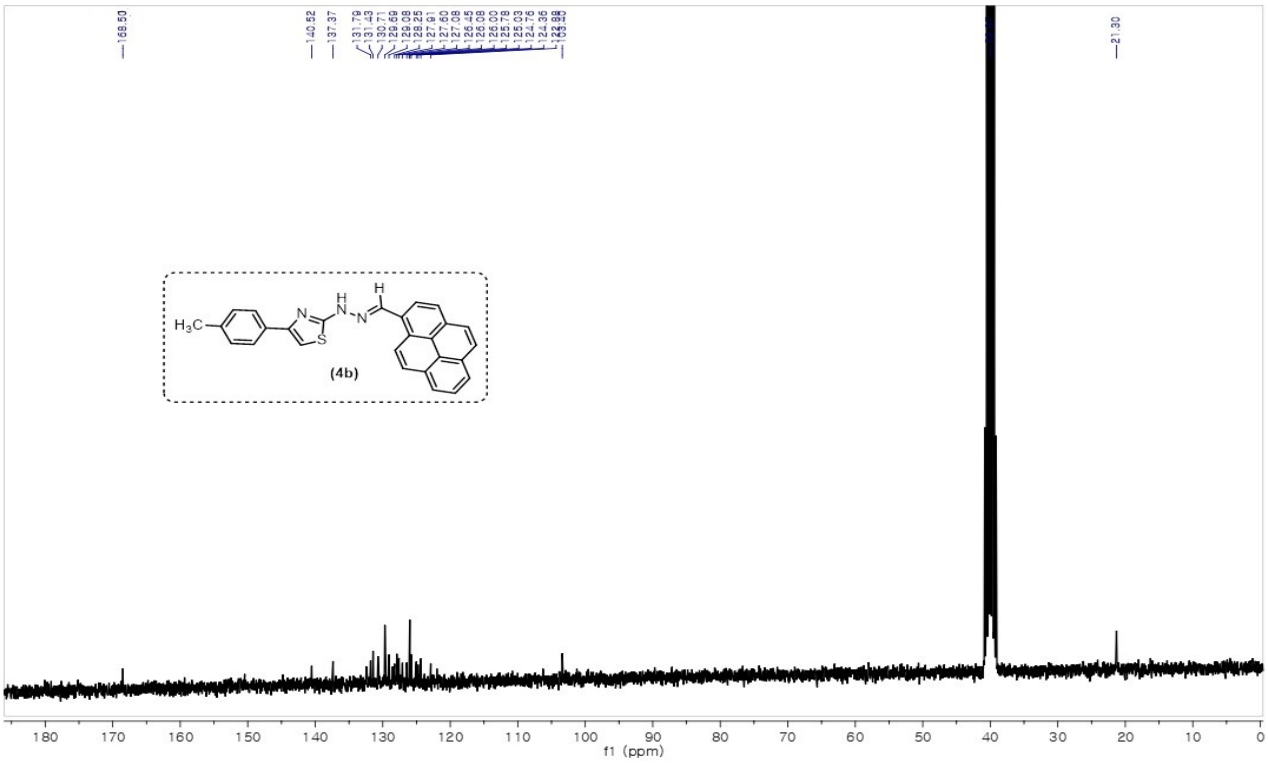

Fig. S15. IR Spectrum of compound (4b)

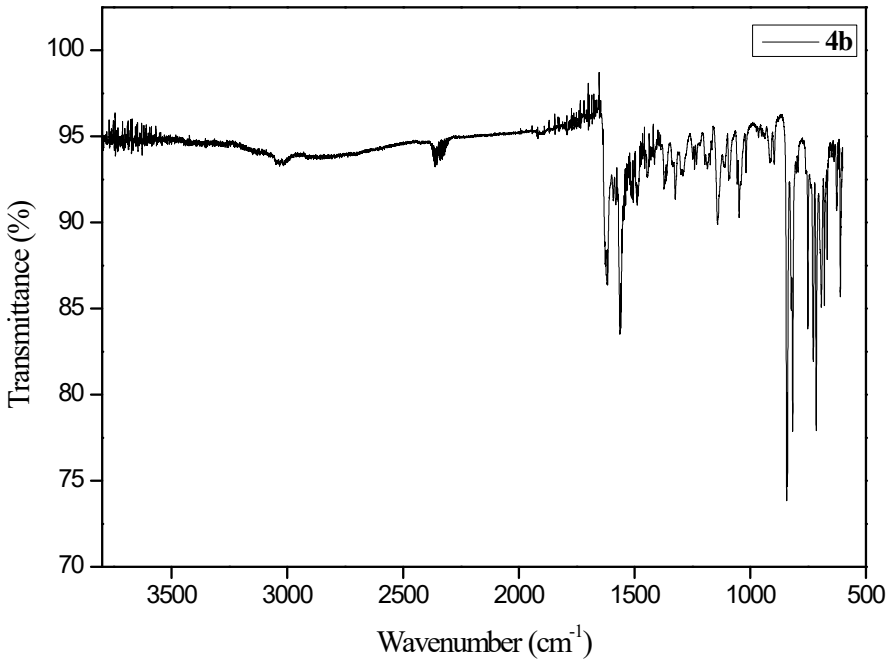

Fig. S16. LC-MS data of compound (4b)

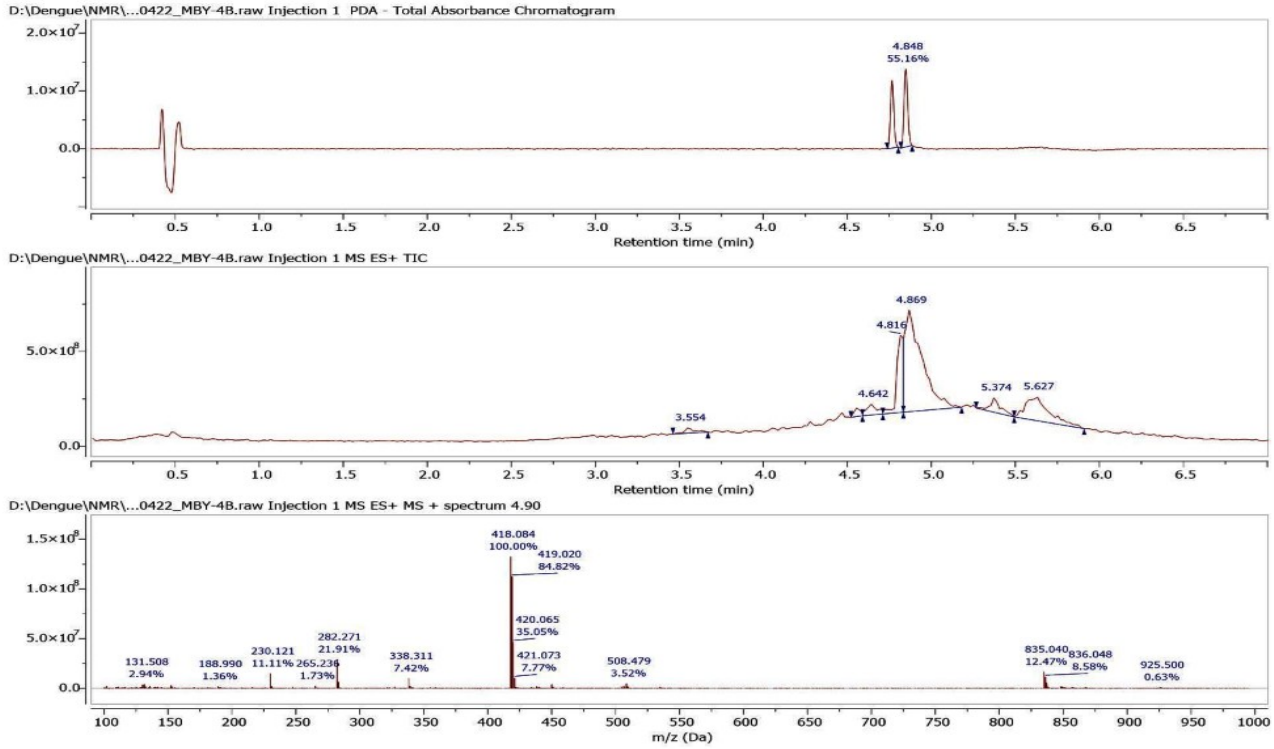

Fig. S17. ^{1}H NMR and Fig. S18. ^{13}C NMR spectra of (4c)

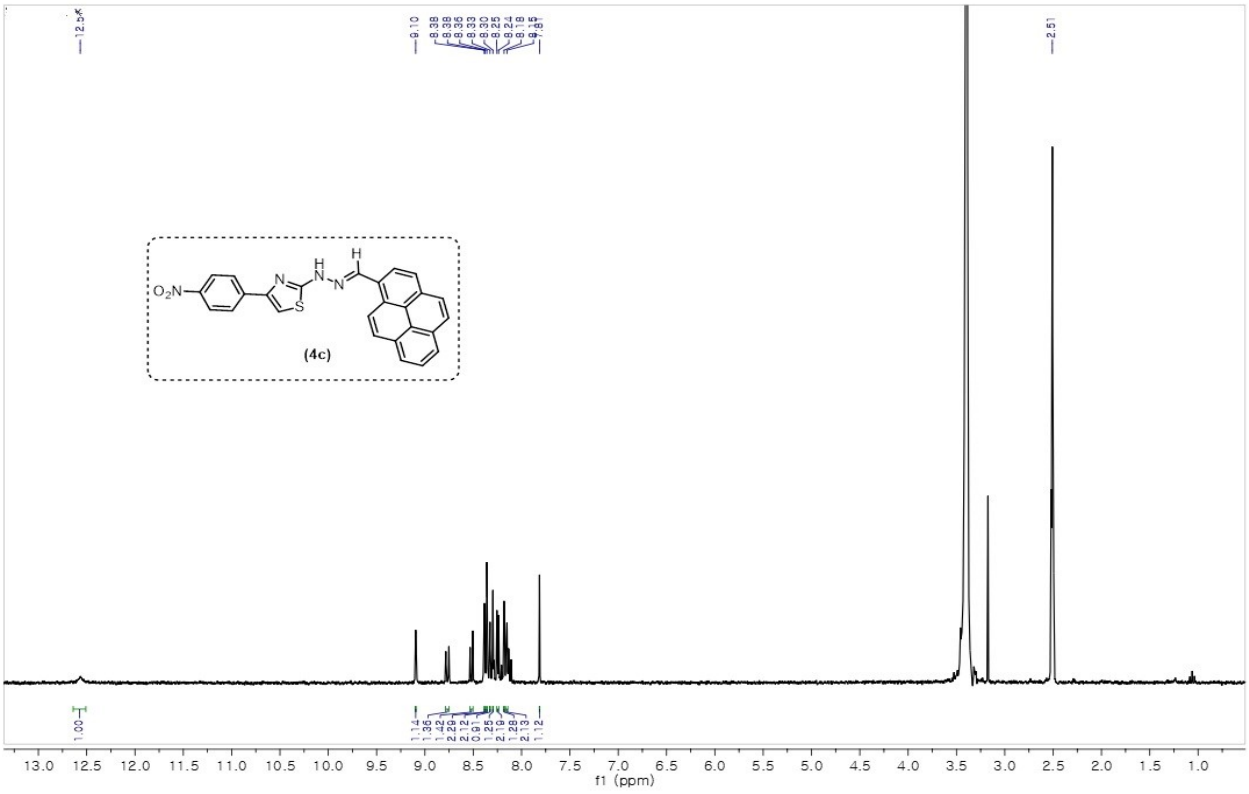

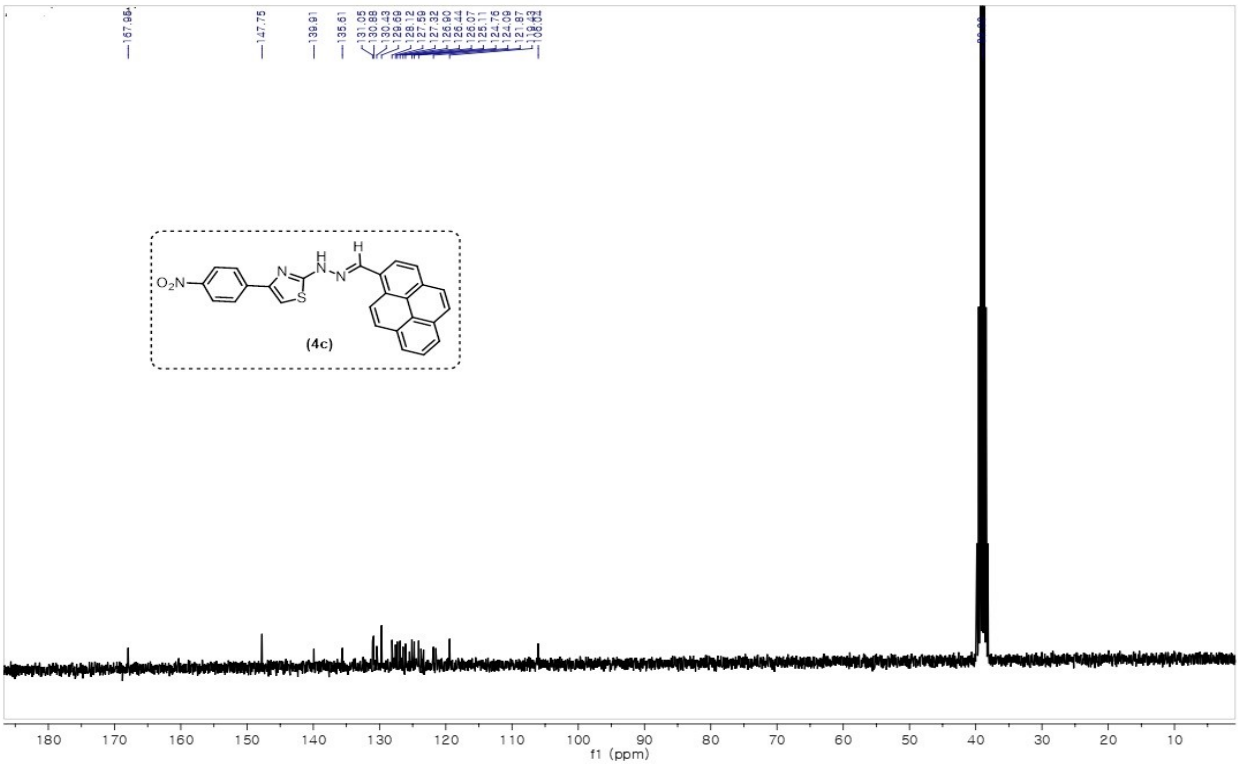

Fig. S19. IR Spectrum of compound (4c)

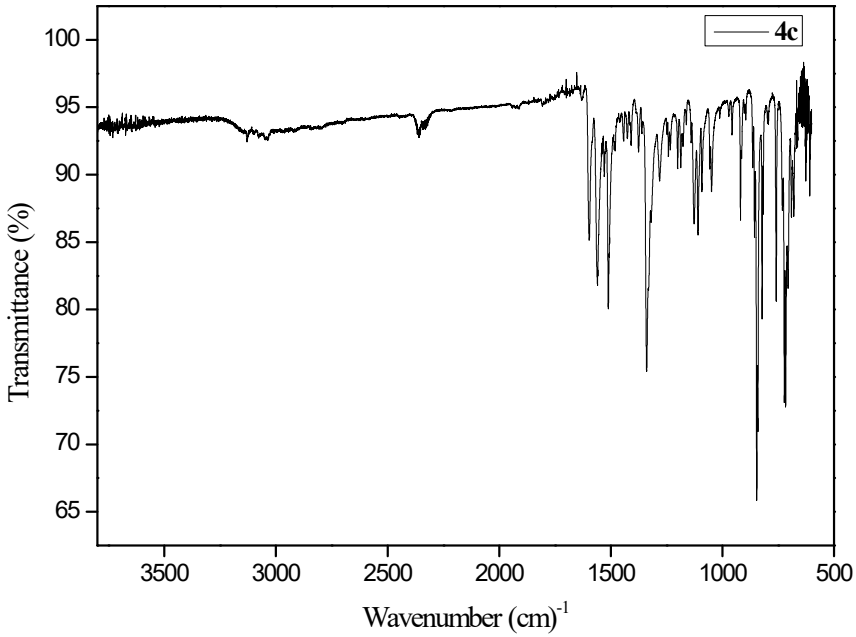

Fig. S20. LC-MS data of compound (4c)

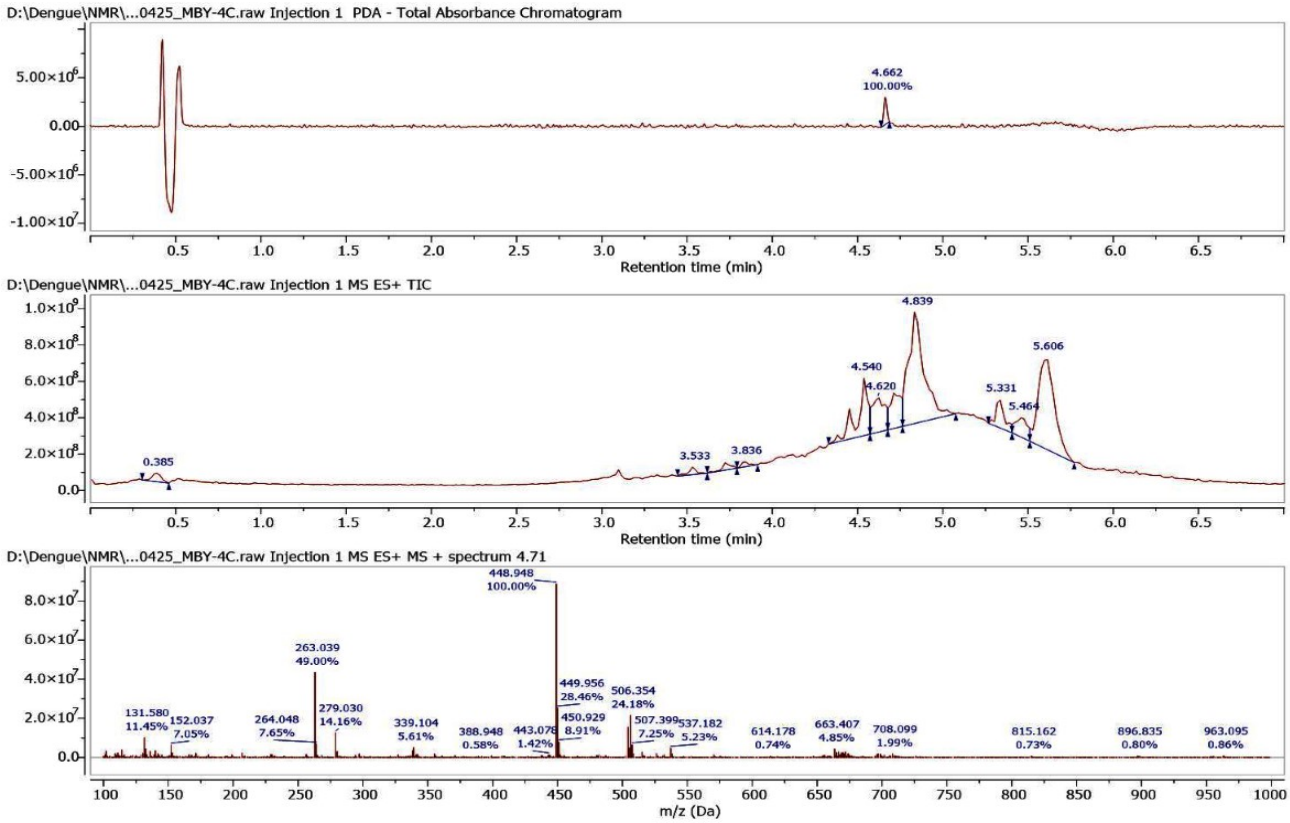

Fig. S21. ^{1}H NMR and Fig. S22. ^{13}C NMR spectra of (4d)

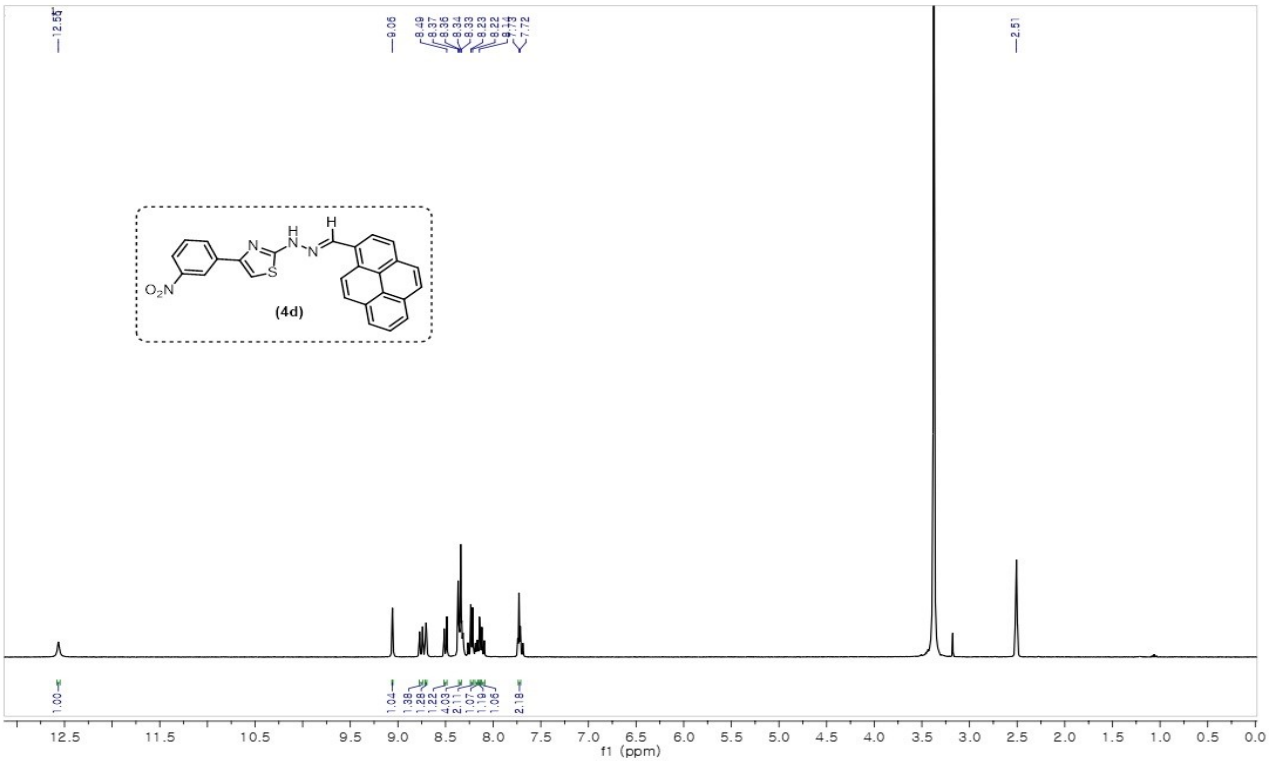
(4d)
f1 (ppm)

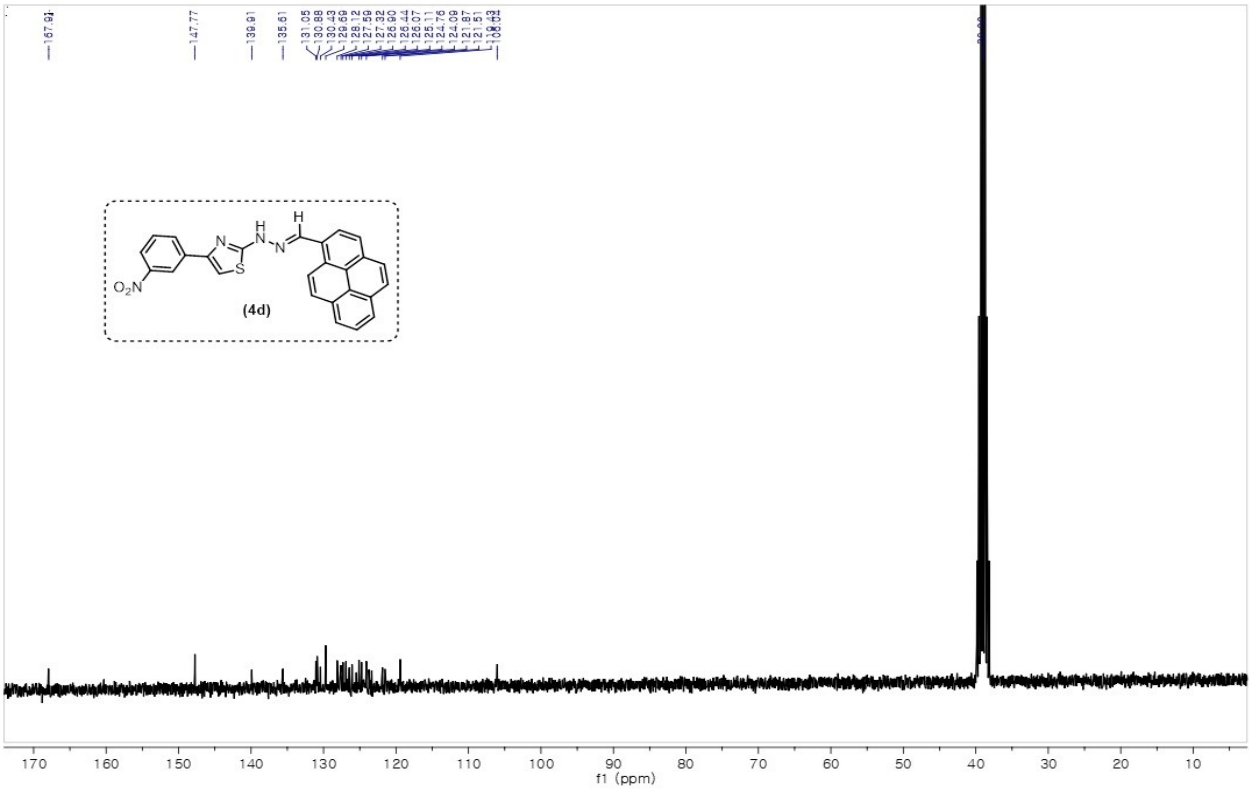
(4d)
f1 (ppm)

Fig. S23. IR Spectrum of compound (4d)

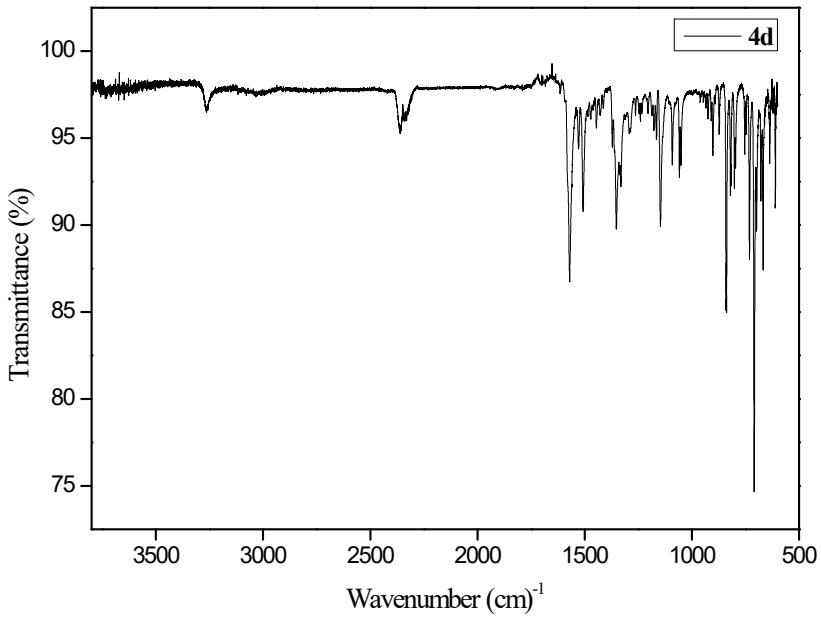

Fig. S24 LC-MS data of compound (4d)

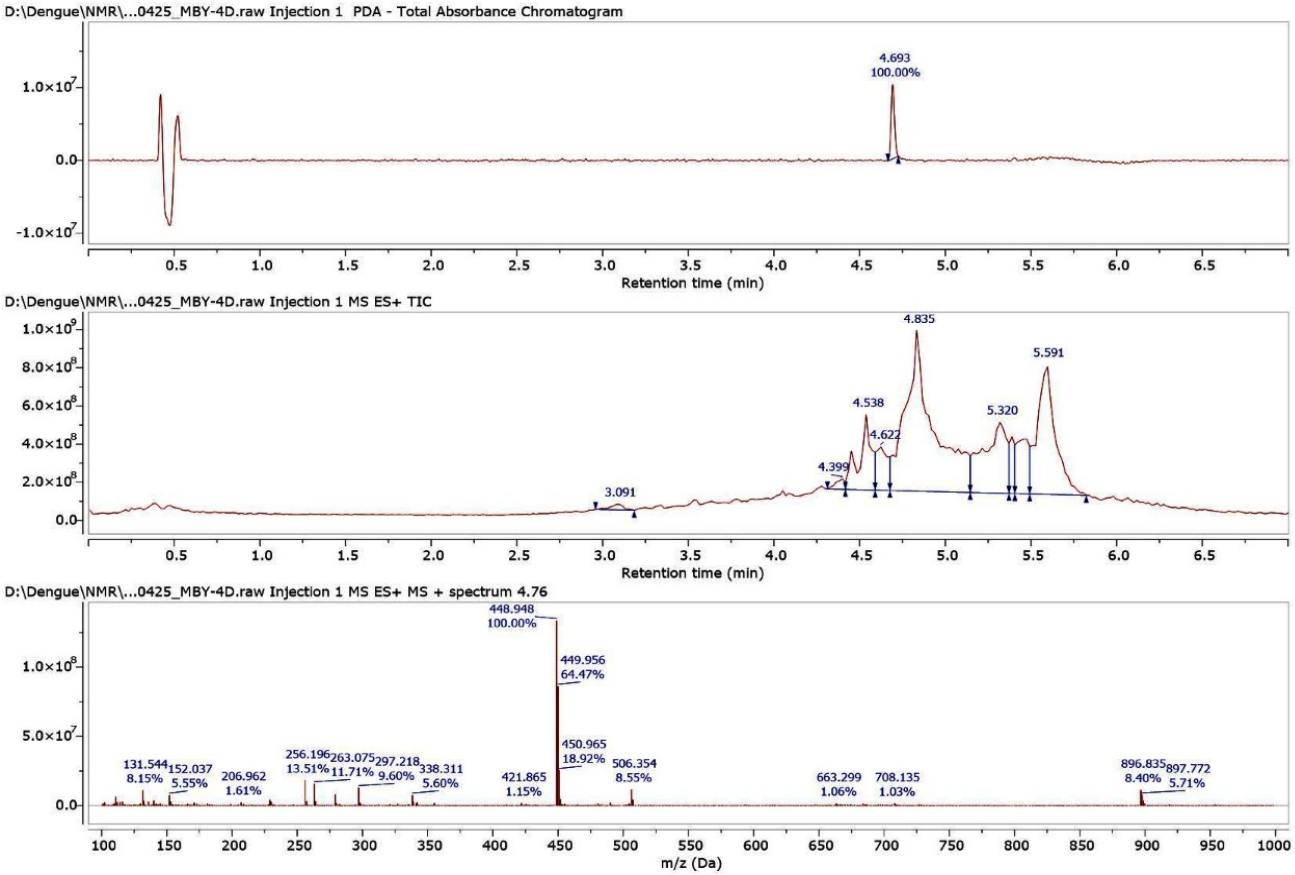

Fig. S25. ^{1}H NMR and Fig. S26 ^{13}C NMR spectra of (4e)

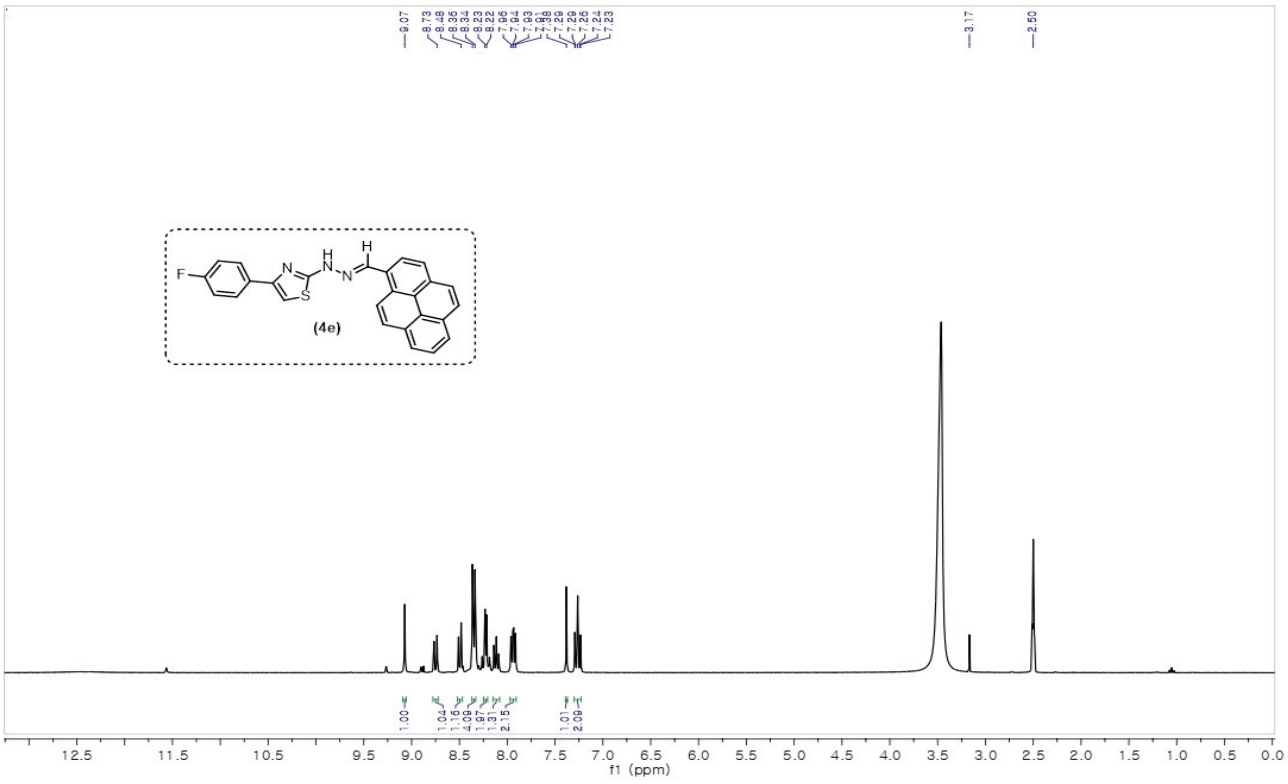

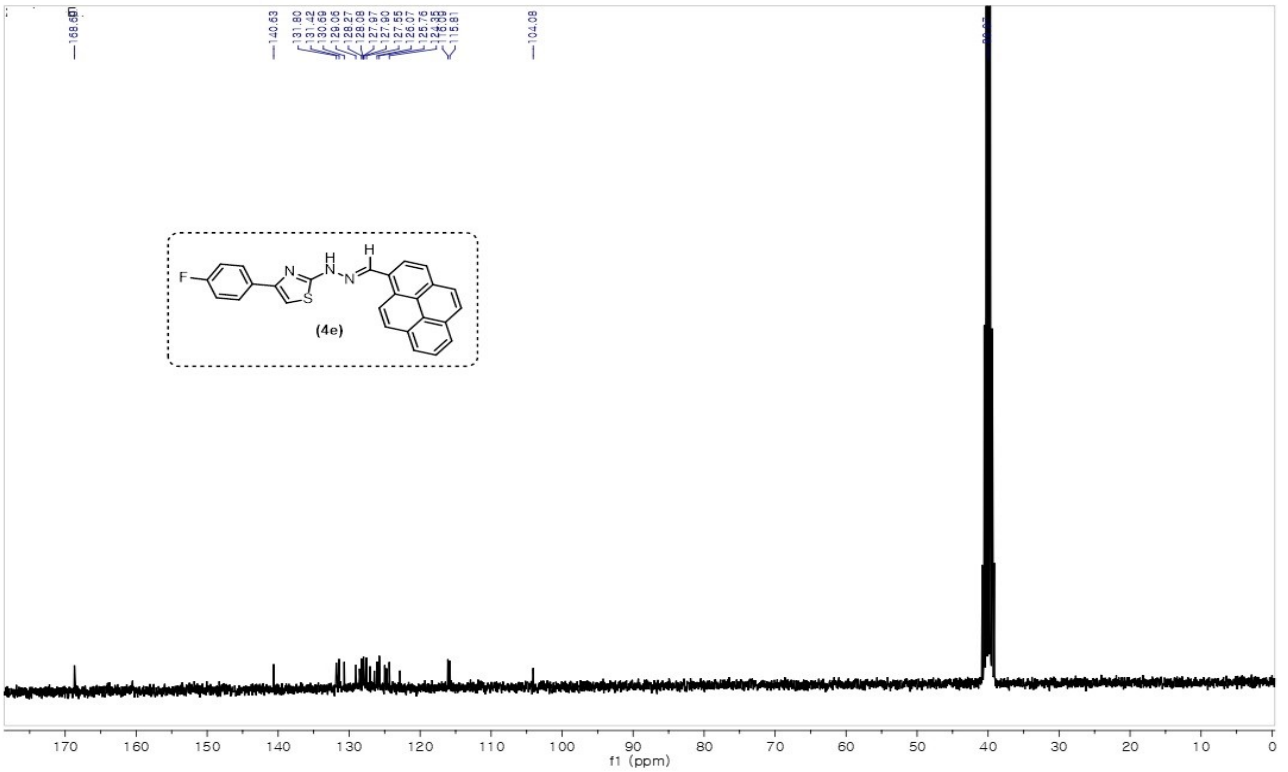

Fig. S27. ^{19}F NMR spectra of compound(4e)

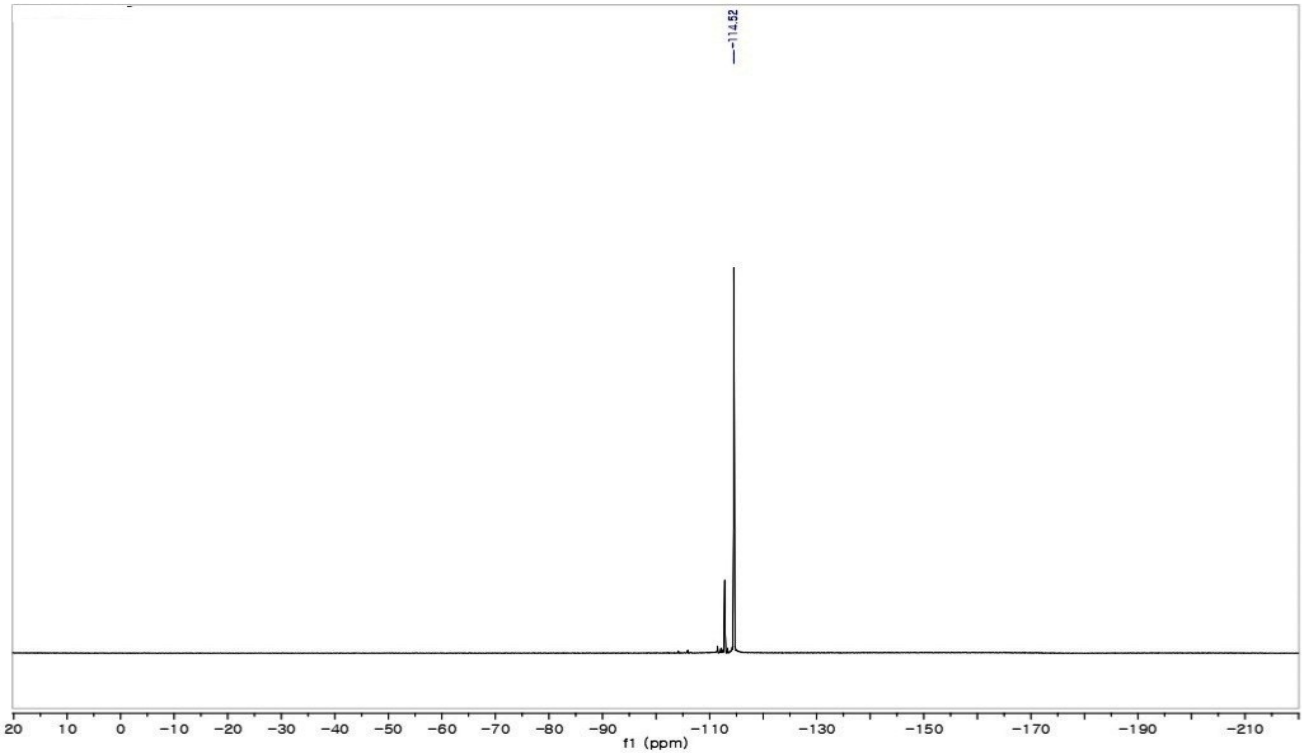

Fig. 28. IR Spectrum of compound (4e)

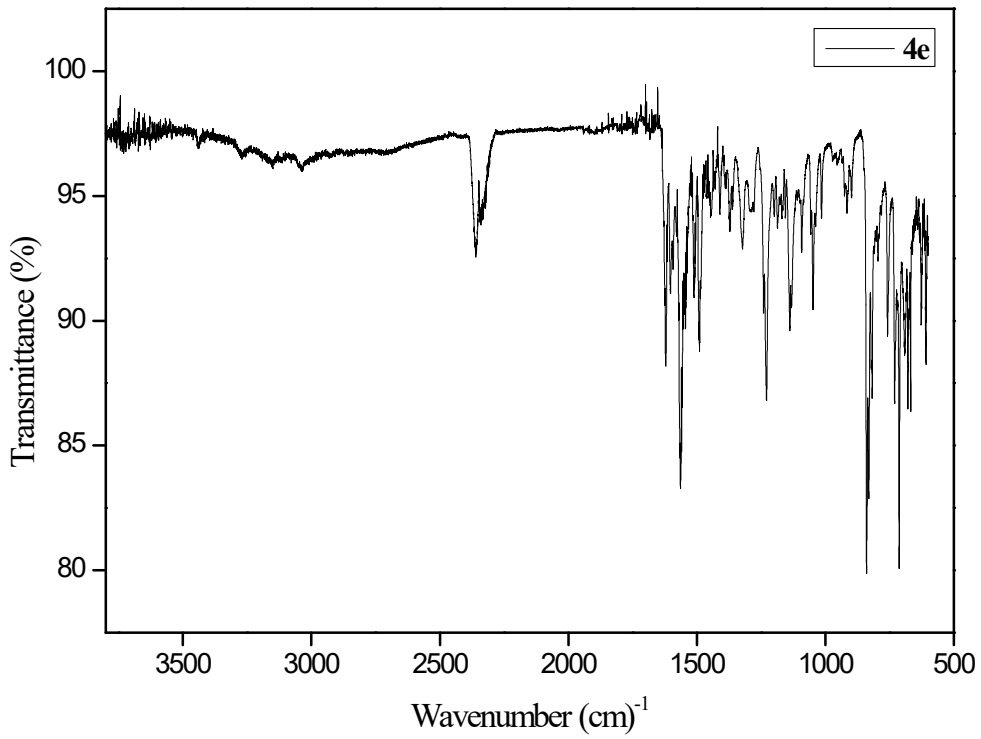

Fig. S29. LC-MS data of compound (4e)

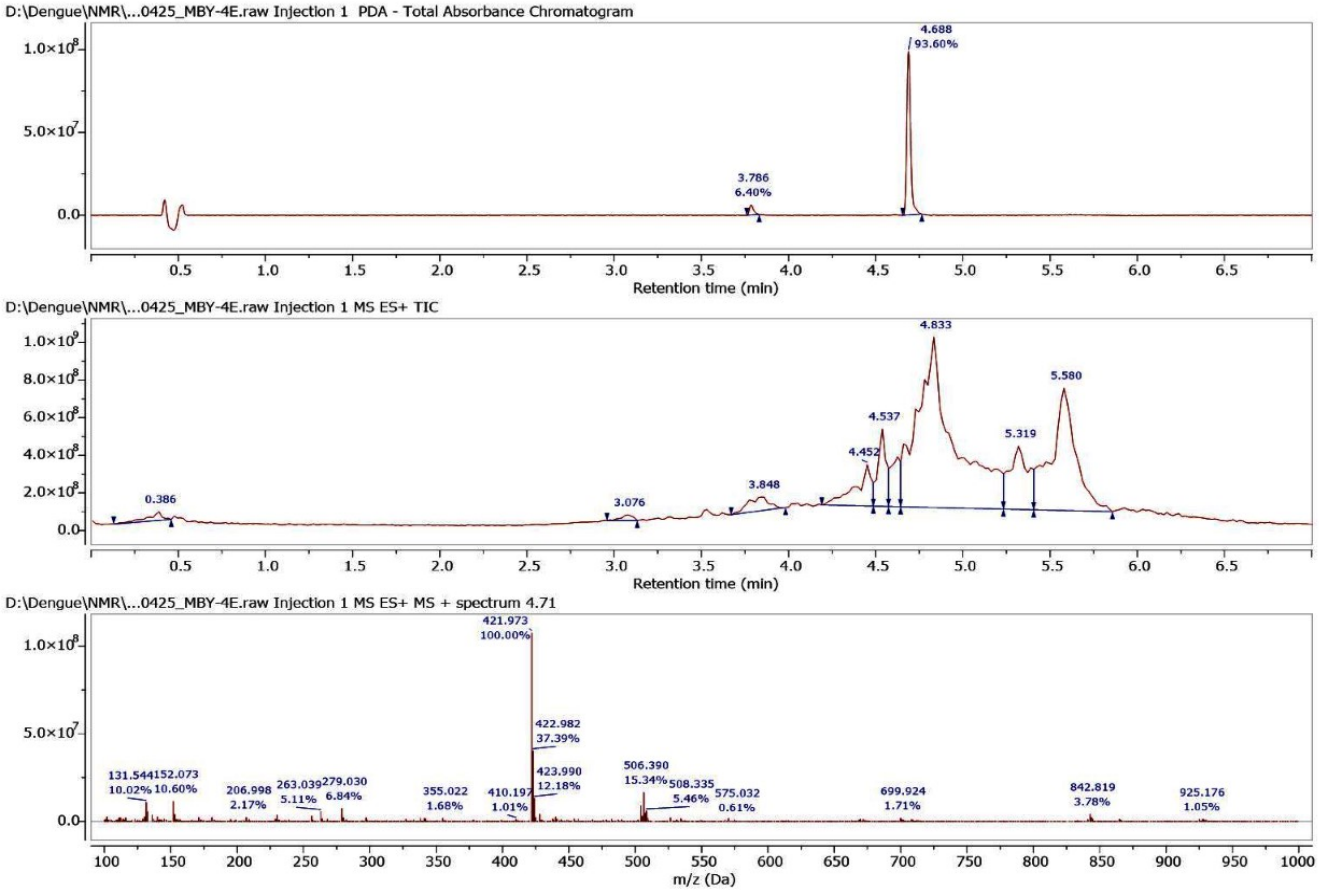

Fig. S30. ^{1}H NMR and Fig. S31. ^{13}C NMR spectra of (4f)

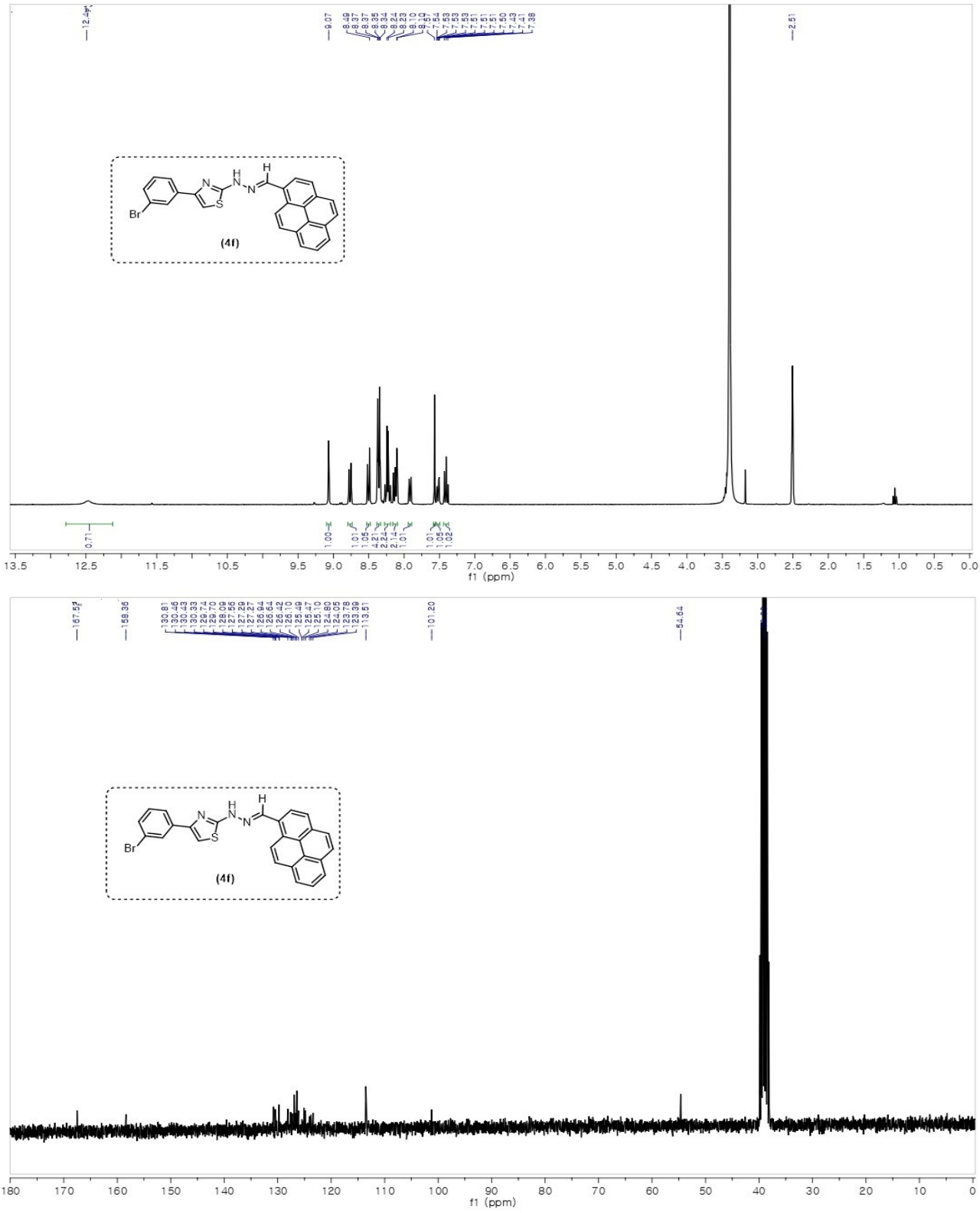

Fig. S32. IR Spectrum of compound (4f)

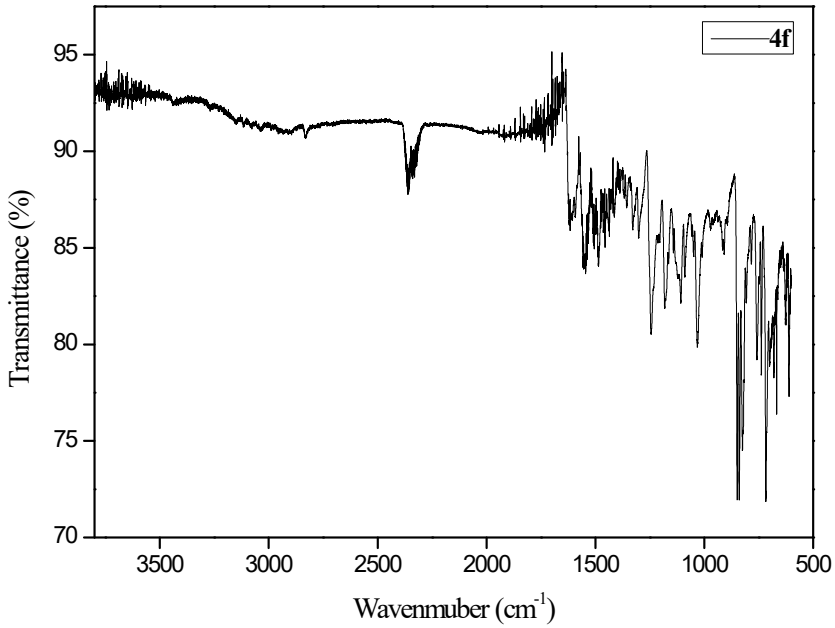

Fig. S33. LC-MS data of compound (4f)

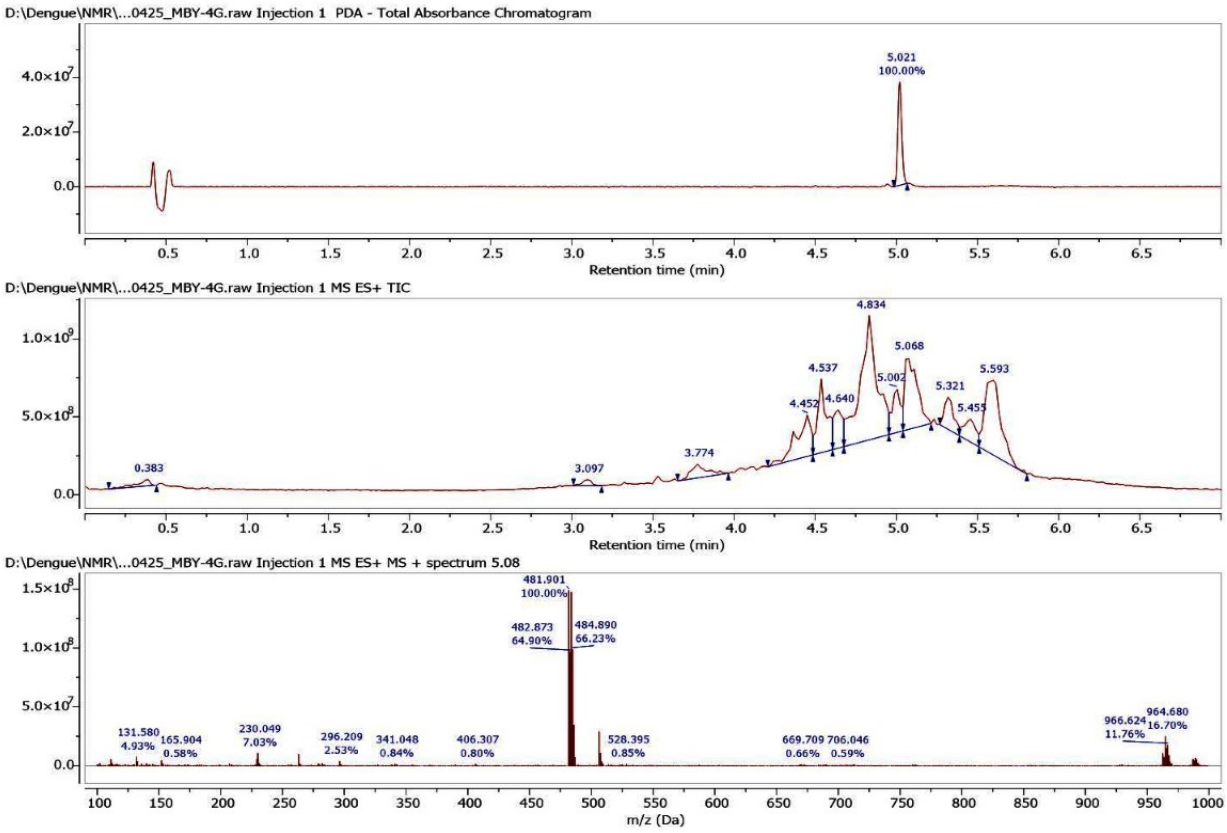

Fig. S34. ^{1}H NMR and Fig. S35. ^{13}C NMR spectra of (4g)

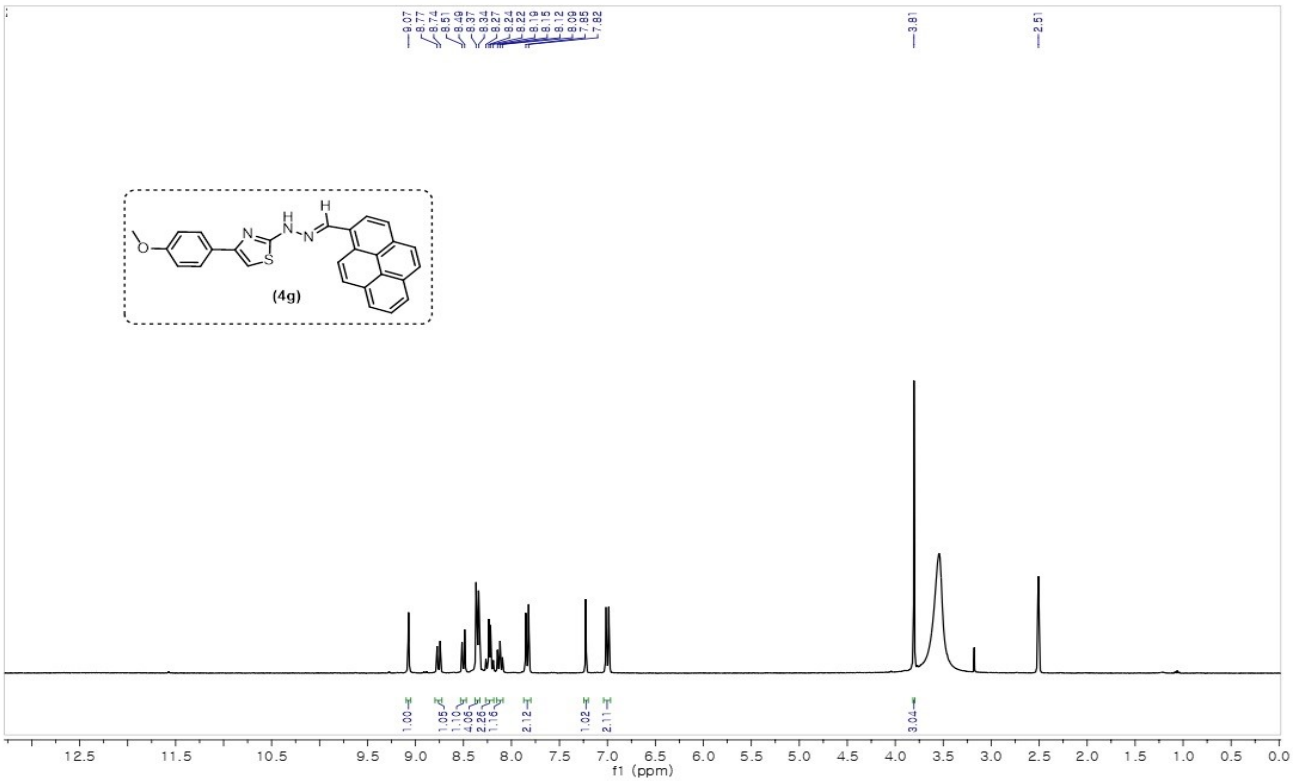

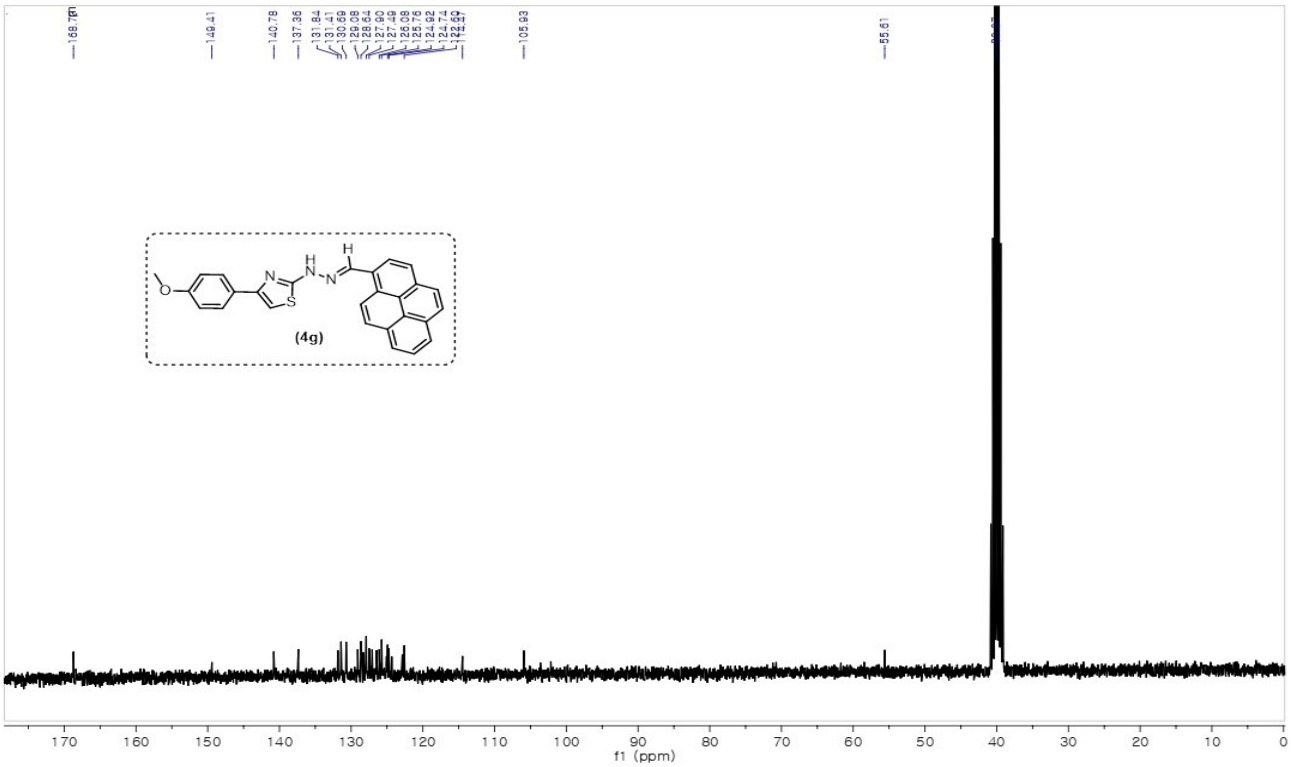

Fig. S36. IR Spectrum of compound (4g)

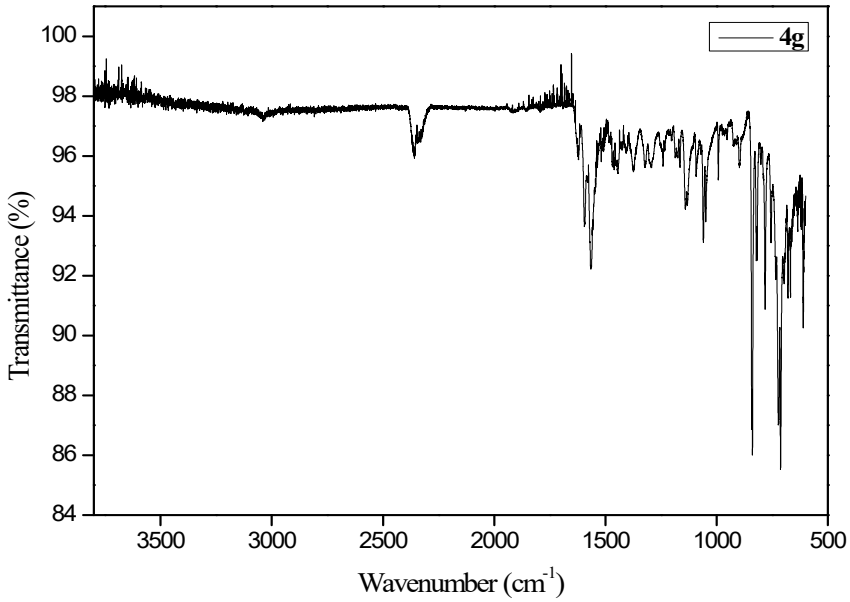

Fig. S37. LC-MS data of compound (4g)

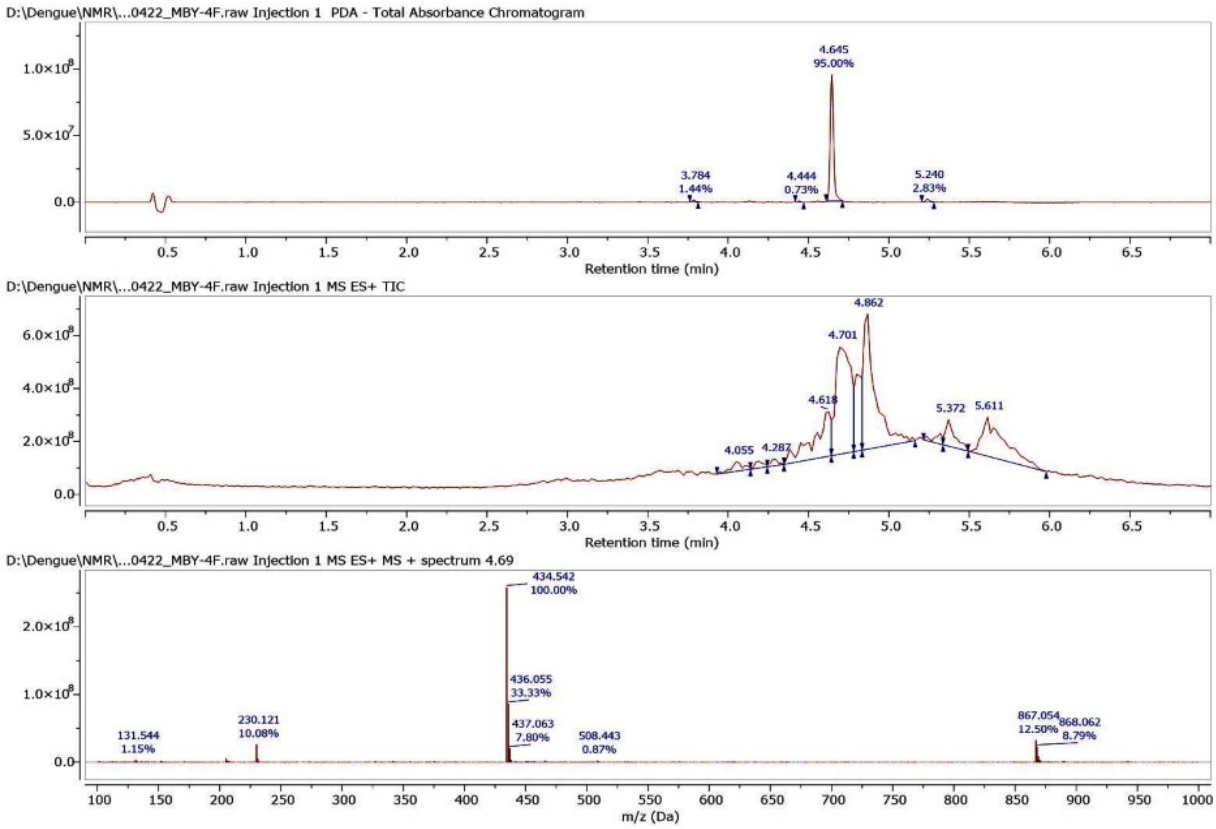

Fig. S38. ^{1}H NMR and Fig. S39 ^{13}C NMR spectra of (4h)

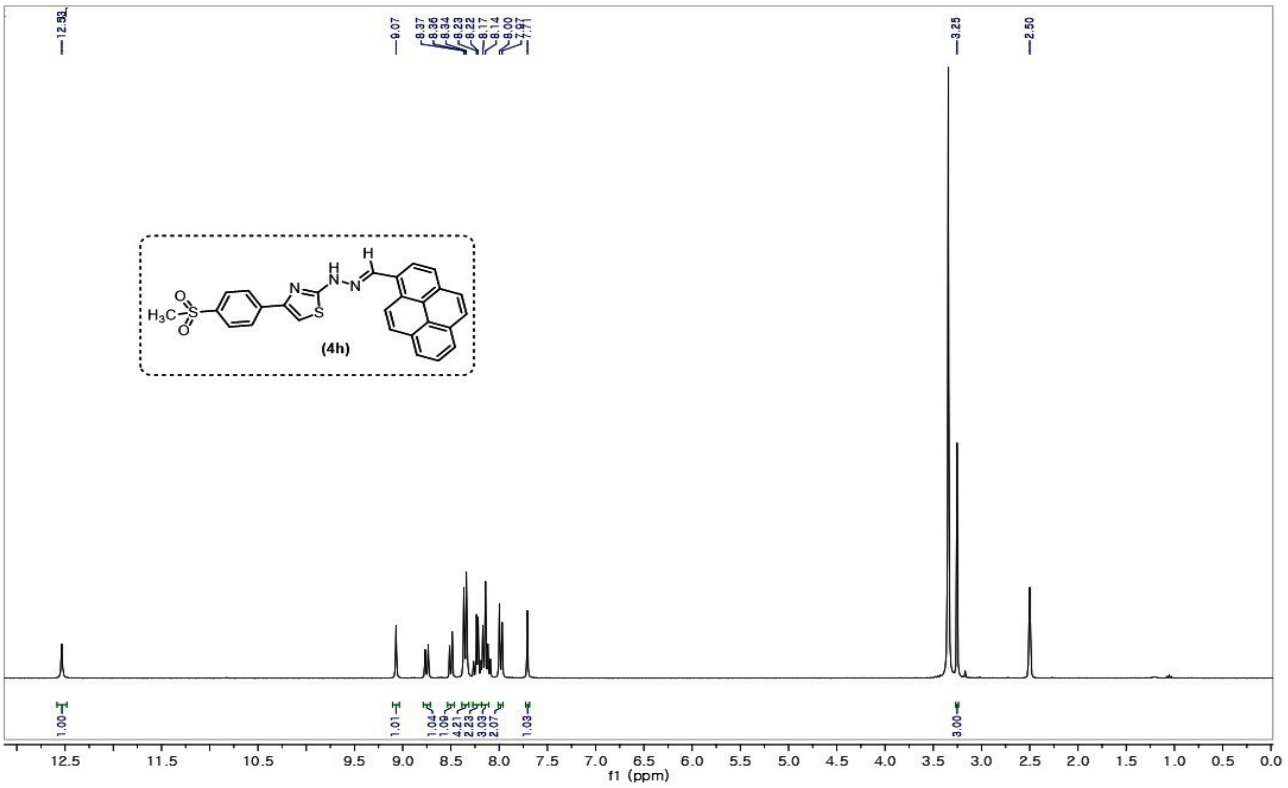

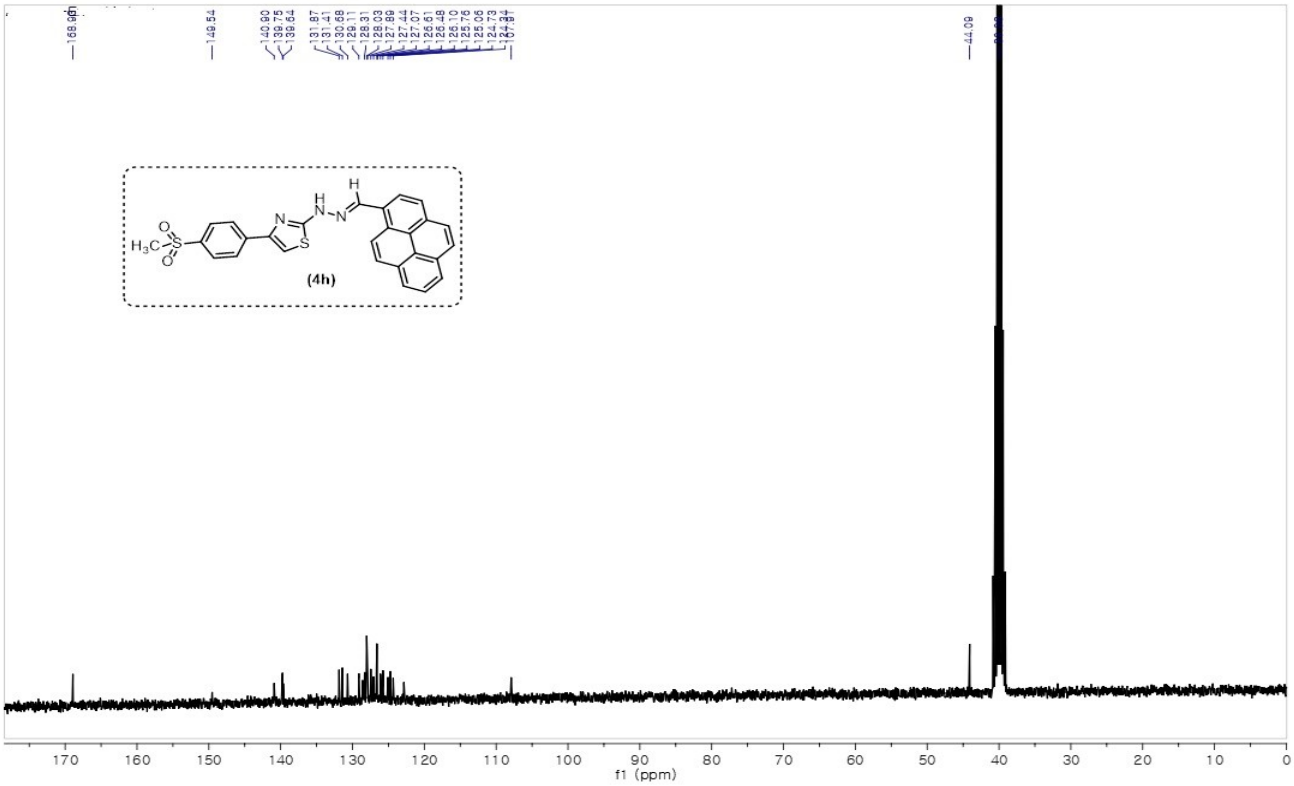

Fig. S40. IR Spectrum of compound (4h)

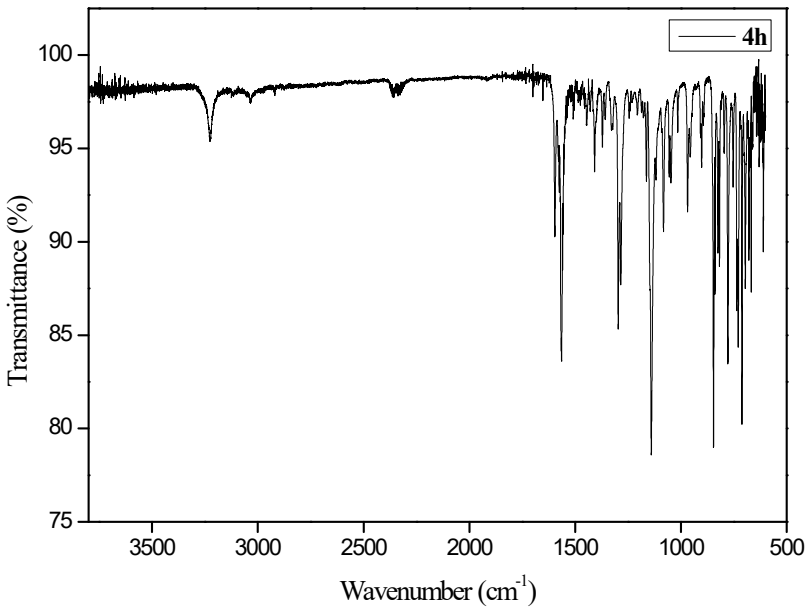

Fig. S41. LC-MS data of compound (4h)

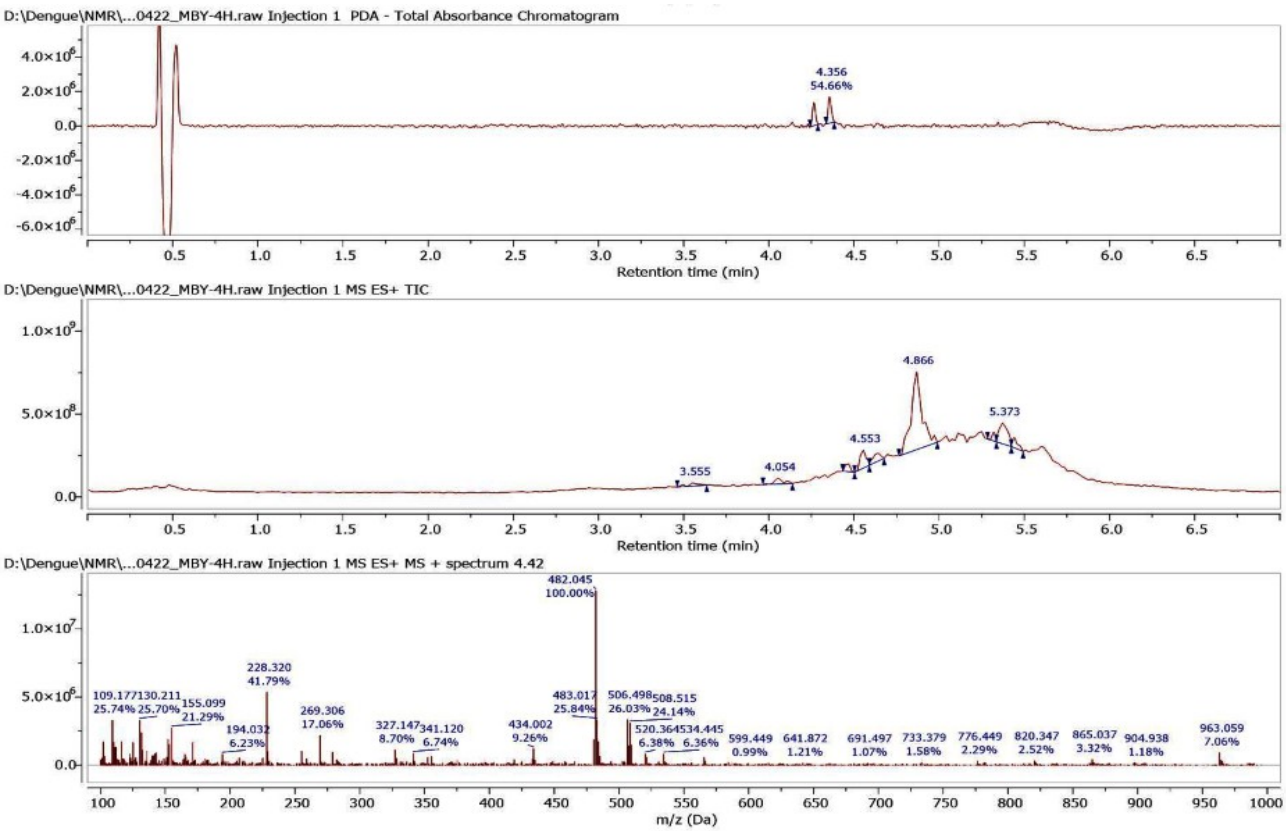

Fig. S42 ^{1}H NMR and Fig. S43 ^{13}C NMR spectra of (4i)

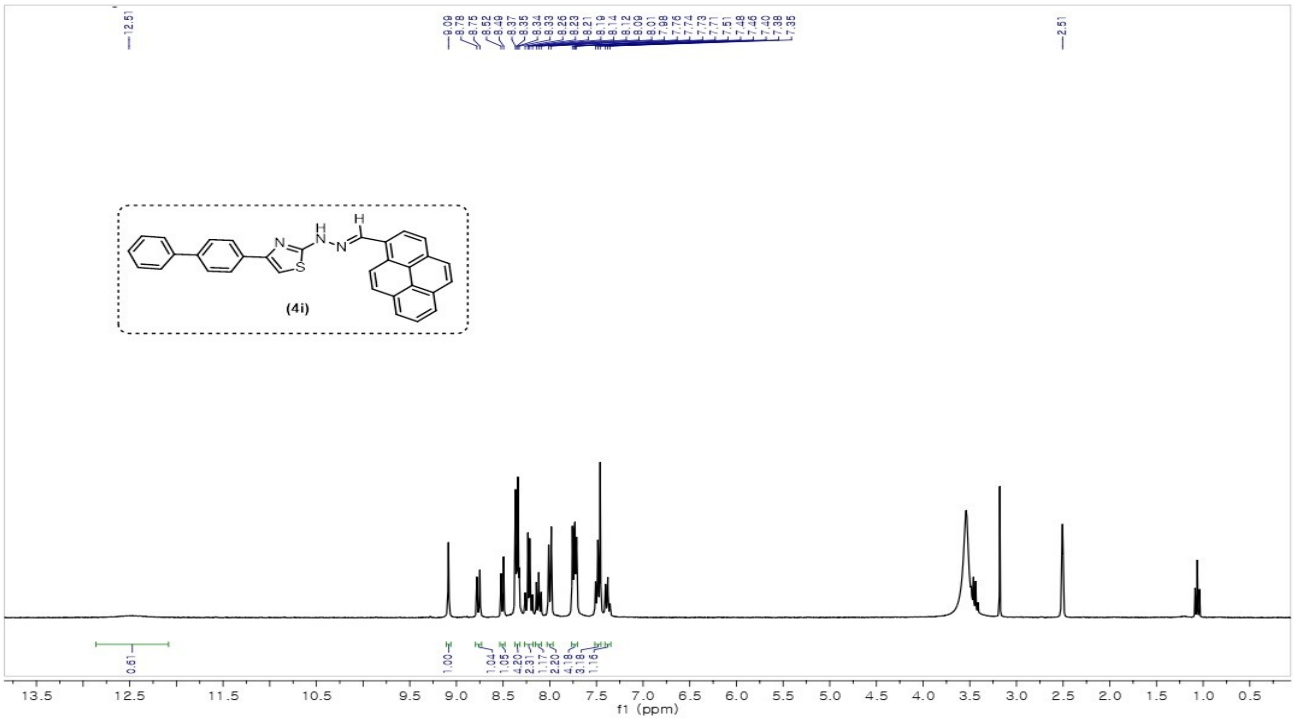

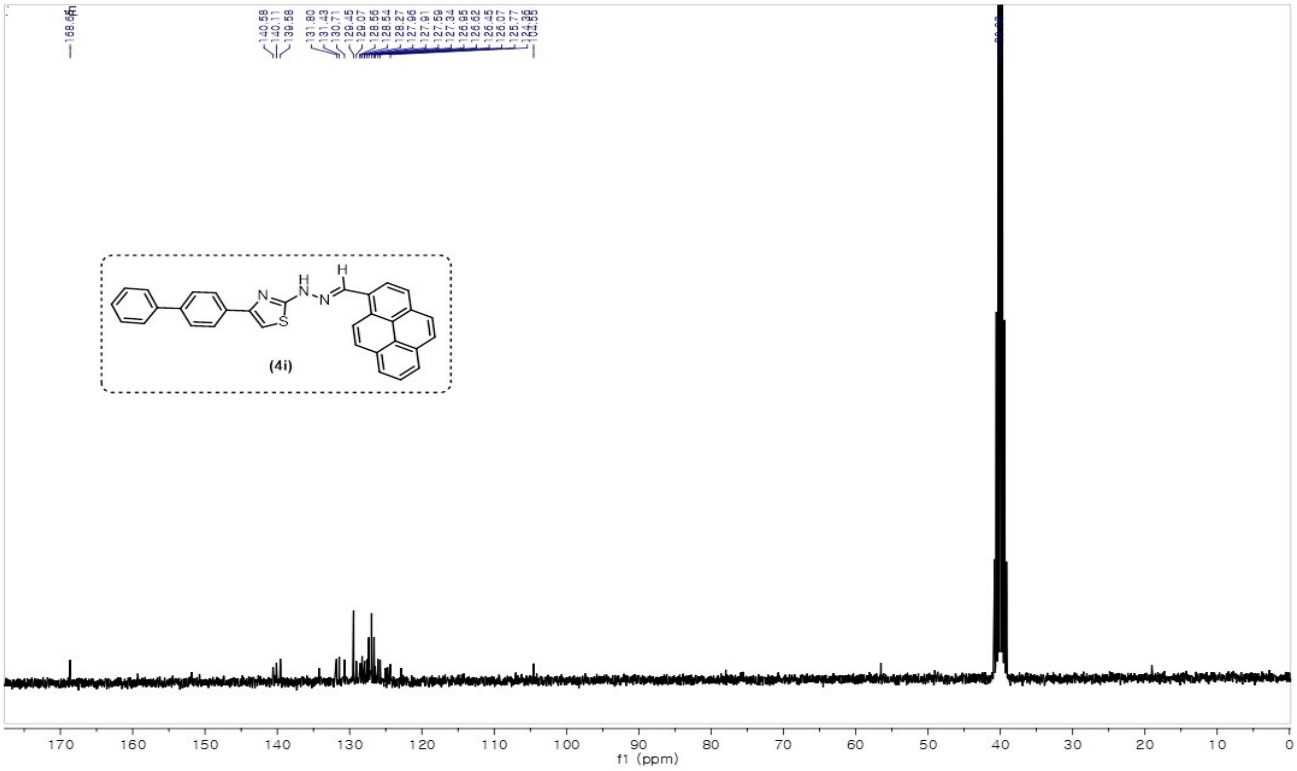

Fig. S44 IR Spectrum of compound (4i)

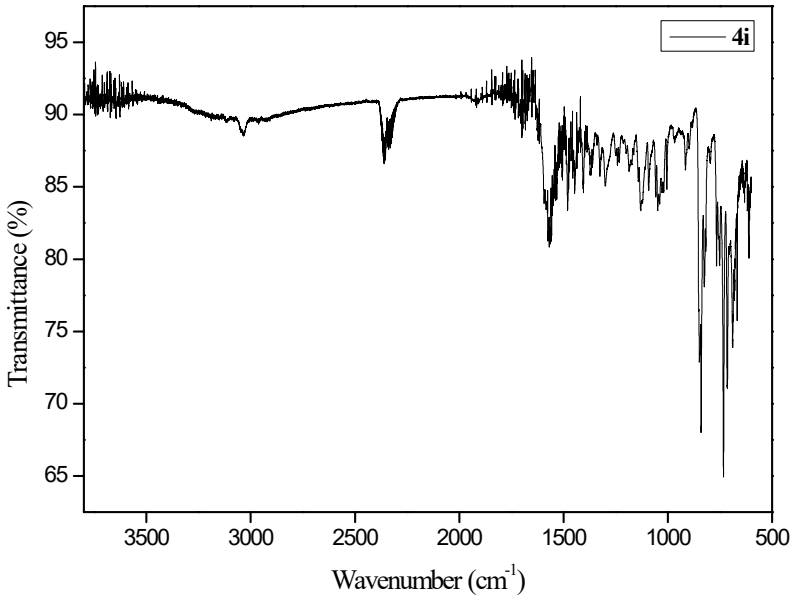

Fig. S45. LC-MS data of compound (4i)

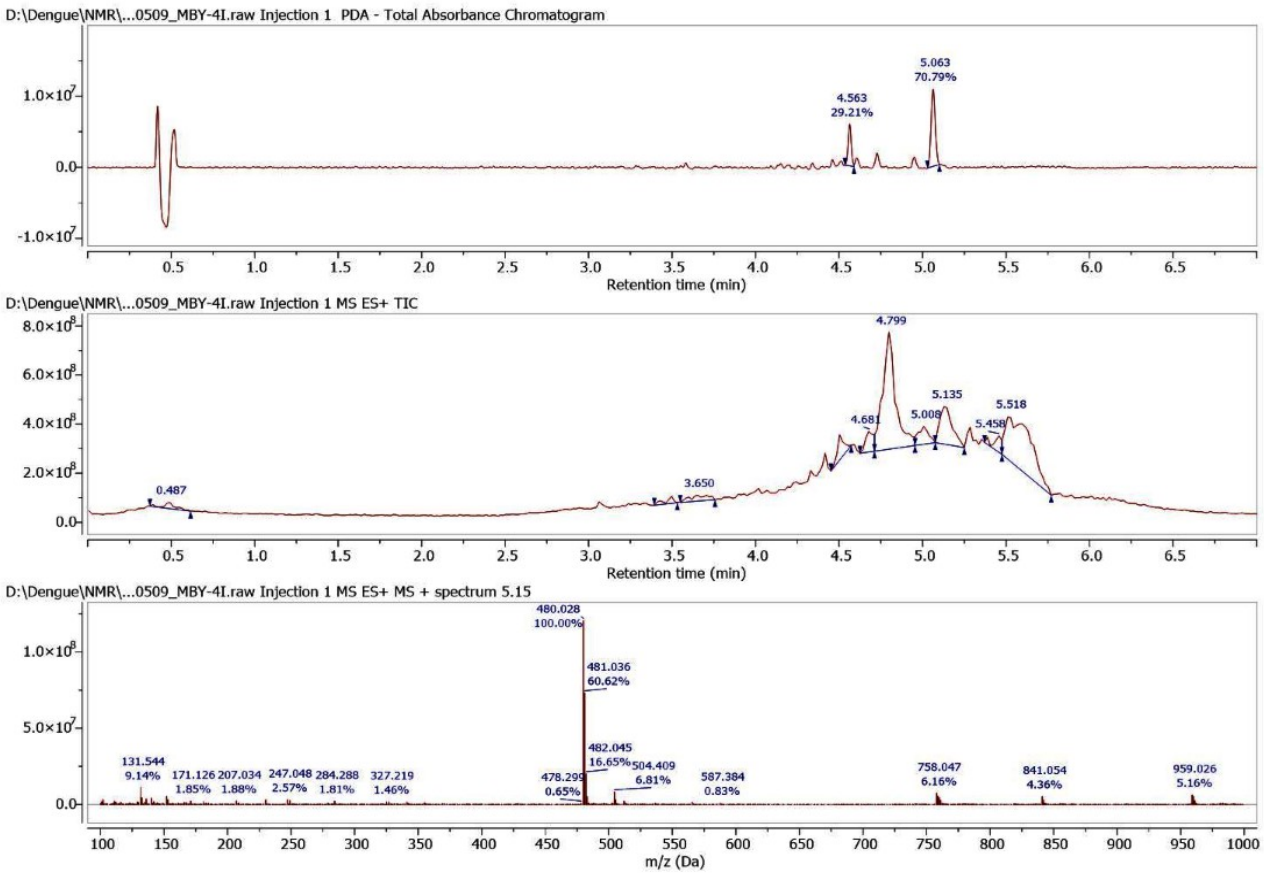

Fig. S46. ^{1}H NMR and Fig. S47. ^{13}C NMR spectra of (4j)

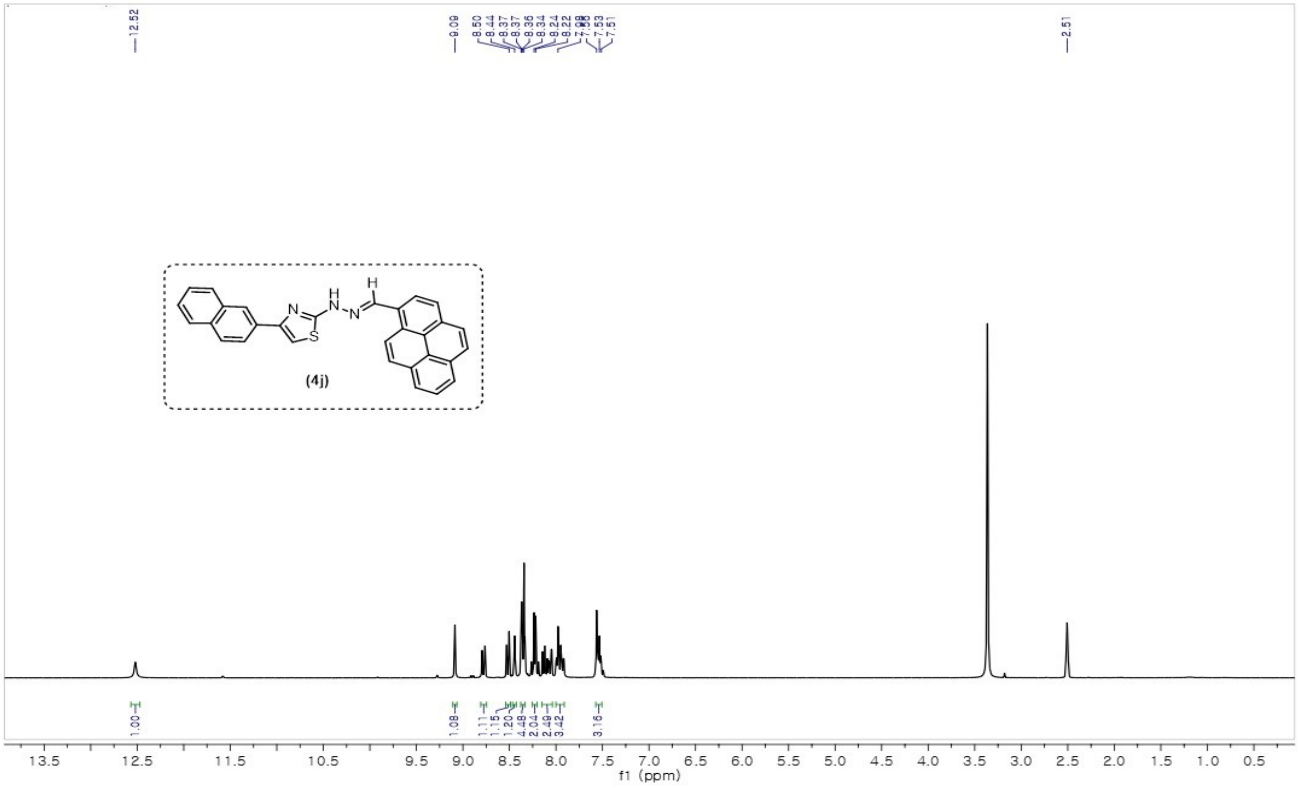

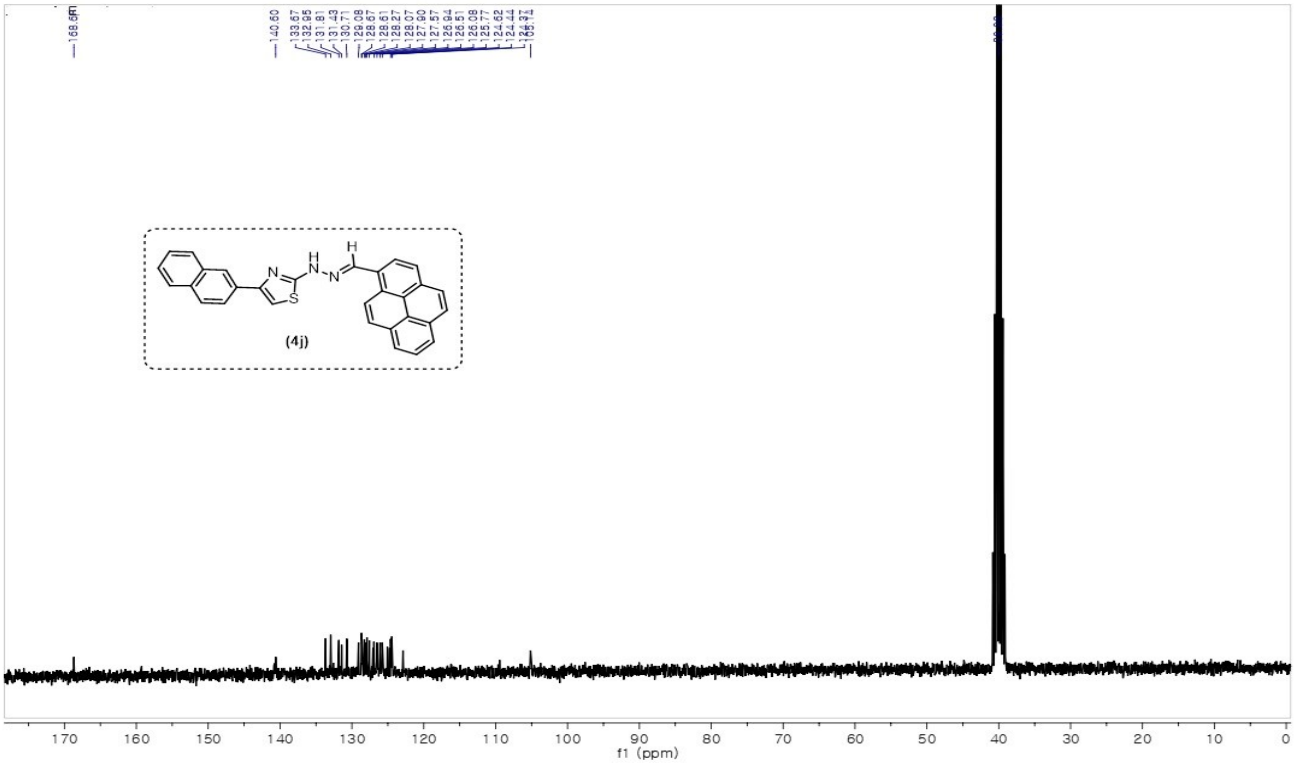

Fig. S48 IR spectra of compound (4j)

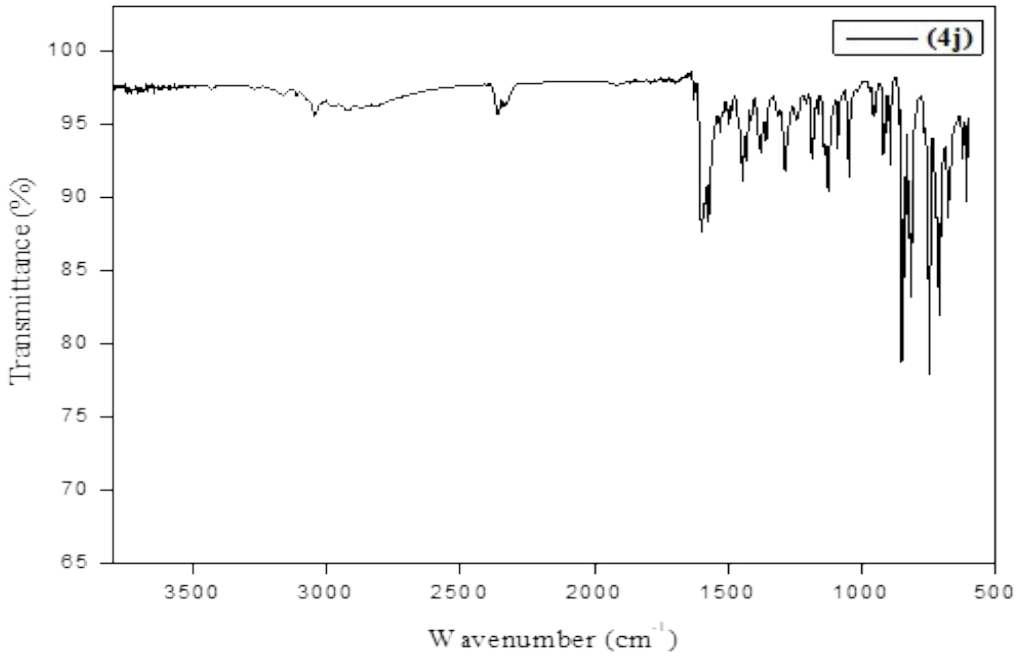

Fig. S49. LC-MS data of compound (4j)

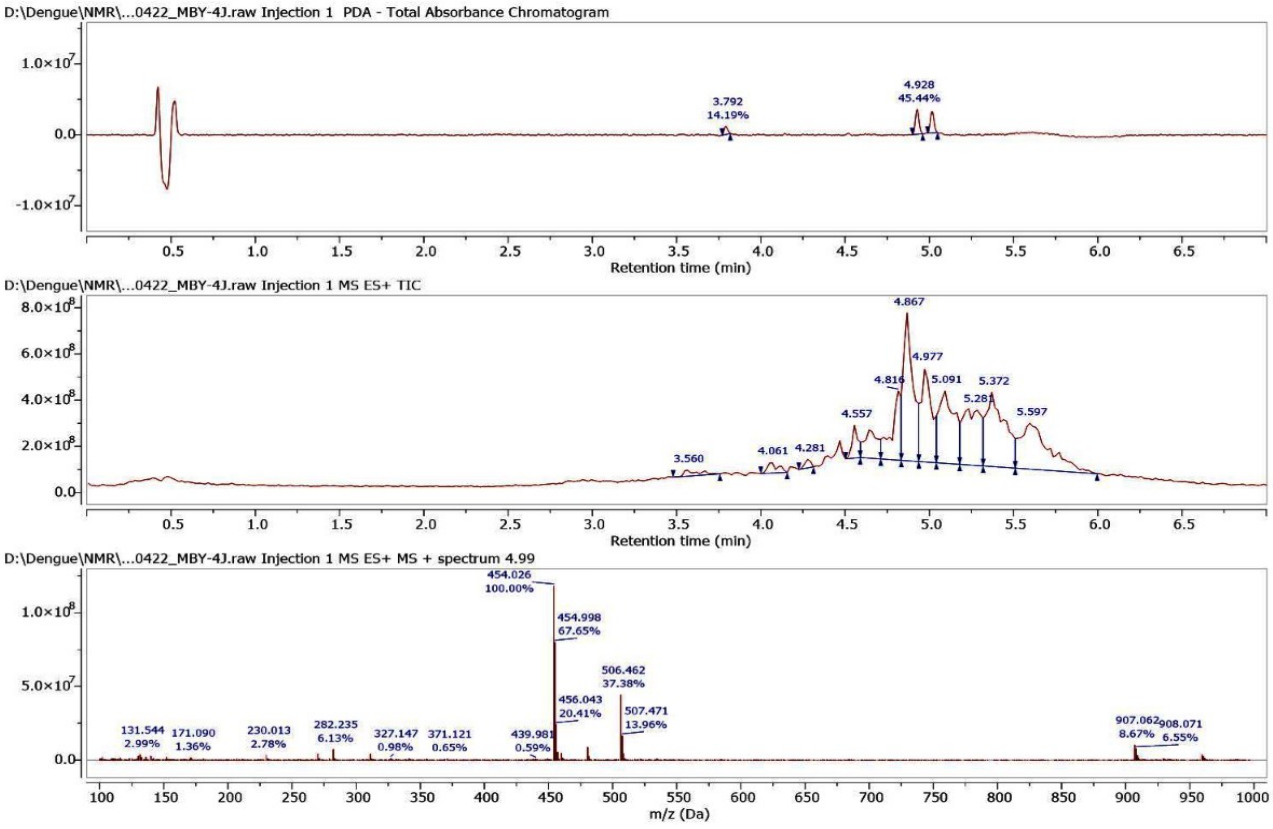

Fig. S50 ^{1}H NMR and Fig. S51 ^{13}C NMR spectra of (4k)

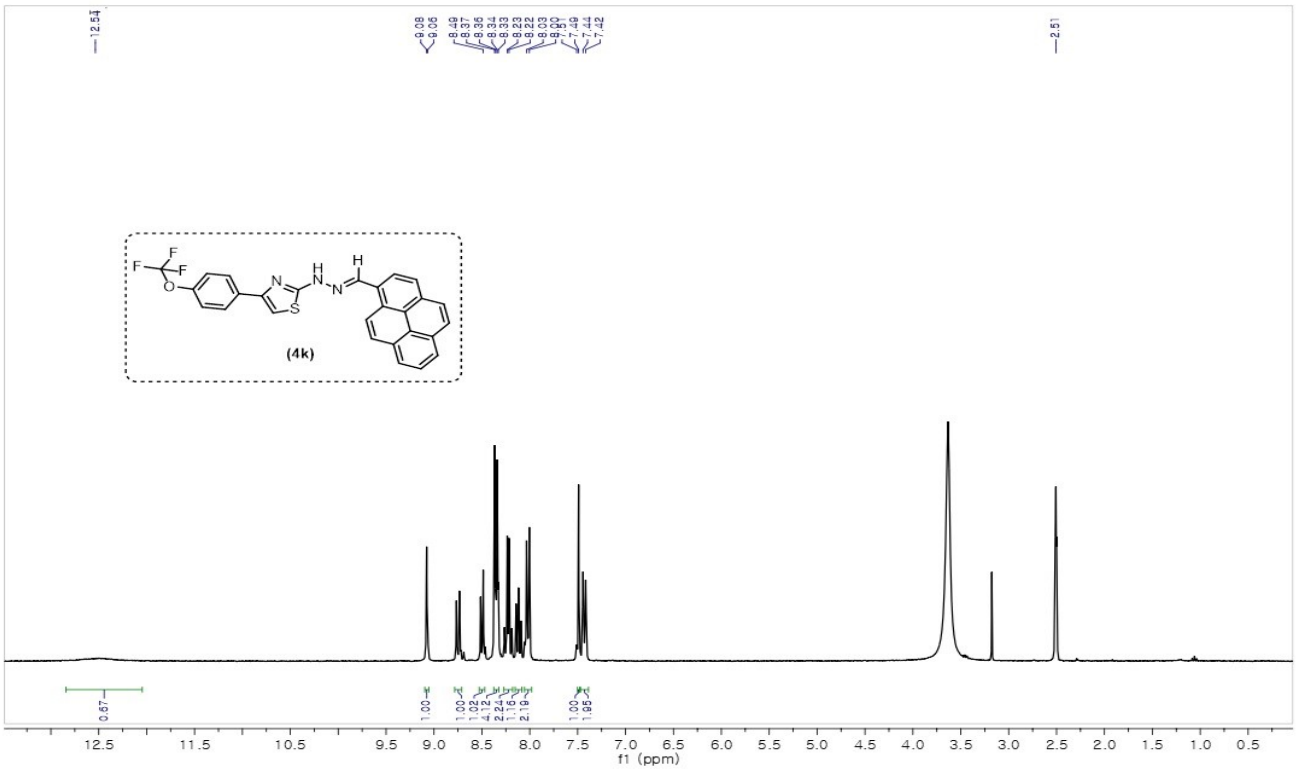

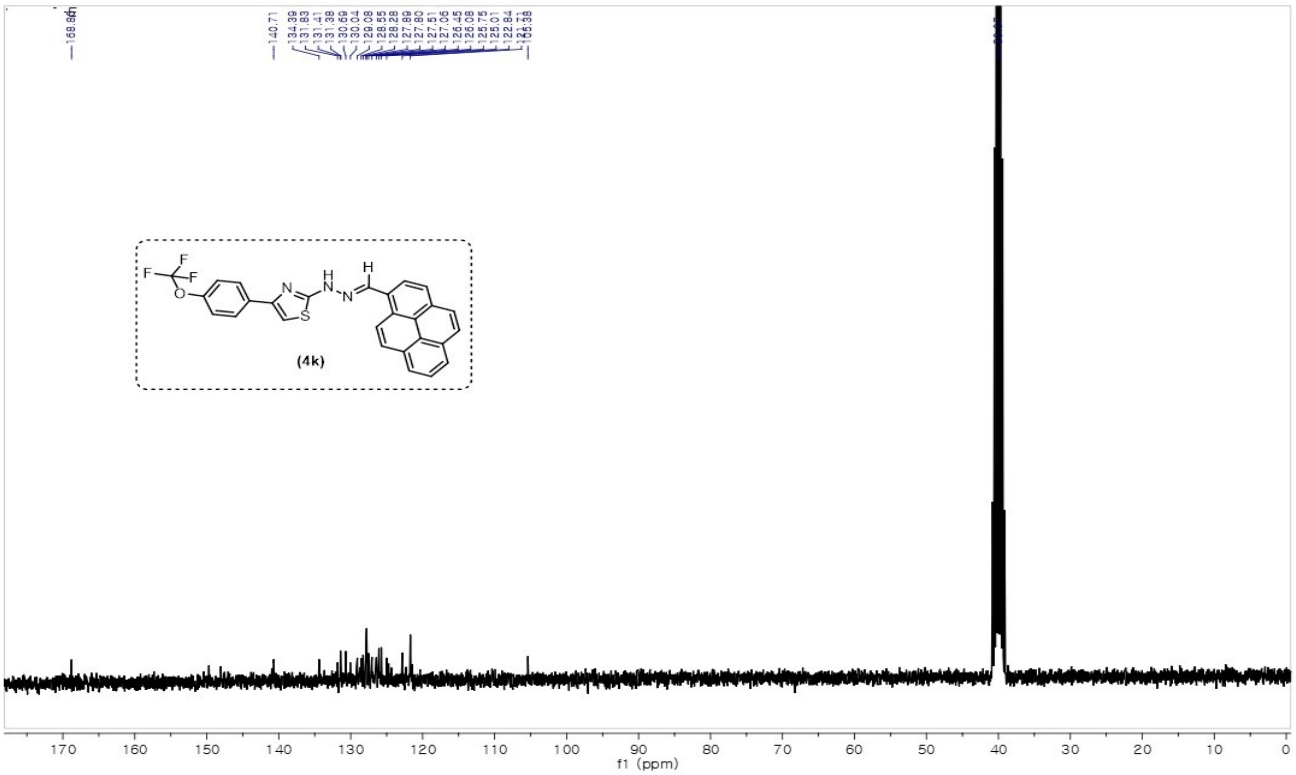

Fig. S52. ^{19}F NMR spectra of compound (4k)

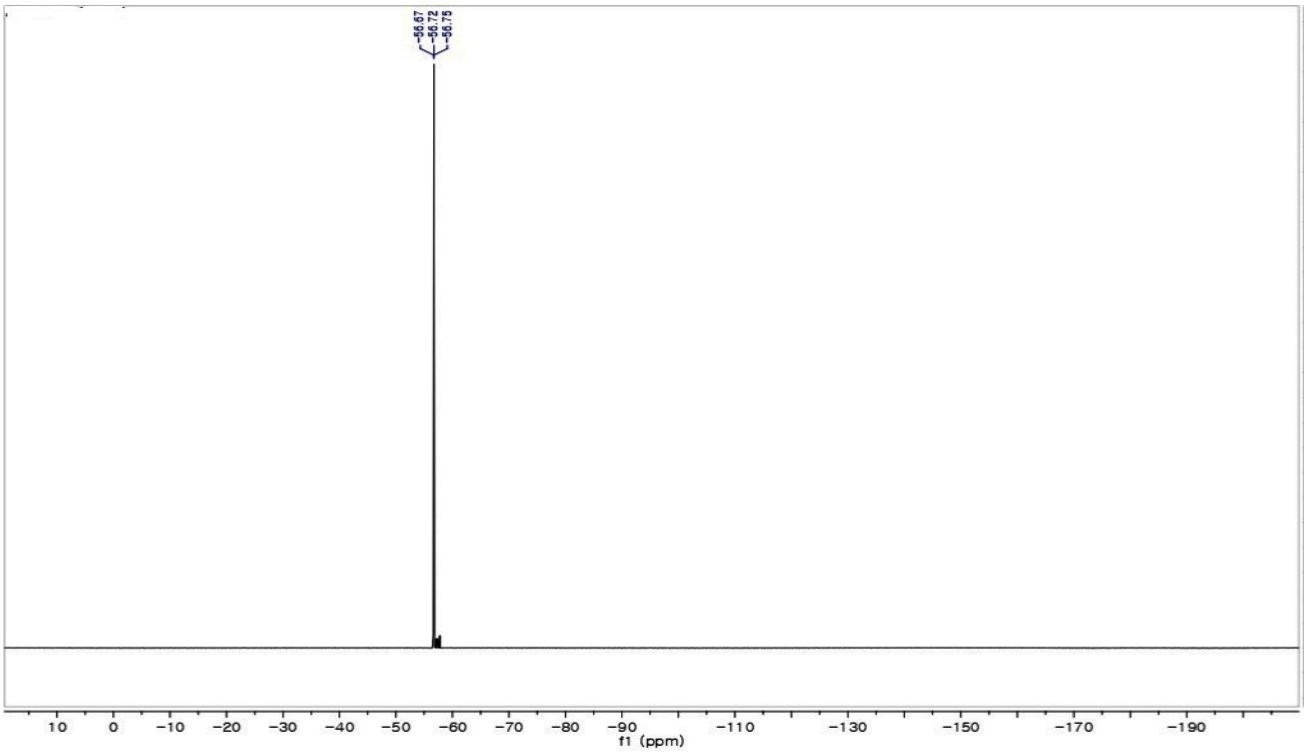

Fig. S53. IR Spectrum of compound (4k)

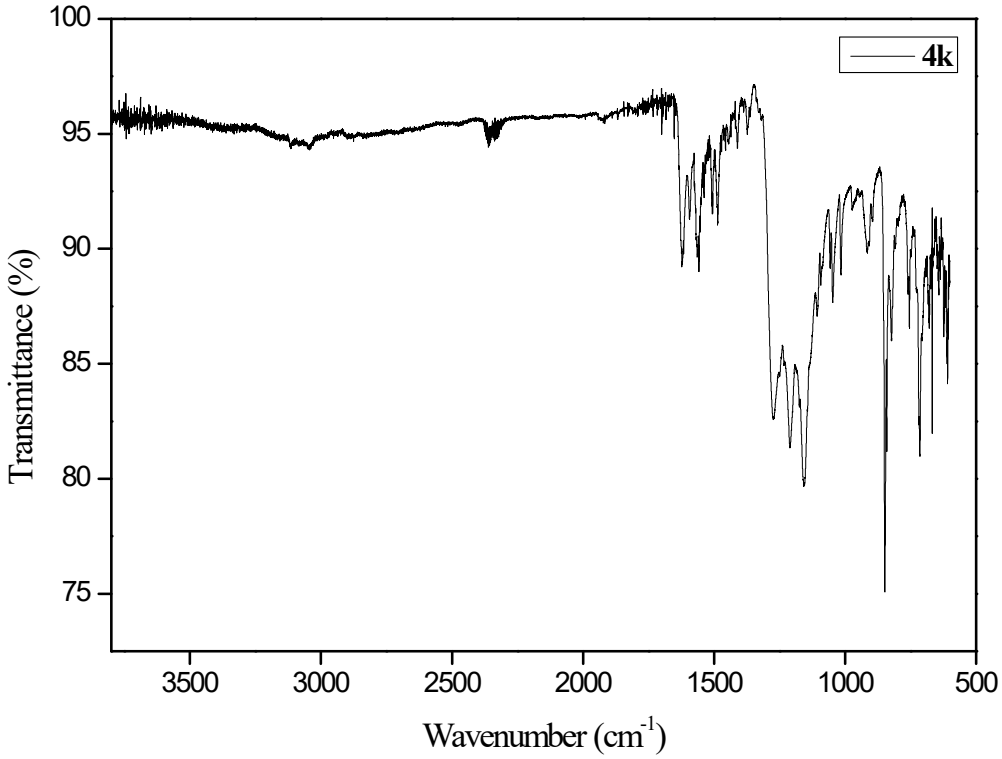

Fig. S54. LC-MS data of compound (4k)

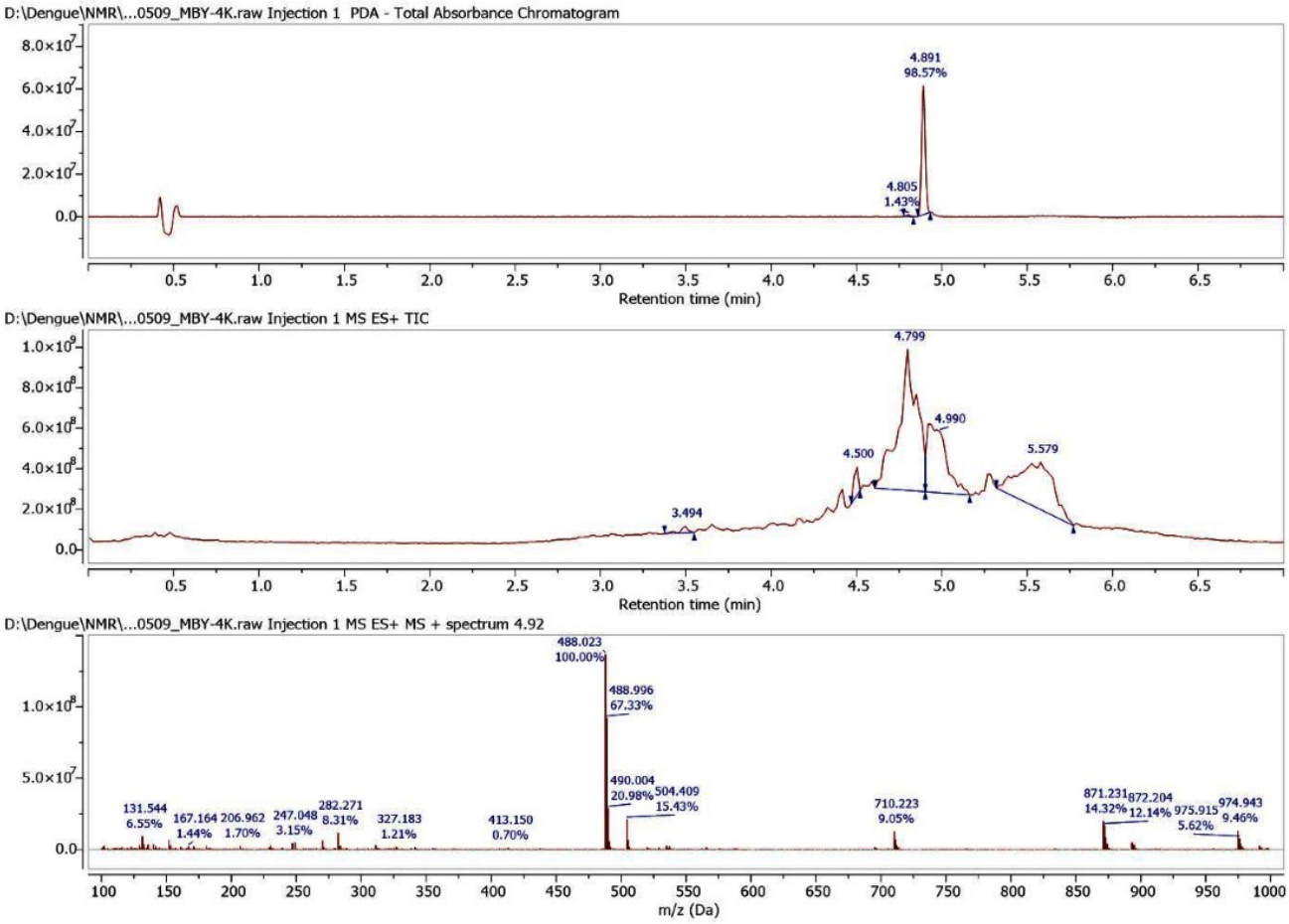

Fig. S55. ^{1}H NMR and Fig. S56. ^{13}C NMR spectra of (4l)

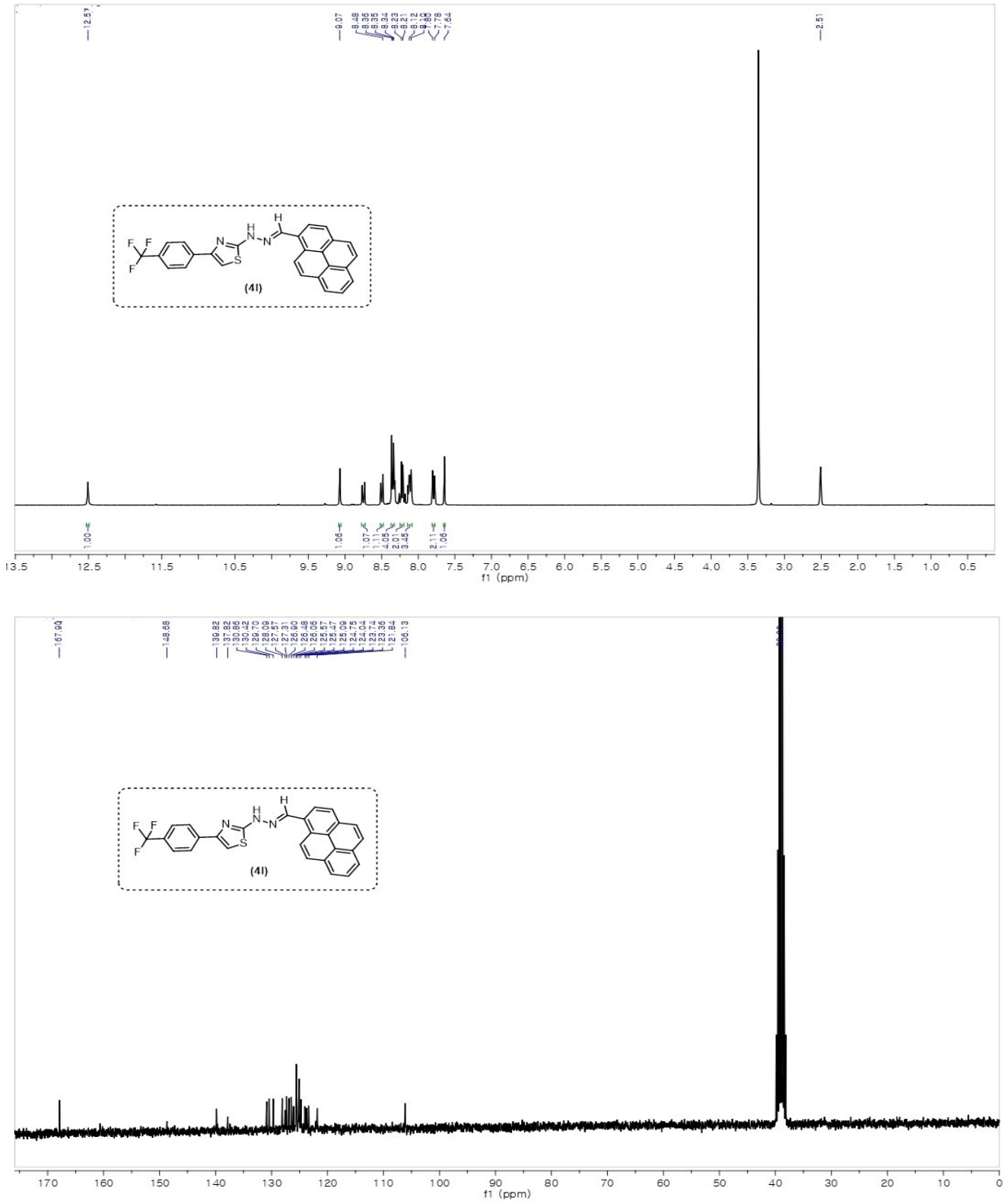

Fig. S57. ^{19}F NMR spectra of compound(4l)

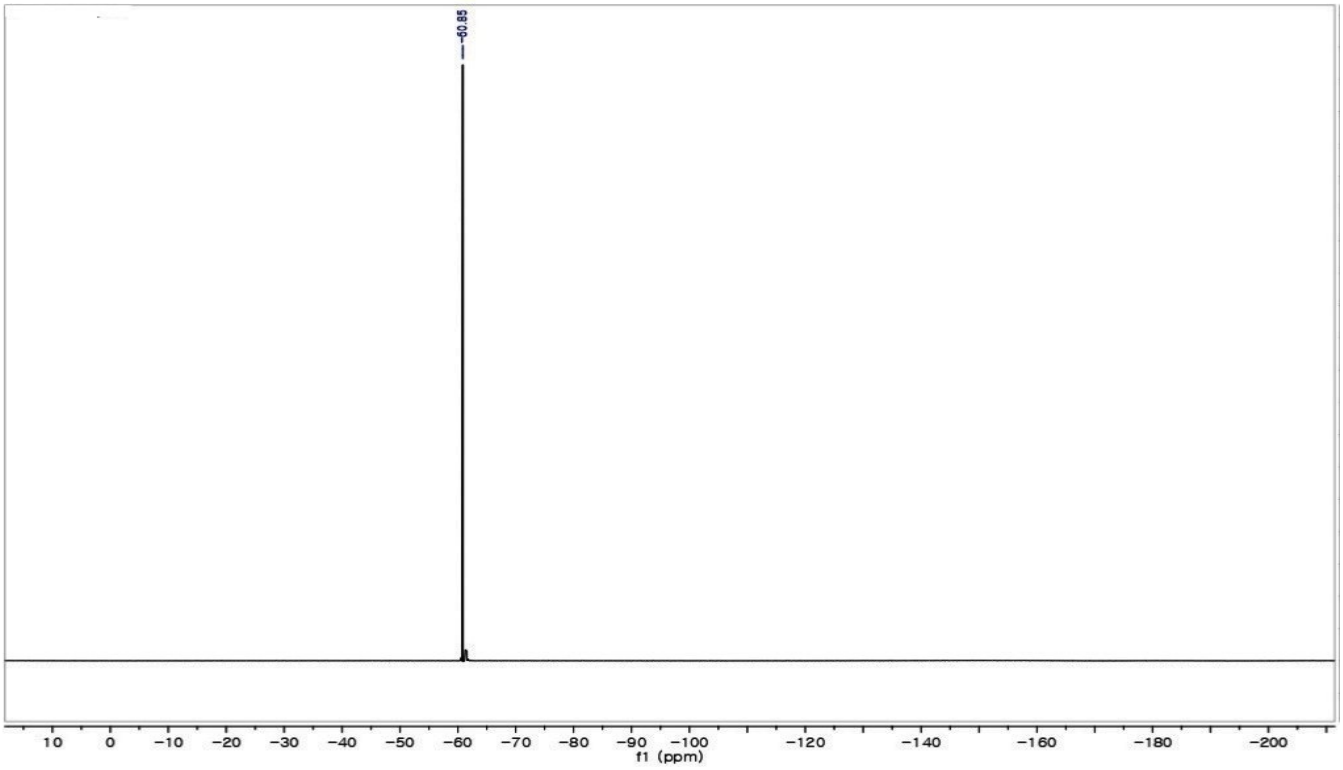

Fig. S58. IR Spectrum of compound (4l)

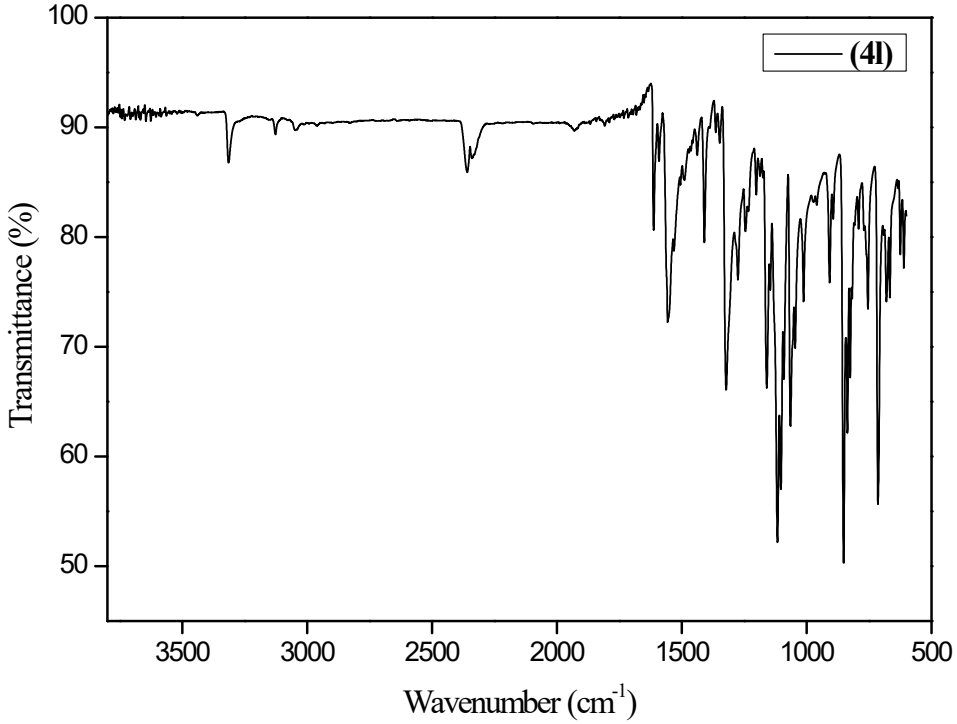

Fig. S59. LC-MS data of compound (4l)

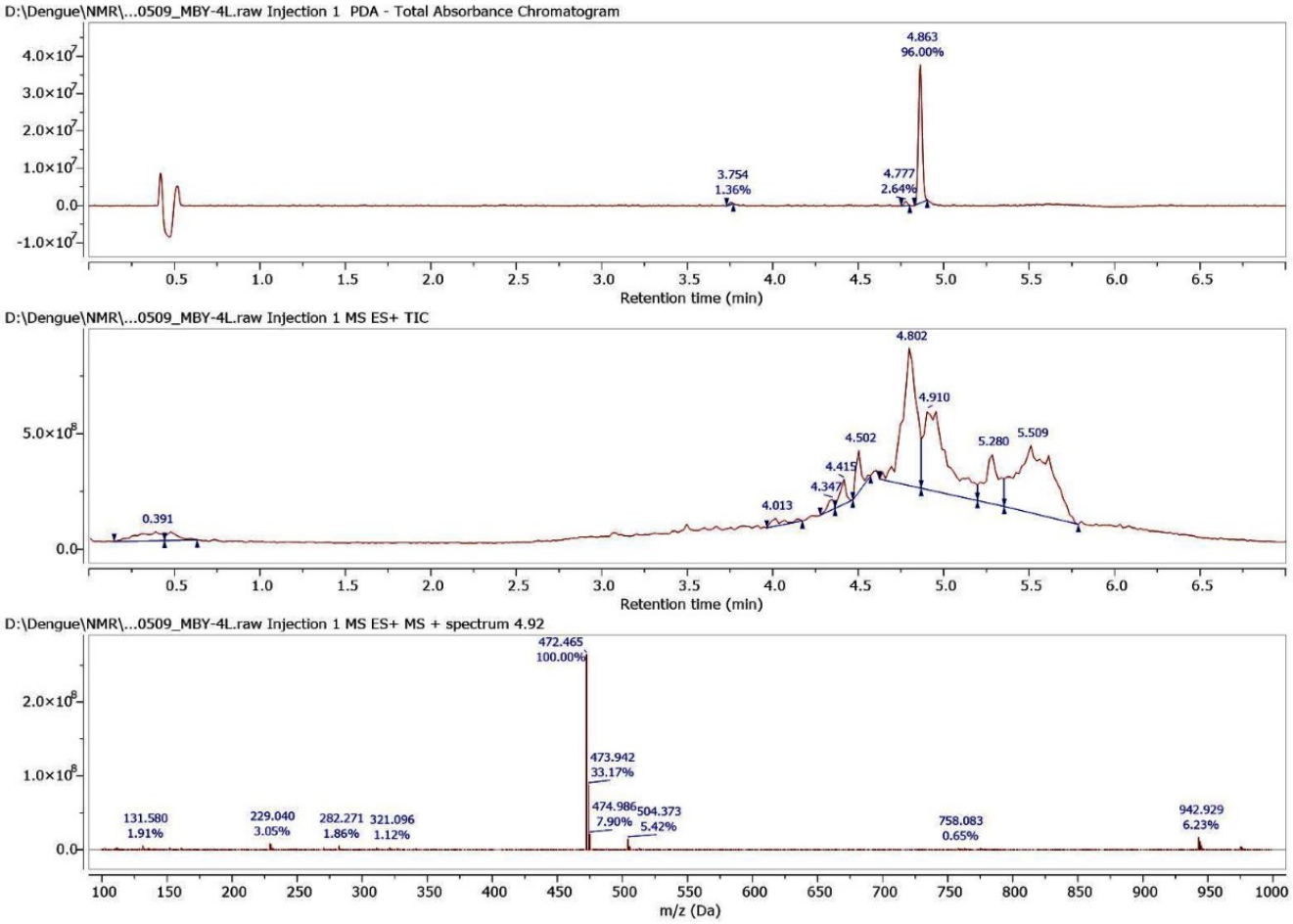

Fig. S60. ^{1}H NMR and Fig. S61. ^{13}C NMR spectra of (4m)

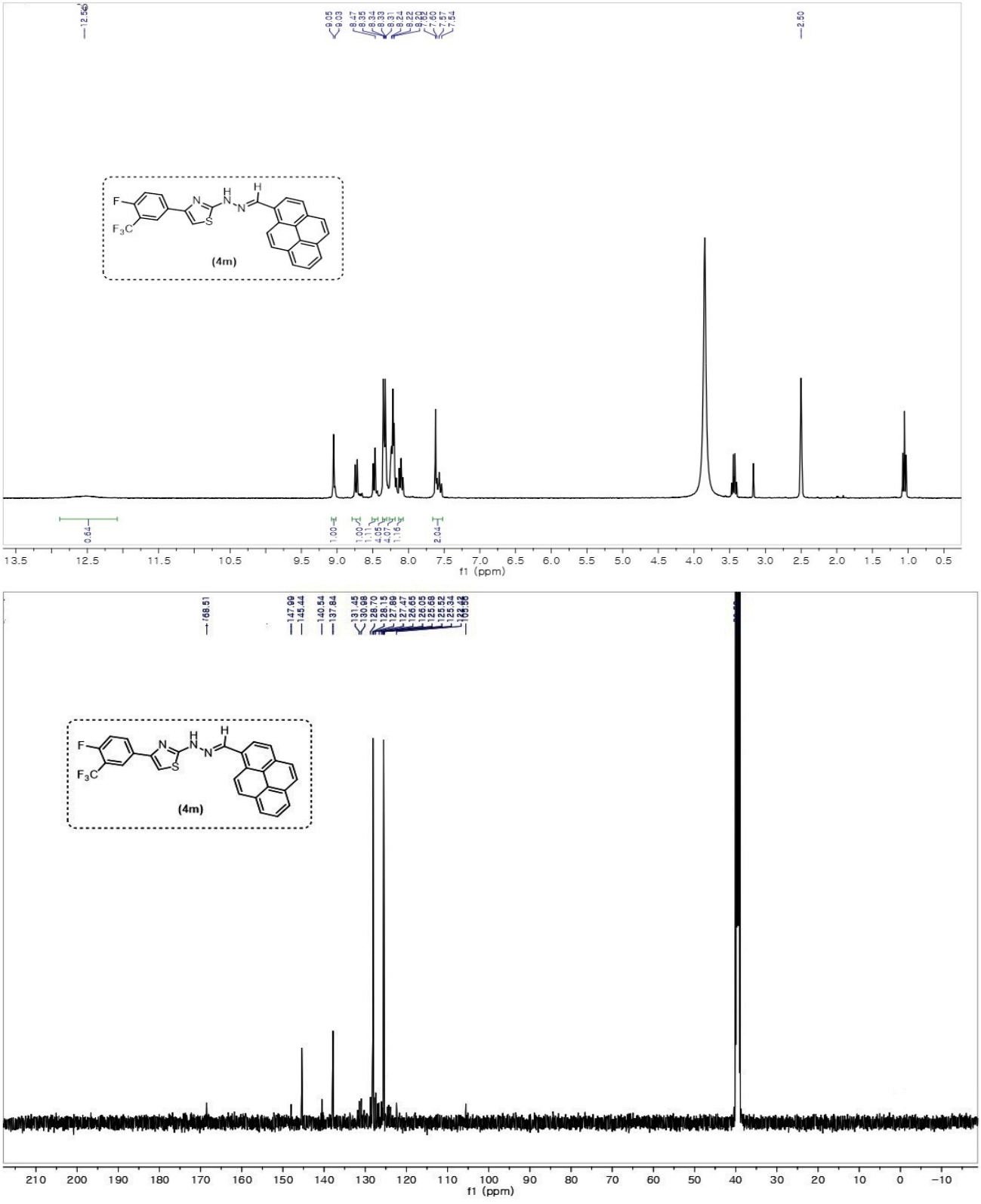

Fig. S62. ^{19}F NMR spectra of compound (4m)

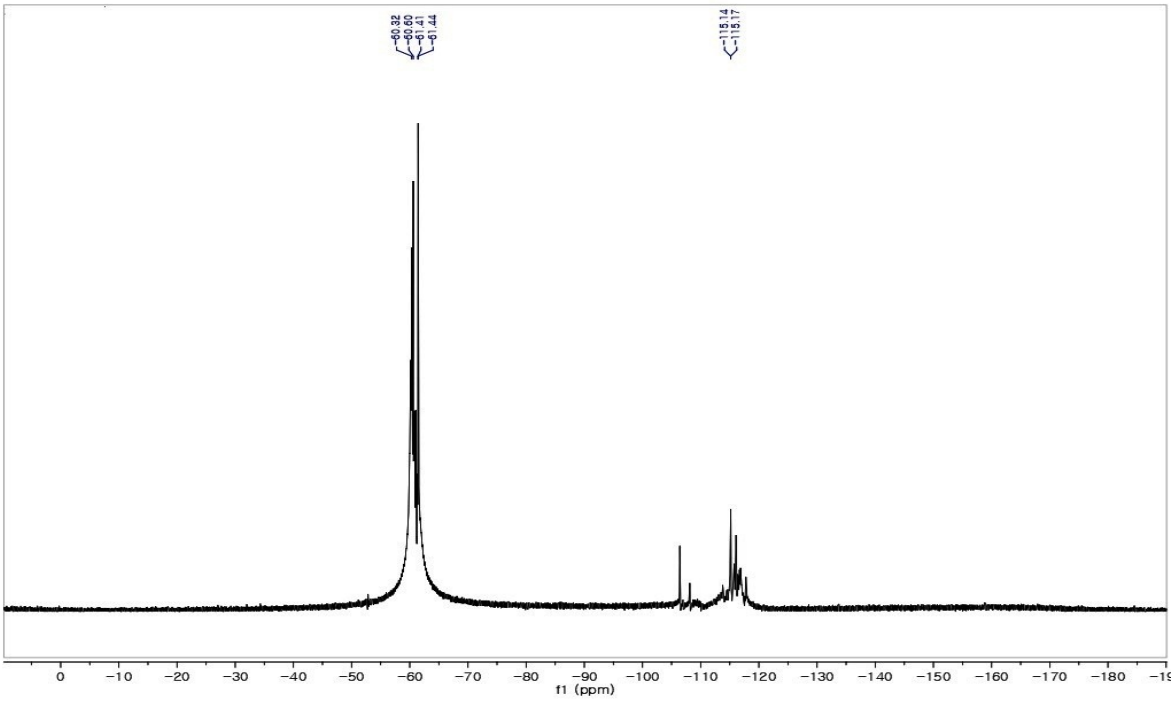

Fig. S63. IR Spectrum of compound (4m)

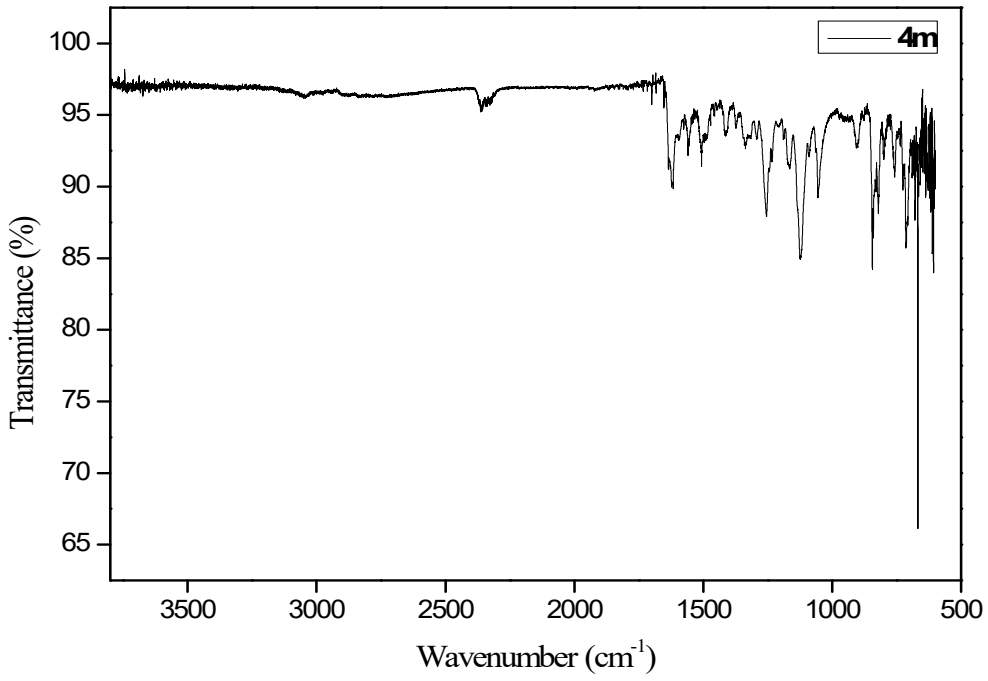

Fig. S64. LC-MS data of compound (4m)

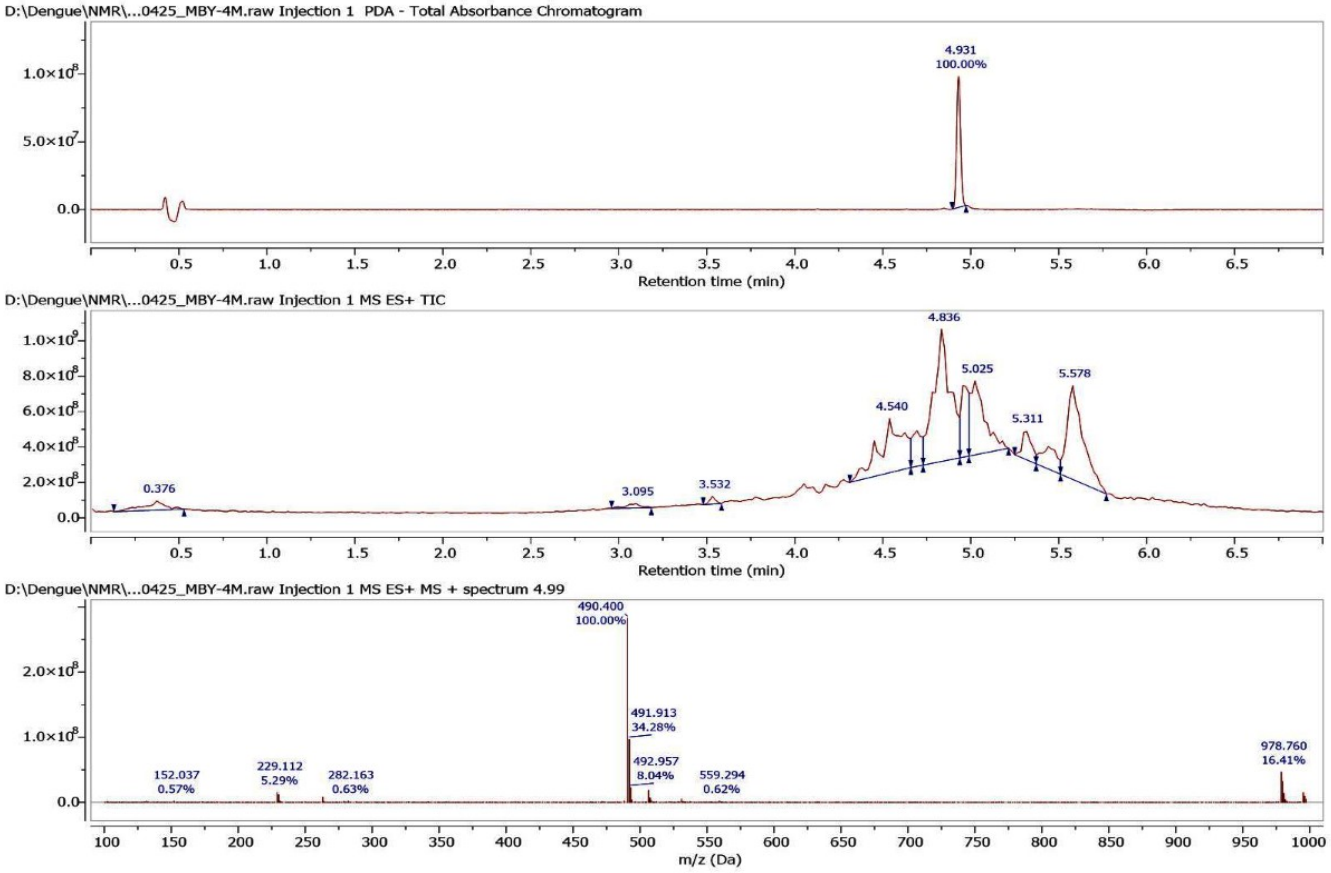

Fig. S65 ^{1}H NMR and Fig. S66 ^{13}C NMR spectra of (4n)

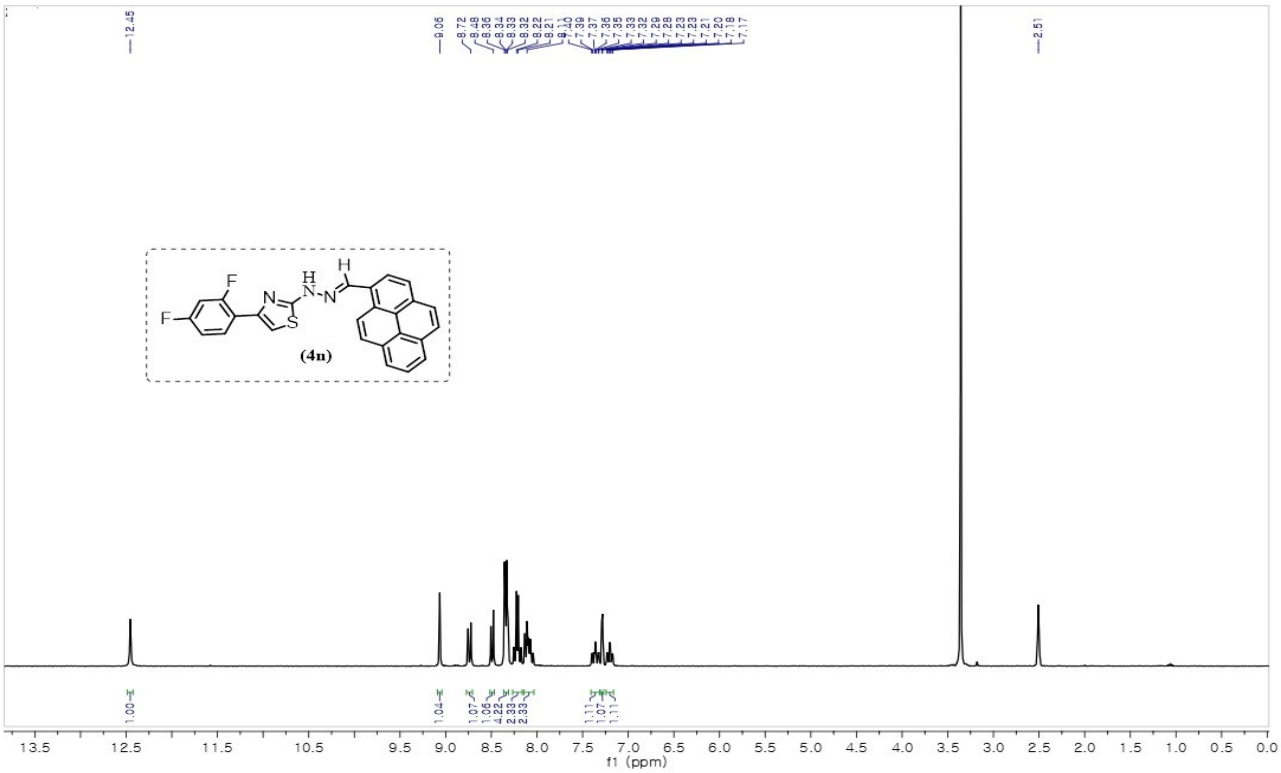

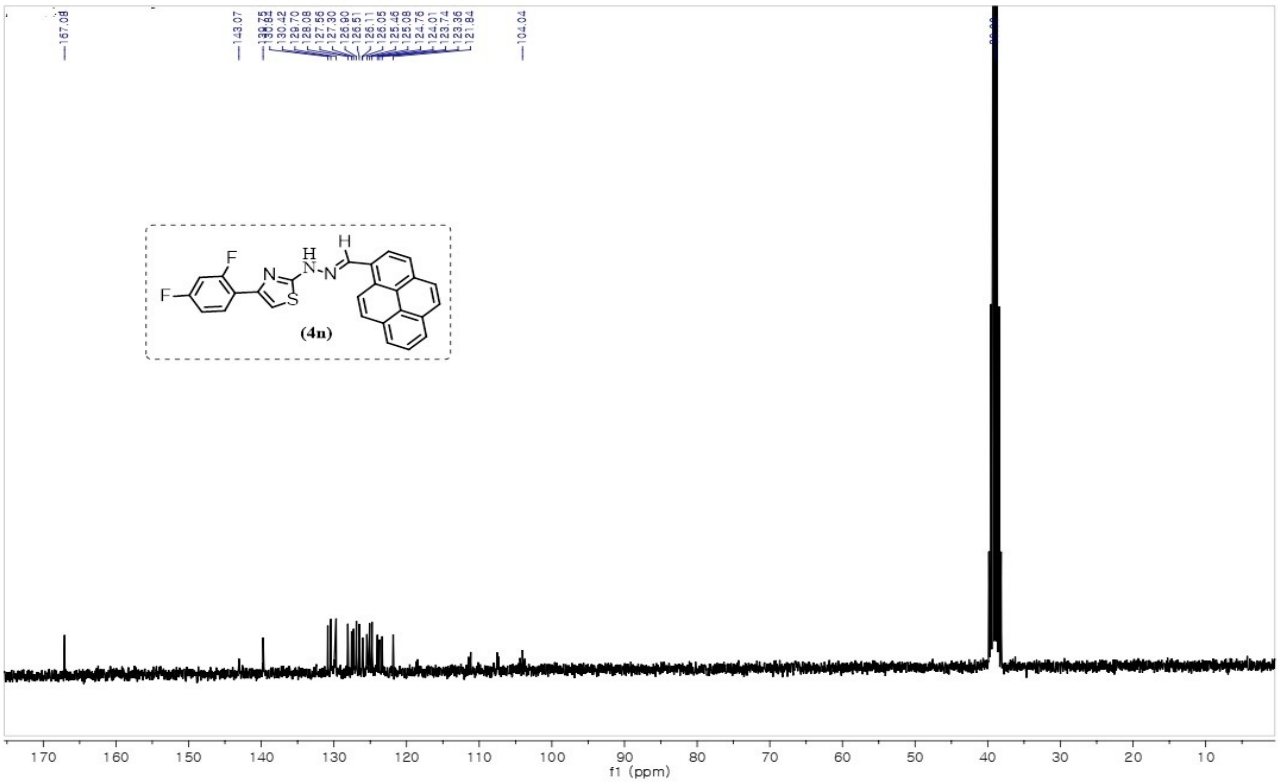

Fig. S67. ^{19}F NMR spectra of (4n)

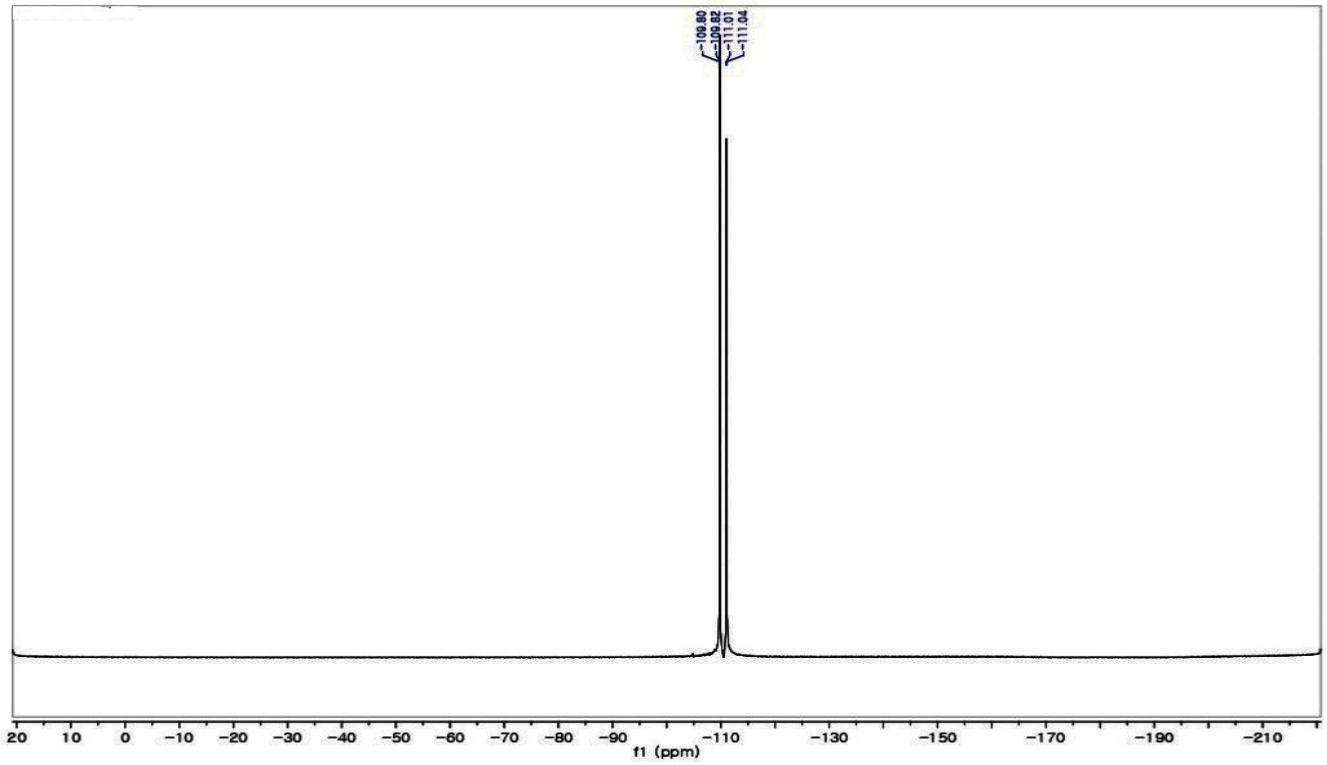

Fig. S68. IR Spectrum of compound (4n)

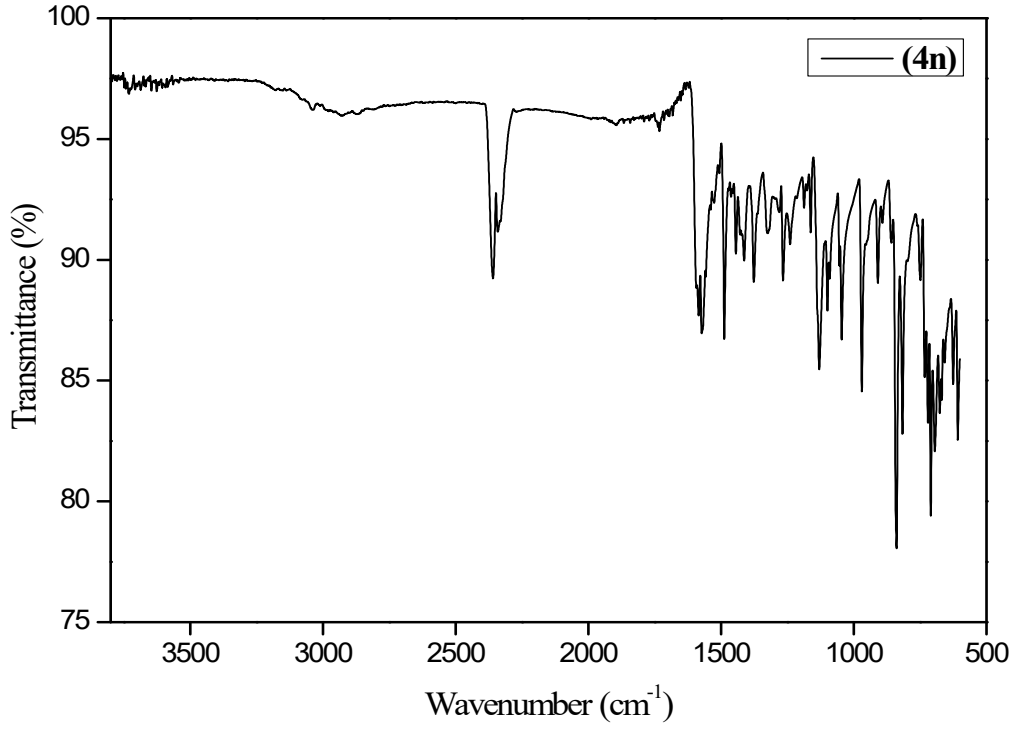

Fig. S69. LC-MS data of compound (4n)

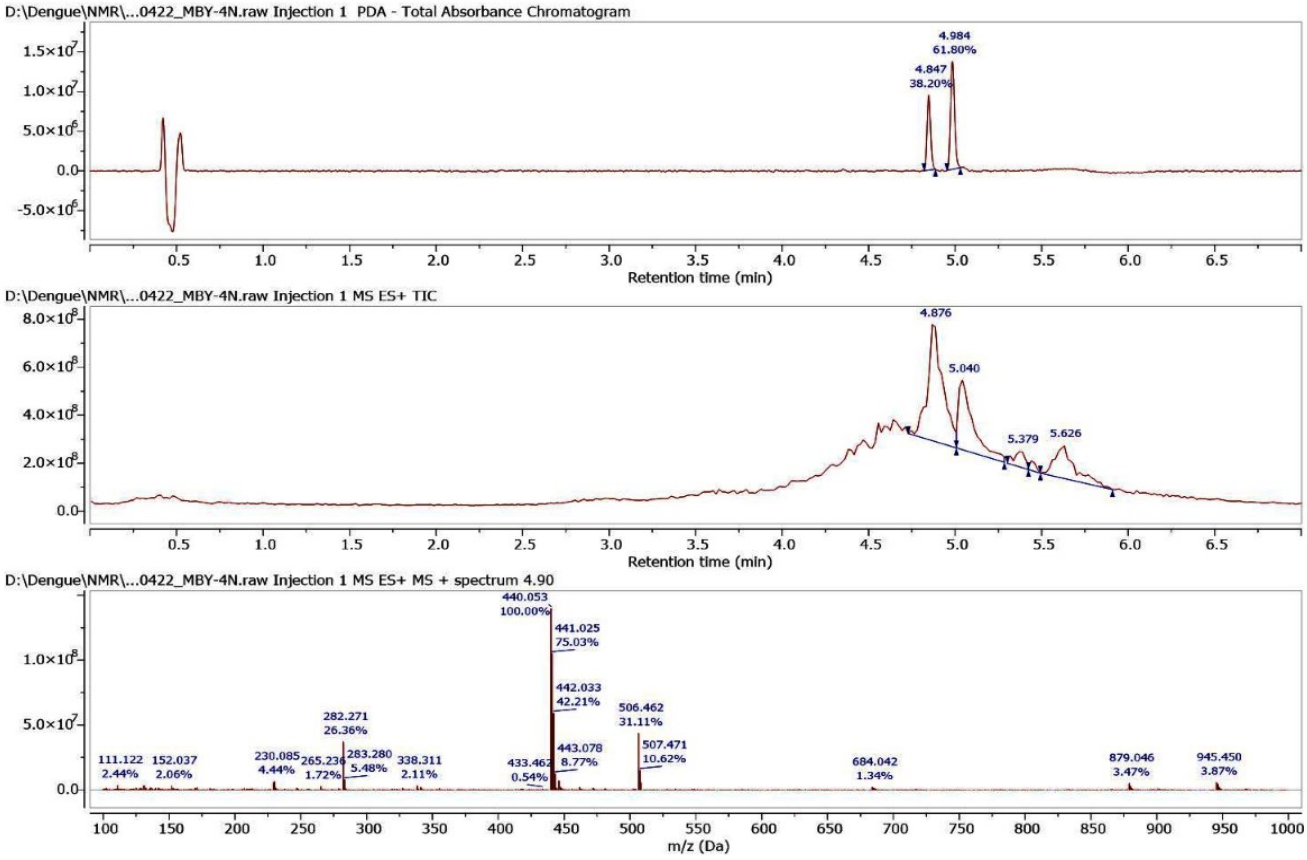

Fig. S70. ^{1}H NMR and Fig. 71. ^{13}C NMR spectra of (4o)

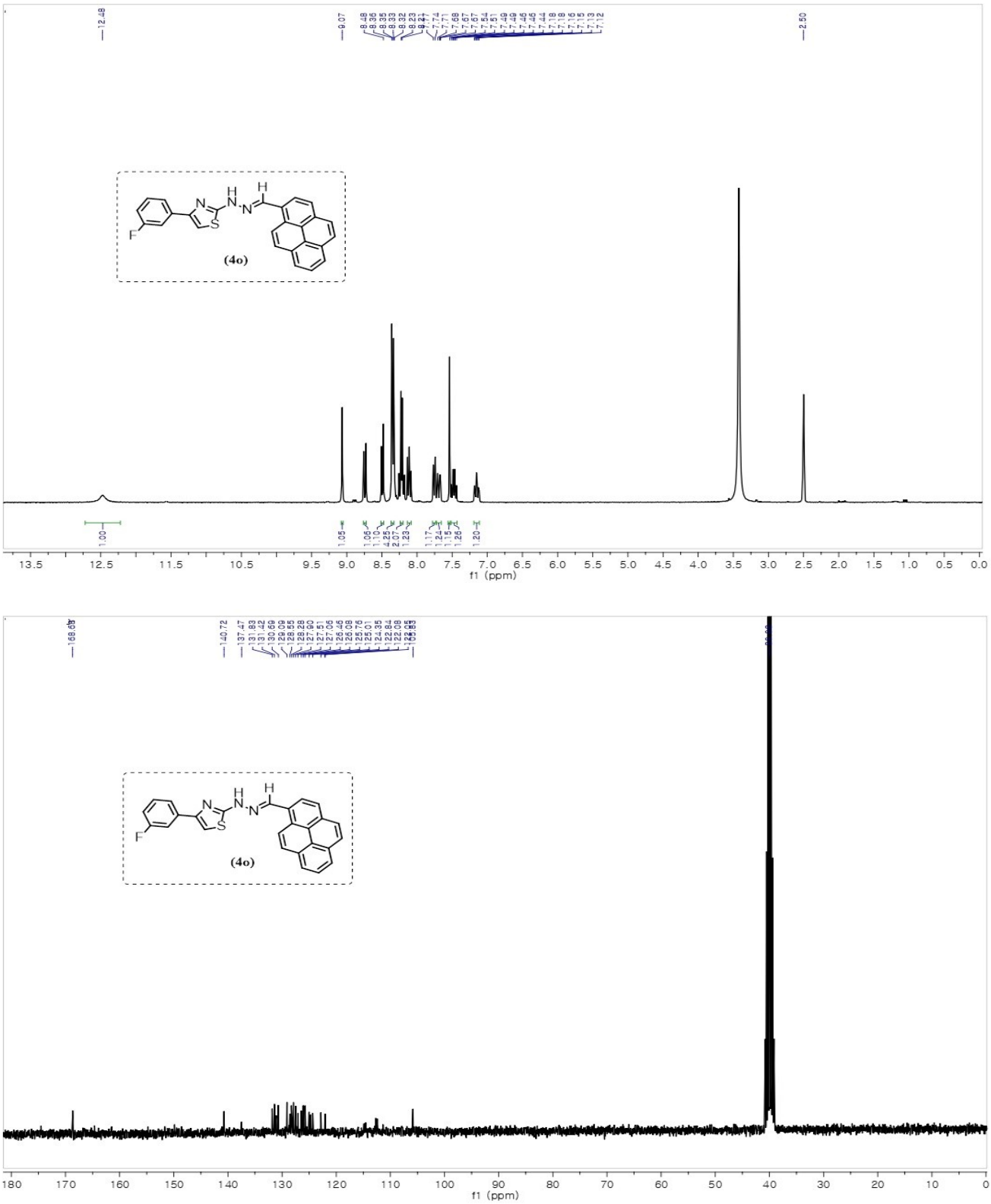

Fig. S72. ^{19}F NMR spectra of compound(4o)

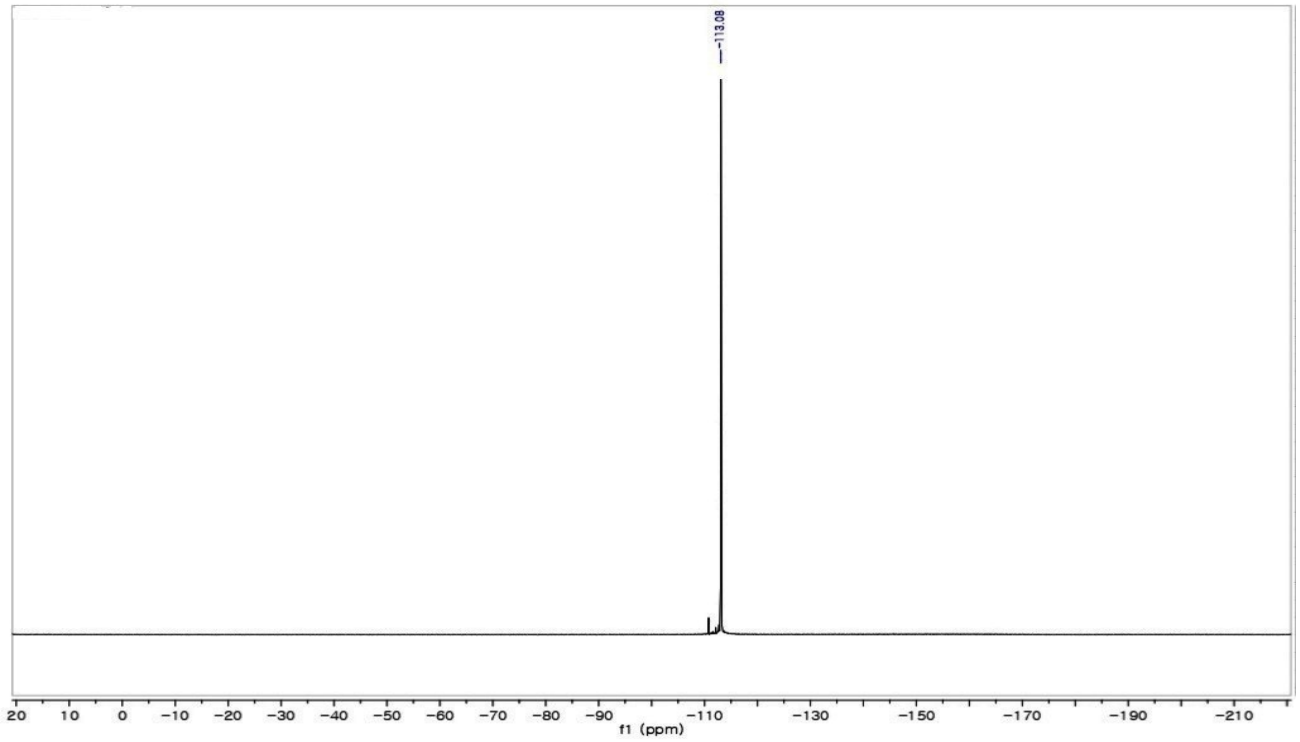

Fig. S73. IR Spectrum of compound (4o)

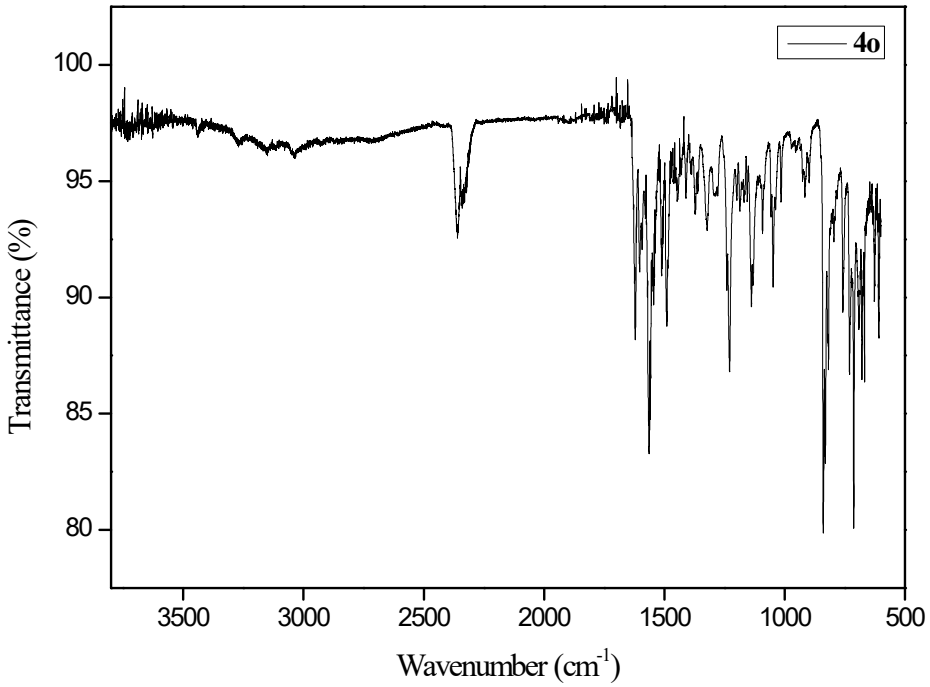

Fig. S74. LC-MS data of compound (4o)